INSIGHTS INTO
THE CRYPTIC MATING BEHAVIOUR OF CHAGA *(INONOTUS OBLIQUUS)*
(HYMENOCHAETACEAE)

by

Benjamin S. J. Bohémier

FACULTY OF NATURAL RESOURCES MANAGEMENT
LAKEHEAD UNIVERSITY
THUNDER BAY, ON, CANADA

August 2025

Insights into the Cryptic Mating Behaviour of Chaga (*Inonotus obliquus*) (Hymenochaetaceae)

by

Benjamin S. J. Bohémier

A Graduate Thesis Submitted in
Partial Fulfillment of the Requirements for the
Degree of Masters of Science in Forestry

Faculty of Natural Resources Management
Lakehead University

August 2025

LIBRARY RIGHTS STATEMENT

In presenting this thesis in partial fulfillment of the requirements of the M. Sc. F. degree at Lakehead University in Thunder Bay, I agree that the University will make it freely available for inspection.

This thesis is made available by my authority solely for the purpose of private study and research and may not be copied or reproduced in whole or in part (except as permitted by Copyright Laws) without my written authority.

Signature:________________________________

Date: ____________________________________

A CAUTION TO THE READER

This M. Sc. F. thesis has been through a semi-formal process of review and comment by at least two faculty members. It is made available for loan by the Faculty of Natural Resources Management for the purpose of advancing the practice of professional and scientific forestry.

The reader should be aware that those opinions and conclusions expressed in this document are those of the student and do not necessarily reflect the opinions of either the thesis supervisor, the faculty, or Lakehead University.

ABSTRACT

Bohémier, B. S. J. 2025. Insights into the Cryptic Mating Behaviour of Chaga (*Inonotus obliquus*) (Hymenochaetaceae). Lakehead University. 191 + xix pp.

Inonotus obliquus(Ach. ex Pers.) Pilàt is a parasitic white heart rot fungus of circumboreal distribution belonging to the family Hymenochaetaceae. It is primarily hosted on birch, but can occur on other hardwoods. Typically, this fungus is recognized by a charcoal-like sterile conk with a yellowish-brown interior that forms on the host tree. Colloquially, this is known as Chaga and is hailed for its health benefits, cultural significance, and economic value. As the name suggests, the sterile conk does not produce any basidiospores. Once in an infection cycle of approximately 10 - 80 years, a spore-producing resupinate and poroid basidioma will form beneath the bark of a recently dead host. This sporadic occurrence makes them difficult to locate and study. The mating system of this fungus has been speculated to be amphithallic (primarily pseudohomothallic + tetrapolar heterothallic).

A clarification of general taxonomy, characteristics of decay, life cycle, medicinal properties, cultivation, conservation, agaricomyceteous mating systems, and the classical/genomic characteristics of *I. obliquus* are provided. Wild strains of *I. obliquus* were isolated from paper birch in North-Western Ontario and examined for *in vitro* growth and fruiting characteristics. A protocol was developed to form fertile fruit bodies reliably under laboratory conditions. The nuclei within basidiospores were examined using Hoechst 33342 and fluorescence microscopy throughout the maturation of basidiomata. It was discovered that the basidiospores of *I. obliquus* have highly variable nuclear characteristics, as they can contain between 1 and 6 nuclei in different ratios at different points in development. Comparisons were made between similar work on Chinese *I. obliquus,* which showed similarity in some cases and major differences in others. Speculation on implications of basidiospore nuclear behaviour are made. As this fungus can reliably fruit *in vitro*, it may grant us a greater understanding of mating in other members of the Hymenochaetaceae as a model organism.

CONTENTS

CHAPTER 1: A COMPREHENSIVE LITERATURE REVIEW OF *INONOTUS OBLIQUUS*

CHAPTER 2: PRELIMINARY INVESTIGATIONS OF *IN VITRO* SPORULATION AND LINEAR GROWTH OF*INONOTUS OBLIQUUS* (HYMENOCHAETACEAE)

CHAPTER 3: *INONOTUS OBLIQUUS* (HYMENOCHAETACEAE) AMPHITHALLISM: CHARACTERIZATION OF HIGHLY VARIABLE BASIDIOSPORE NUCLEAR BEHAVIOURS

TABLES

CHAPTER 2: PRELIMINARY INVESTIGATIONS OF *IN VITRO* SPORULATION AND LINEAR GROWTH OF *INONOTUS OBLIQUUS* (HYMENOCHAETACEAE)

APPENDIX I

CHAPTER 3: *INONOTUS OBLIQUUS* (HYMENOCHAETACEAE) AMPHITHALLISM: CHARACTERIZATION OF HIGHLY VARIABLE BASIDIOSPORE NUCLEAR BEHAVIOURS

APPENDIX II

FIGURES

CHAPTER 1: A COMPREHENSIVE LITERATURE REVIEW OF *INONOTUS OBLIQUUS*

CHAPTER 2: PRELIMINARY INVESTIGATIONS OF *IN VITRO* SPORULATION AND LINEAR GROWTH OF *INONOTUS OBLIQUUS* (HYMENOCHAETACEAE)

APPENDIX 1

CHAPTER 3: *INONOTUS OBLIQUUS* (HYMENOCHAETACEAE) AMPHITHALLISM: CHARACTERIZATION OF HIGHLY VARIABLE BASIDIOSPORE NUCLEAR BEHAVIOURS

ACKNOWLEDGEMENTS

First and foremost, I’d like to acknowledge Dr. Leonard Hutchison for providing guidance, and financial support as I’ve pursued a career in mycology. The knowledge and skills I’ve learned in BB-1050 will carry me far as I navigate this evolving field. Thank you for trusting me to explore the complex and amazing world of fungal mating systems and nuclear behaviour in agaricomycetes.

Thank you to my family for their emotional and financial support throughout this challenging degree. Thank you to Audrey Nerino for emotional support and listening to me ramble about chaga. Thanks to all my friends for their emotional support.

Thank you to the members of my committee for being incredibly kind and relaxed as I navigated this massive project. Thank you to Dr. G. Hausner for being an external reviewer on this thesis. Wren Mengelli for aiding me with genetics. I want to acknowledge Greg Kepka from the instrumentation lab for getting me set up with the epifluorescence microscope. Thank you to Dr. Ashley Thomson for lending me vital equipment for my research. Thank you to all students I got to TA in Forest Pathology and Biology of the Fungi; it was great helping you all. I’d like to acknowledge Dr. Rob Mackereth for validating my reasoning for the Bayesian model in Chapter 3.

Thank you to the Ontario government (Ontario Graduate Scholarship (OGS)) and the Sonoma County Mycological Association (SOMA) for financial support.

Thank you to Ohio Mushroom DNA Lab (Kyle Canan) for sequencing my cultures and Sidnee Ober-Singleton for assisting me in troubleshooting fluorescent microscopy and Hoechst dye.

This thesis is dedicated to the memory of Dr. George L. Barron for his immense contributions to mycology. His influence on our laboratory and my formative years as a mycologist will be carried on into the future.

GENERAL INTRODUCTION

Inonotus obliquus (Ach. ex Pers.) Pilàt is typically recognized by growths of charcoal-like sterile conks on parasitized birch trees, which are colloquially known as chaga. This fungus can be found worldwide and is commonly associated with boreal or sub-boreal forests. It has a long history of medicinal and cultural use. These conks aren't a typical "mushroom"; they do not produce any spores and are likely nutrient sinks for sexual reproduction. The basidiomata (fruit bodies) do not occur in plain view, but instead, beneath the bark of dead birch trees and look nothing like the conspicuous sterile conk. They are flat, porous fruit bodies that produce prolific spores once in a life cycle and are extremely rare. These structures typically form after host tree death, but the fungus continues to form sterile conks for as long as its host can survive; this can be up to 80 years or longer. Its rarity has eluded mycologists for decades, making it incredibly difficult to study. Throughout this project, a method to form basidiomata *in vitro* was developed, which was followed by the analysis of abnormal basidiospore nuclear characteristics. This document aims to elucidate the "cryptic" mating behaviour of *I. obliquus*, with a particular focus on its life cycle, mating system, and the mating mechanisms of other Agaricomycetes.

CHAPTER 1:

A COMPREHENSIVE LITERATURE REVIEW OF *INONOTUS OBLIQUUS*

INTRODUCTION

Inonotus obliquus (Ach. Ex Pers.) Pilàt is a circumboreal white heart rot fungus belonging to the Hymenochaetaceae, a family of the Phylum Basidiomycota. *Inonotus obliquus* has an affinity for attacking *Betula* species; however, it can occasionally be hosted on *Fagus, Ulmus, Ostrya*, *Alnus,* and *Acer.* (Gilbertson and Ryvarden, 1986; Brydon-Williams *et al*. 2021; Minter and Soliman, 2022). It is found in Russia, Poland, Northern Europe, most of the Baltic countries, North America, and Asia (Gilbertson & Ryvarden, 1986; Zheng *et al*, 2010; Rogers, 2012). Typically, this fungus is recognized by the production of sterile conks, which are black, fissured, and charcoal-like perennial aggregates of somatic hyphae that form on the main stem of its hosts and can range in size from roughly 4 cm to 30 cm in diameter and weigh up to 16 kg (Sinadskij, 1973; Lee *et al.* 2008) (Figure 1-1). They only form or amass size while their host is alive (Shigo, 1965; Rivoire, 2020). The term "sterile conk" refers to the lack of sporulating agents present in these structures; not that they are dead - they are alive and actively growing. The charcoal-like appearance of these conks is caused by a heavy melanization of the exterior, but the interior is corky, with a yellowish-brown context; some term this structure a "sclerotium" or "pseudosclerotium" because of its general physical similarities. There are many theories from the community as to its purpose (some with heavy emphasis on the truth of what they claim), but to date, there have been no formal studies unveiling the enigma that is the sterile conk. At the moment, the most reasonable working theory is that it may be a storage sink of nutrients for growth and sporulation (Bunyard, 2015). However, "the jury is still out", so to speak, on its true functionality.

Figure 1-1. *Inonotus obliquus* sterile conk (chaga) on white birch. Source: Researcher

The sterile conk bears many names originating from various cultures around the world: chaga (which is derived from the Russian Komi word *čága* meaning "fungus growing on a tree" or "tinder"), clinker, canker, *kreftkjuke* (when translated from Norwegian meaning "cancer polypore"), *Pakuri* in Finnish, *Wiskakecakomikih* by the Cree, and the Chipewyan call it *Cha'a'ihtthi* (Rogers, 2012). Since the 16th and 17th centuries, the sterile conk of *Inonotus obliquus* has been held in high regard as a potent medicinal folk remedy in many of the aforementioned countries, especially Russia and Siberia and is used to treat cancers, gastritis, ulcers, liver conditions, heart disease, tuberculosis, intestinal worms, and is also used as "soap water" to wash external sexual organs during menstruation or after birth (Saar, 1991; Kim *et al.* 2006; Lee *et al.* 2008; Lemieszek *et al.* 2011; Rogers, 2012). It is most commonly brewed as a tea or made into a tincture. In the former USSR, *I. obliquus* extract enriched by 0.175% $CoCl_2$ and 0.2% $CoSO_4$ is sold as an official medicine and was sold as *Befunginum* (Tumanova *et al.* 1989). Only since the 21st century has Chaga begun to attract the interest of the scientific community. Extracts from the sterile conk and its cultivated mycelium have been examined to possess anti-tumour, anti-viral, hypoglycemic, and other properties that will be elaborated upon later in the text. (Ichimura *et al.* 1999; Kim *et al.* 2005; Cha *et al.* 2005; Kim *et al.* 2006; Chen *et al.* 2006; Lemieszek *et al.* 2011; Shibnev *et al.* 2011; Wang *et al.* 2017; Basal *et al* 2021; Teplykova *et al.* 2022). In recent years, Chaga (as well as other medicinal mushrooms) has become highly commercialized, where it can be sold in its raw wild form, tea bags, tinctures, hot chocolate mixes, coffee, capsules, gummies, etc. The chaga market was estimated to reach market value of US $1.05 billion by 2024 (Fact.MR, 2024). However, there have still not been any formal human trials.

While the primary focus of this species has been on the sterile conk, its basidiomata, sexual cycle, and mating are largely understudied while being equally, if not more, enigmatic than its sterile counterpart. The fruiting body of *I. obliquus* is incredibly inconspicuous, rare, and easily missed if one does not know where and when to search for it. Even to the avid Chaga harvester/enthusiast, it can be easily overlooked as it appears nothing like its sterile form that has received so much interest and praise. Its basidiomata (fruiting body) is simply a resupinate (flat) and poroid (porous) mass that ruptures and forms beneath the bark of recently deceased host trees and has a somewhat similar colour to its substratum (Figures 1-2 & 1-3) (Gilbertson & Ryvarden, 1986; Bunyard 2015; Rivoire, 2020). Interestingly, when seeing one in the wild, it bears an almost iridescent or metallic shine that is difficult to describe unless seen with your own eyes. The namesake of *I. obliquus* or formerly *Poria obliqua* (Ach. ex Pers.) Karst. refers to the oblique direction of pore formation relative to the host stem. Interestingly, this fruit body will only form once during an infection cycle of approximately 30 to 80 years (Shigo, 1965; Černý, 1976; Gilbertson & Ryvarden, 1986; Bunyard, 2015; Maine Forest Service, 2023). Bunyard (2015) was the first to formally describe its association with beetles of the genus *Orchesia* Latreille that likely act as primary basidiospore dispersers for the fungus. Due to the fruitbody forming so rarely and the difficulty of conducting mating experiments for members of the Hymenochaetaceae, it has been challenging to study (Rajchenberg *et al*. 2015). Recently, *I. obliquus* was examined by Sun *et al.* (2023) and found to exhibit traits of an amphithallic mating system, as its primary mode of reproduction was pseudohomothallic with tetrapolar heterothallic tendencies. This is a classic example of amphithallism *sensu* Lange (1952). Additionally, Sun *et al.* (2023) observed anucleate, uninucleate, binucleate, trinucleate, and tetranucleate basidiospores. With its potential medicinal and commercial applications, the literature available on *I. obliquus* is highly imbalanced, as it is dominated by research focusing on secondary metabolites, potential medicinal use, and commercialization, while we still lack a fundamental understanding of its biology, mating, and ecological function.

Figure 1-2. Basidiomata of *Inonotus obliquus* on yellow birch on Madeline Island, Wisconsin. Whole structure. Source: Benjamin Bohémier

Figure 1-3. Basidiomata of *Inonotus obliquus* on yellow birch on Madeline Island, Wisconsin. Pore structure. Source: Benjamin Bohémier

The introduction of this literature review serves to familiarize the reader with this taxon such that complex topics can be discussed that relate more closely to the following chapters of this dissertation. This review covers a wide variety of topics that aim to provide *I. obliquus* taxonomic history, life cycle, mating system and genomics, nuclear behaviour, decay mechanisms, cultivation, medicinal use of the sterile conk and more. Find below a foundation of highly valuable knowledge on which this work was built, and in turn, for you, the reader, to stand on as you explore

Inonotus obliquus and the Hymenochaetaceae in this document. To begin, here is a quote by John R. Raper from his crucial book *Genetics of Sexuality in Higher Fungi*:

"Sexuality in higher fungi is no more mystifying than elsewhere; the facts, examined in proper sequence, are simple enough, but it does seem that there are quite a few of them" (Raper, 1966)

FOUNDATIONS OF TAXONOMY

Inonotus obliquus belongs to the order Hymenochaetales and the family Hymenochaetaceae of the Agaricomycetes; the hymenochaetoid clade. Important modern conceptualizations of these rankings are provided. Finer focus will be made on the genus *Inonotus* P. Karst. and the species *Inonotus obliquus* with regards to descriptions and taxonomic history.

The Hymenochaetales

The Hymenochaetales (*sensu* Oberwinkler (1977)) is an early-diverging order within the Agaricomycetes, estimated to have diverged approximately 259 Mya (He *et al.* 2019). As of October 2023, this order contained roughly 1200 species, and more than 780,000 occurrences have been reported worldwide (Zhao *et al.* 2024). Species in this clade are primarily wood-inhabiting white-rot fungi, but they also complete a multitude of ecological functions, such as saprotrophy, parasitism, and mutualism (Larsson *et al.* 2006; Zhao *et al.* 2024). The members of the Hymenochaetales produce incredibly morphologically diverse basidiomata forms, such as poroid, corticoid, hydnoid, clavarioid, spathulate, and agaricoid (Larsson *et al.* 2006; Zhao *et al.* 2024) (Figure 1-4). *Hymenochaete* Lév., the type genus of the order, is an important and well-studied saprotrophic genus that forms resupinate *Stereum*-like pilei that cause a white fibrous or pocket rot in deadwood (Parmasto *et al.* 2014). *Onnia tomentosa* (Fries) P. Karsten is an incredibly important root rot pathogen of spruce and pine in North America, which causes significant economic loss and tree mortality (Germain *et al.* 2009). The genera *Coltricia* Gray and *Coltriciella* Murill have been found to form ectomycorrhizas with woody plants (Tedersoo *et al.* 2007). Additionally, the basal Hymenochaetales agaricoid taxon *Rickenella fibula* (Bull.) Raithelh. maintains a commensal endophytic relationship with bryophytes (Korotkin, 2017). As the diversity of macro and microscopic characters is great in the modern concept of Hymenochaetales *sensu stricto*, there is no particular one that unites the order, save for ultrastructural characteristics of their parenthosomes, which is an important and variable structure in the dolipore septa of Agaricomycetes (Hibbett & Thorn, 2001). Members of this order almost all possess imperforate parenthosomes, save for *Peniophorella praetermissa* P. Karst. which has been found to have perforate parenthosomes (Hibbett *et al.* 2014). Members of *Peniophorella* P. Karst. form their own family in the order; Peniophorellaceae (Zhao *et al.* 2024).

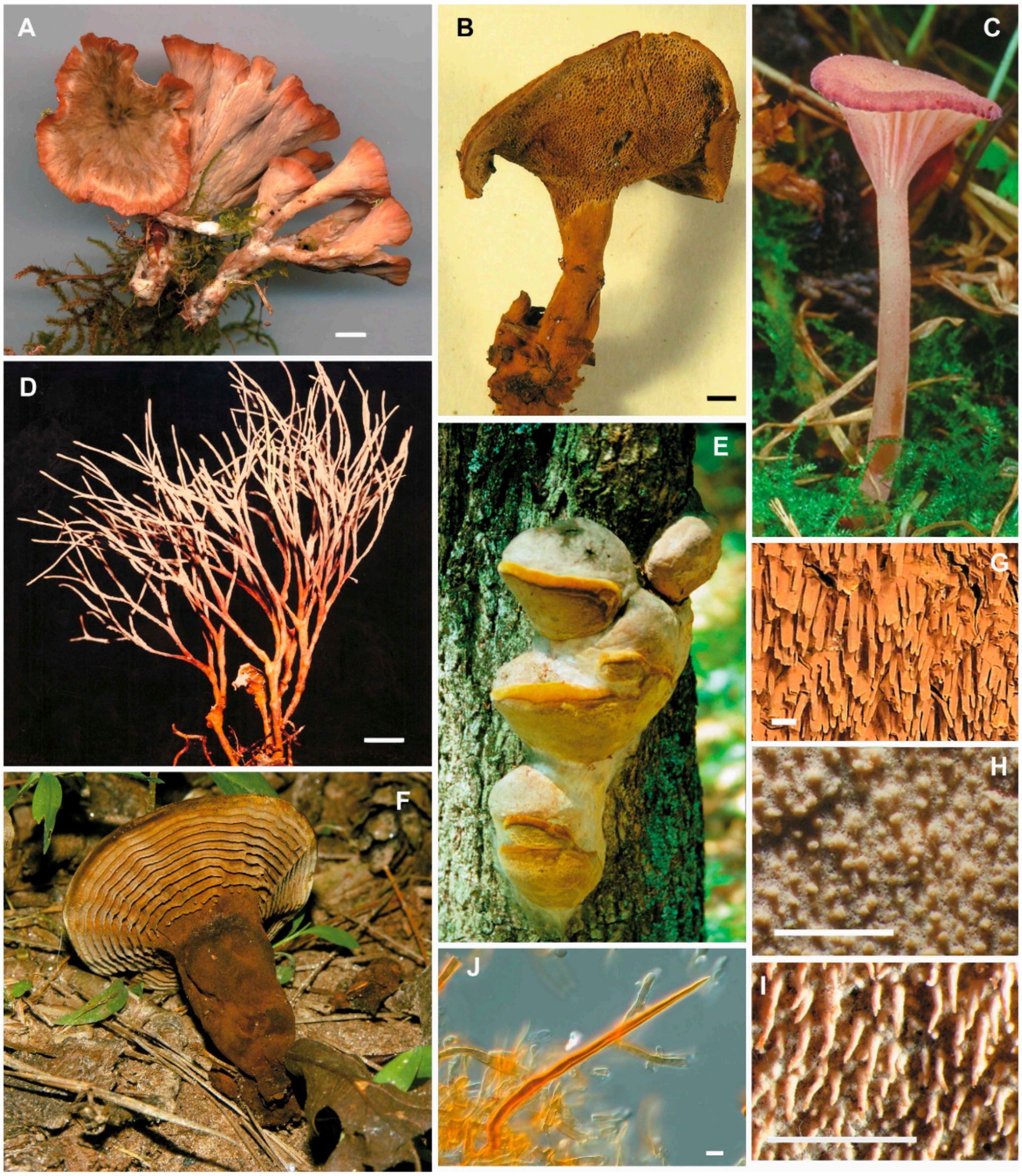

Figure 1-4. Macro and micro characters in Hymenochaetales. A–J. Basidiome and hymenophore types. A. *Cotylidia pannosa* (Sowerby) Reid, (photo David Mitchel, www.nifg.org.uk/photos.htm) B. *Coltricia perennis* (L.) Murrill. C. *Contumyces rosella* (Moser) Red., Monc., Vilg. & Lutz. D. *Clavariachaete rubiginosa* (Berk. & Curt. ex Cooke) Corn. (photo Roy Halling) E. *Phellinus robustus* (P. Karst.) Bour. & Galz. (photo Andrej Kunca, Forest Research Institute, Slovakia, www.forestryimages.org) F. *Coltricia montagnei* (Fr.) Murrill (photo Dianna Smith, www.mushroomexpert.com). G. *Hydnoporia olivacea* (Schwein.) Teix. H. *Resinicium bicolor* (Alb. & Schwein.) Parmasto hymenium. I. *Hyphodontia arguta* (Fr.) Erikss. hymenium J. hymenial setae *in Hymenochaete cinnamomea.* Source: Larsson *et al*. (2006)

Descriptions of the hymenochaetoid-clade or hymenochaetaceous fungi date back to Patouillard (1900) the *Série des Ignaires*, which united genera of varying basidiomata morphology based on possessing setae (sword-like cystidial structures in the hymenium or hyphae), golden to brown colouration of basidiomata, and the darkening of tissue in potassium hydroxide (xanthochroic reaction). The presence of setae sometimes lacks in certain taxa, but the colour of basidiomata and the reaction of tissue in KOH were unanimously shared characters in this group (Fiasson & Niemelä, 1984). Donk (1948) recognized the group as family **Hymenochaetaceae.** Oberwinkler (1977) raised this family to the order Hymenochaetales. Fiasson & Niemelä (1984) in *The Hymenochaetales: A Revision of European Poroid Taxa* provided an early definition and classification of the Hymenochaetales. They defined the Hymenochaetales as follows: Homobasidiomycetes with poroid, smooth or spiny hymenophore; hyphae golden to brown, xanthochroic and consistently simple-septate; setae present in most species; parenthesomes nonperforated in most species; capable of synthesizing styrylpyrones; producing white-rot or seldom imperfect brown-rot.

Since Oberwinkler (1977) raised the Hymenochaetales, it has received many major revisions and is to be interpreted much more broadly (Larsson *et al.* 2006). The description for the Hymenochaetales *sensu* Oberwinkler (1977) provided by Fiasson & Niemelä (1984) is now akin to the family Hymenochaetaceae sensu Donk (1948). Hibbett & Donogue (1998) displayed the broadness of the Hymenochaetales in the first comprehensive molecular study of the Homobasidiomycetes (Agaricomycetes *sensu lato*), where genera such as *Trichaptum* Murrill, which do not possess setae or a xanthocroic reaction, were closely related to the Hymenochaetales. However, it did possess an imperforated parenthosome. Hibbett & Thorn (2001), in their hallmark paper on the phylogeny of the Homobasidiomycetes, were the first to describe the Hymenochaetales accounting for molecular data. Through the combined work of Moncalvo *et al.* (2002) and Redhead *et al.* (2002), some omphalinoid agaric genera, such as *Rickenella* Raithelh. and *Cantharellopsis* Kuyper*,* were basally placed in the Hymenochaetales.

Zhao *et al.* (2024) provided the most up-to-date and comprehensive report on the phylogenomics and evolution of the Hymenochaetales. As it stands, the order is comprised of 10 accepted families: **Hymenochaetaceae**, Coltriciaceae, Hirschioporaceae, Schizoporaceae, Rigidoporaceae, Peniophorellaceae, Sideraceae, Resiniciaceae, Skvortzoviaceae, and Rickenellaceae. They found that the divergence time for these families is likely to have taken place 123-163 mya. Additionally, corticoid basidiomata are likely an ancestral morphology in the Hymenochaetales, which was quickly overtaken by the poroid basidiomata roughly 130-150 Mya, thought to be caused by the rapid radiation of Hymenochaetaceae.

The Hymenochaetaceae

The Hymenochaetaceae is the largest family in the Hymenochaetales, containing roughly 35 genera and 900 species that are currently accepted (Ghobad-Nejhad *et al*. 2024). As described above, the Hymenochaetaceae fits very close to the description provided by Fiasson & Niemelä (1984). In addition to their description, members of the Hymenochaetaceae produce annual or perennial basidiomata that can be woody, resupinate, and effused-reflexed to pileate that are typically broadly attached to their substrate or are sometimes stipitate (Dai, 2010; Rajchenberg *et al.* 2015; Wu *et al*. 2022; Ghobad-Nejhad *et al*. 2024) (Figure 1-5). The hyphae do not bear clamp connections, and their hyphal system is typically monomitic or dimitic. Many species are important forest pathogens, such as *Onnia tomentosa* and *Phellinus tremulae* (Bondartsev) Bondartsev & P.N.Borisov (Mallet & Myrholm, 1995; Germain *et al*. 2009). In terms of cultural features, taxa within the family are virtually impossible to separate unless knowledge regarding hosts and habitat is provided (Nobles 1965; Stalpers, 1978). The two most important genera in this family are *Phellinus* Quél and ***Inonotus*** P. Karst.. *Phellinus* contains 220 species (Larsen & Cobb-Poulle, 1990), *Inonotus* with 101 species (Ryvarden, 2005). It is likely that these numbers are incomplete (Wagner & Fischer, 2002). Over time, many of these genera have been split (Larsson *et al.* 2006). Historically, these two genera have been split based on hyphal systems and fruiting body persistence, but this separation has been proven to be artificial (Wagner & Fischer, 2002).

Figure 5-1. Examples of basidiomata in the Hymenochaetaceae. A. *Arambarria destruens* Rajchenb. & Pildain. B. *Nothophellinus andinopatagonicus* (Wright & Deschamps) Rajchenb. & Pildain. C-D. *Phellinopsis andina* (Plank & Ryv.) Rajch. & Pildain. C. young basidioma. D. mature basidioma. E. *Phellinus livescens* (Speg.) Rajchenb. D. *Pseudoinonotus crustosus* (Speg.) Rajchenb. & Pildain (photograph by P. Sandoval). Source: Rajchenberg *et al.* (2015)

The Genus *Inonotus*

As stated above, *Inonotus* is one of the largest and most important genera in the Hymenochaetaceae in which members are poroid, and cause a white-rot in dead or living hardwoods or conifers. To begin, the original description of the genus by P. Karsten is provided as sourced from Ryvarden (2005) in his synopsis of the genus *Inonotus*:

"INONOTUS P. Karsten, Medd. Soc. Fauna Fl. Fenn. 5:39, 1880. Basidiomata annual, resupinate, effused-reflexed, sessile, or rarely laterally stipitate, tissue yellowish to reddish-brown, darkening in KOH; pileus surface hirsute, hispid, tomentose, or glabrous, yellowish to reddish-brown, often darkened and rimose in age; context brown, soft-fibrous to tough-corky; hyphal system monomitic; hyphae simple-septate, in most species ranging from thin-walled and almost hyaline to thick-walled and brownish in KOH, much branched, setal hyphae present in context or trama of some species; hymenial setae present in most species, usually hymenial or subhymenial in origin, subulate to ventricose, pointed, pale to dark brown in KOH; basidia clavate to broadly ellipsoid, 4-sterigmate, simple-septate at the base; basidiospores cylindrical, ellipsoid to ovoid or subglobose, hyaline or golden to reddish brown, smooth, negative or dextrinoid in Melzer's reagent; causing a white rot of living and dead conifers and hardwoods.

Type species: *Polyporus hispidus* Bull.:Fr.

Remarks: The genus is usually easy to recognize by its brown, annual basidiomata with a fibrous to soft or fragile consistency. The generative hyphae are generally wider than those of the related genus *Phellinus* that is characterized by its woody, perennial basidiomata and dimitic hyphal system."

Until the release of Wagner and Fisher (2002), *Inonotus sensu stricto* consisted only of taxa with a monomitic hyphal system and annual basidiomata. It was shown that the concept of *Inonotus s.s.* should be broadened to taxa that have perennial basidiomata, a dimitic hyphal system, or intermediate forms. They also found *Inonotus sensu lato* to be highly polyphyletic and was separated into genera such as *Inocutis, Onnia*, and *Inonotopsis.*

The Species *Inonotus obliquus*

As much regarding the species has already been described and will be further expanded upon throughout this literature review, this section will focus on taxonomic history and a description that is the combination of works by Campbell & Davidson (1938), Domański (1965), Černý (1976), Stalpers (1978), Ryvarden (2005), Pietka & Grzywacz (2006), Dai (2010), Bunyard (2015), Rivoire (2020), Wu *et al*. (2021) and observations of the researcher. With regards to measurements, of basidiospores, basidia, and setae, they do not vary much from one another in descriptions, thus, those that report a higher "n" are used. Any contradictions in descriptions will be addressed and marked with an asterisk.

Inonotus obliquus (Ach. ex Pers.) Pilát

Basidiomata: Basidiomata annual; forming only once in an infection cycle beneath the bark of dead standing or fallen host tree, ruptures bark, resupinate, poroid, can be up to 3-4m in length and 50cm wide, becomes hard and brittle when dry, easily separable, pore surface iridescent reddish-brown, 1-7 pores per mm, often elongate, young pores yellow to olive, old pores reddish-brown, pores oblique, polygonalspherical, 20-30° relative to stem, entire dissepiments; become lacerate, context bright yellowish-brown, faintly zonate, corky, largely 1mm thick, margin of basidioma can be thicker; 2.5-4mm

Hymenium: Tramal hyphae/subhymenium strongly agglutinated, hyaline thin-walled to yellowish thick-walled, hyphal setae absent or very rare in trama, frequent hymenial setae, subulate, ventricose, reddish-brown, thick-walled, 11-24(-40) x 5-8 µm, some deep-rooted

Basidia: subclavate, 11-24 x 5-8, four sterigmata**, sterigmata 2-2.5µm in length, basal septum, often with large guttule

Basidiospores: hyaline to pale yellow-brownish*, broadly ellipsoid to ovoid, sometimes with prominent hilar appendage, (7.1-) 7.2-<u>8.6</u>-10.0 (-10.1) x 4.4-<u>5.5</u>-6.6 µm, Q = 1.4-<u>1.6</u>-1.8 (-1.9), n = 70

Sterile conk: not producing conidia or chlamydospores***, sterile, black exterior, fissured, charcoal-like, brittle, hard to separate, two types of generative hyphae, some are rare 1.5-2µm wide, sinuous, branching, thin walls, others more common, 4-6 (-8) µm wide, parallel, thick brown walls, only will develop when host is living, interior mottled yellowish-brown, patches of hyaline young hyphae, corky, dense intricate core, difficult to separate, numerous generative hyphae, branching, 1.25-2 (2.5) µm wide, thin to thick walls, brownish, setal hyphae inside, 2-3.3 (-6) µm wide, thick walled, reddish-brown, lumen often consistent, sterile conk is dominant stage of life cycle, only will develop when host is living, 4-30cm in diameter, up to 16kg

Hyphal system: monomitic, generative hyphae dark brown in KOH, thin to moderately thick-walled, frequent branching, 3.5-7µm wide

Culture characters: hyphal setae sometimes present in aerial mycelium, up to 250 µm long and 5-8 µm in diameter, dependent on colony age and media, colony at first white, antimony yellow, apricot yellow or mustard yellow, rarely cinnamon buff or buckthorn brown, colonies sometimes zonate, inverse often with black melanized zonation when 2-3 weeks old, aerial hyphae 2-5µm, hyphae without clamps

Host: Primarily *Betula*, rarely on *Alnus*, *Fagus*, and *Ostrya*

* Wu *et al.* (2021) and Dai (2010) report that basidiospores are purely hyaline, not to pale yellow or pale brownish. Yellowish colour can be difficult to distinguish under the microscope, or if the spore print is too thin. All other descriptions report yellowish spores. Their collections were made in Mongolia; interesting difference.

** Campbell and Davidson (1938) mention that basidia are sometimes bisterigmate. This contradicts every other available observation that describes the basidia as tetrasterigmate.

*** Domański (1965) reports that the sterile conk produces chlamydospores, which contradicts every other account of *I. obliquus*. Likely contamination.

Inonotus obliquus - taxonomic history

Campbell & Davidson (1938) and Balandaykin & Zmitrovich (2015) provided a detailed accounting of the taxonomic history of *Inonotus obliquus* (Ach ex Pers.) Pilát, from which I summarized here: *Inonotus obliquus* has quite a long taxonomic history filled with disputes, arguments and assumptions about this mysterious fungus and its formation of the culturally significant sterile conk. Myasoedov (1896), author of *Album of the Most Harmful Wood-Parasitizing Fungi*, had initially attributed the sterile conk to *Polyporus laevigatus* Fr. (syn: *Phellinus laevigatus* (P. Karst.) Bourdot et Galzin). However, Prof. Borodin (the album editor) suggested that the fungus described as *P. laevigatus* was not consistent with the then-current descriptions, and that true identification of the Chaga fungus was required. Lindroth (1904) described the sterile conks as aborted basidiomata of *Polyporus nigricans* Fries. (modern syn: *Phellinus igniarius* (L.) Quél.). Bondarstev (1912), on the basis of hyphal structure, determined that the Chaga fungus was perhaps a sterile form of *Fomes igniarius* (L.) Fr. (modern syn: *Phellinus igniarius*) which was supported by Yachevskii (1913).

Weir (1915) observed fruiting bodies of *F. igniarius* and sterile conks appearing on the same tree and considered the two to be the same species. He suggested that sterile conks were unable to develop into basidiomata because of humidity, cyclical freezing and thawing, and certain chemicals from the wound which arrested the mycelium's development from a vegetative state to a sexual one. In subsequent years, it was formally named *Fomes igniarius f. sterilis* Vanin. Katayevskaya (1928) examined *F. igniarius* and the sterile conk in culture and found that there were discernable microscopic differences between the two; however, she remained with the position that both were originating from the same species. Verrall (1937) concluded after completing an in-depth analysis of cultural variation among *F. igniarius* and considering that both the latter and the sterile conk come from the same host tree, that they are both the same species.

Campbell (1938) described the cultural characteristics of many species of *Fomes* and the sterile fungus. It was determined that the sterile fungus demonstrated characteristics which could be readily separable from other species of *Fomes*. Campbell & Davidson (1938) were the first to describe that the sterile conk was likely formed by *Poria obliqua* (Pers) (modern syn: *Inonotus obliquus* (Ach Ex Pers.) Pilát): In August of 1937, a resupinate species of *Poria* was collected from a dead *Betula allgheniensis* Britt. in Massachusetts. The *Poria* split the bark wood layer outward and exposed the resupinate hymenium. In this instance, Campbell & Davidson (1938) reported that the basidiomata ran the entire length of the snag and was 3.6m long. Upon further investigation in the Harvard Forest, these resupinate poroid fruiting bodies were found only on dead-standing trees of the genus *Betula* which bore sterile conks on their stems. This observation was the first to associate sterile conks with *Poria*. The specimens collected were sent off to the Division of Forest Pathology in Washington to be cultured in the laboratory. Spores and tissue yielded a culture that was identical to that of the sterile conk. This proved that a *Poria obliqua*-like fungus analogous to that in Europe (syn: *Inonotus obliquus*) was most likely the fruiting stage of sterile conks. Zabel (1947) and Bondarstev (1953) both supported this description. Kuzntesova-Zarudnaya (1955) terminated the attribution of sterile conk formation to *Phellinus* species because cultural studies of the fungus were insufficient for exact identification. Eventually, the description *Inonotus obliquus* was supported by all taxonomists (Ryvarden & Gilbertson, 1986). A question that now stands is whether the circumboreally distributed *I. obliquus* is a single species or a complex. That is yet to be examined, and could reveal some interesting questions about this taxon.

In addition, here are all the known synonyms of *Inonotus obliquus* (Ach. ex Pers.) Pilat (1942) in order: *Boletus obliquus* Ach. ex Pers. (1801), *Polyporus obliquus* (Ach. ex Pers.) Fr. (1821), *Physisporus obliquus* (Ach ex Pers.) Chevall. (1826), *Poria obliqua* (Ach ex Pers.) Karst. (1881), *Fomes obliquus* (Ach. ex Pers.) Cooke (1885), *Mucronoporus obliqua* (Ach. ex Pers.) Ellis & Everh. (1889), *Scindalma obliquum*, (Ach. ex Pers.) Kuntze (1898), *Phellinus obliquus* (Ach ex Pers.) Pat. (1900), *Xanthochrous obliquus* (Ach. ex Pers.) Bourd. & Galzin (1928), and *Fuscoporia obliqua* (Ach. ex Pers.) Aoshi. (1951).

INFECTION CYCLE

The Sterile Conk and Decay

Inonotus obliquus occurs almost exclusively on trees of the genus *Betula* (*B. papyrifera* Marshall, *B. pendula* Roth, *B. pubescens* Ehrh., *B. alleghaniensis* Britt., *B. lenta* L., *B. occidentalis* Hook., *B. populifolia* Marshall. However, *I. obliquus* has been reported to occur on *Alnus rubra*, *Fagus grandifolia* Ehrh., *F. sylvatica* L*., Acer rubrum* L., *Ostrya virginiana* (Mill.) K. Koch., *Quercus* L. and *Populus* L. (Brydon-Williams *et al*. 2021). *Inonotus obliquus* begins infection like many other decay fungi by entering through wounds in the tree. These wounds can be broken branch stubs, old cankers, entry or exit holes from boring insects, weather damage, etc. Balandaykin & Zmitrovich (2015) observed that anthropogenic disturbance increases the incidence of the sterile conk in stands of birch. Brydon-Williams *et al*. (2021) surveyed 2611 birch trees from 2017-2018 in the White Mountain National Forest in New Hampshire, USA and determined that there is a positive correlation between sterile conk presence and birch tree age, DBH, and site elevation. Through this survey, a low incidence of sterile conk was observed at only 2% of the birch trees observed. Kuz'michev *et al.* (2001) reported sterile conk incidence to vary widely from 1-20% on birch in Russian forests. Generally, infection of *I. obliquus* will occur in the middle to lower trunk but can begin infection in any area where wounds have occurred at approximately 4.5m (Brydon-Williams, 2019). Upon germination of basidiospores within the host tree, this fungus inflicts a white rot type of decay in the heartwood and colonizes the sapwood in areas where the sterile conk erupts through the bark (Lee *et al*, 2008; Blanchette, 1982). Sterile conk formation will typically occur one to two years following infection from basidiospores forming only on the main stem and not on branches (Pilz, 2004). *Inonotus obliquus* is a stress-tolerant primary colonizer of living birch trees and does not require a pre-decomposed substrate. This fungus infects the host tree for approximately 10-80 years and only forms sterile conks whilst the tree is still alive (Shigo, 1965; Černý, 1976; Gilbertson & Ryvarden, 1986; Bunyard, 2015). These conks typically form at or near the site of initial infection and generally form on trees aged 30 years or older (Campbell & Davidson 1938; Balandaykin & Zmitrovich, 2015). Shigo (1969) examined how these conks are incited and reported that a wedge of mycelium is pushed into the outer bark. As a result, immense pressure is built up which splits bark and kills cambial tissue. Throughout the infection time, trees can produce from one to six sterile conks throughout the life of the tree (Sinclair & Lyon*,* 2005). These sterile conks can reach masses of three to five kg after initial formation and have been reported to achieve a weight of up to sixteen kg (Sinadskij 1973; Gammerman *et al.* 1975). Bark surrounding the sterile conk is swollen due to increased wood production and thickened bark. A high proportion of sterile conks generally indicates that an extensive decay column has formed. While the ecological purpose of these sterile conks is unknown, what is certain is that *I. obliquus* spends a substantial amount of energy during its life to produce them. A theory for its production will be elaborated in the following section, as context of the fruiting body is required.

As the infection begins to spread, the tree will respond with defence mechanisms in an attempt to contain decay as described in the extensive work of forester and pathologist Al Shigo, who coined the phenomenon CODIT (Compartmentalization of Decay in Trees) (Shigo, 1984). Mechanical and chemical barriers will be produced in an attempt to inhibit the further spread of decay and compartmentalize it. These barriers are observed as discoloured wood surrounding areas of existing decay. Blanchette (1982) completed an in-depth study examining how the decay of *I. obliquus* progresses. The decay of *I. obliquus* associated with sterile conks on the living stems of birch is observed as large, nested columns of white-rotted wood delimited by old barrier zones of discoloured wood. In most cases, wood-colonizing fungi require significant time and the succession of other microorganisms to ameliorate the environment of discoloured barrier zones for colonization (Shigo, 1969). *Inonotus obliquus* does not require this successional stage and is able to break down internal compartments produced by the tree. The fungus continually reinvades the tree and attacks recently formed cells. Occlusions of vessel and parenchyma tissue can be both colonized and destroyed by *I. obliquus*. The mosaic appearance of decay is caused by the repeated formation of discoloured barrier zones and their colonization. However, extensively plugged tissues are colonized at a slower rate, thus decay is still slowed in some regions. Decay columns can grow quite extensively and elongate as much as 35.56 cm annually (Pilz, 2004). The work of Blanchette (1982) considered *I. obliquus* an exception to the rules of CODIT as it has developed means to evade and overcome host tree defence mechanisms. It is not entirely known if *I. obliquus* is the sole reason for tree mortality from canker girdling or if other opportunistic pathogens are responsible in the later stages of decay (Pilz, 2004; Brydon-Williams, 2019). Colonized sapwood at the point of sterile conk formation predisposes the host tree to windthrow (Gilbertson & Ryvarden, 1986)

The Basidioma, Life Cycle, and Dispersal

Life cycle

The basidioma of *I. obliquus* is a resupinate poroid hymenium that forms from mid-summer to late autumn beneath the bark of recently deceased host trees (Bunyard, 2015) (see above for description). Cha *et al* (2011) and Zabel (1947) reported occurrences of the structure on living birch and beech, but this is very rare. The bark is ruptured and cracked open as basidiomata develop. Lõhmus & Lõhmus (2024) reported this as an important mechanism for bark removal on dead standing birch trees in Estonia, creating habitat for a multitude of species of fungi, lichens, and others (Figure 1-6). It is quite unusual for basidiomycetous fungi to form fruiting bodies beneath the bark of host trees and has only been reported to occur in *Inonotus andersonii* (Ellis & Everh.) Nikol. (Millman, 2012).

Figure 1-6. Example of habitat in *I. obliquus* ruptured bark post-sporulation. (a) the creation of microhabitat in ruptured bark – red circle shows wildlife in bark rupture. (b) slugs and snails feeding/living in enclosed bark rupture habitat on old fragments of basidiomata. Terrace Bay, Ontario. Source: Researcher

In formal literature, *I. obliquus* is reported to form its fruit body once in an infection cycle or a life cycle (Campbell & Davidson, 1938; Gilbertson & Ryvarden, 1986; Pietka & Grywacz, 2006; Bunyard, 2015). Pringle & Taylor (2002) describe fungi that reproduce once in their life as being **semelparous**, while those that reproduce multiple times in their life are described as being **iteroparous.** By this definition, *I. obliquus* follows a semelparous life cycle. However, semelparous fungi are known to complete fast life cycles of only a few days due to the exhaustion of ephemeral food sources; coprophilous (dung-loving) fungi such as *Coprinus* Pers. are an example of this. On the contrary, *I. obliquus*, while semelparous, can have an incredibly long life cycle of multiple decades (10 – 80 years); thus does not follow the typical definition of short-lived semelparous fungi (Shigo, 1965; Černý, 1976; Pringle & Taylor, 2002). In some ways, this strategy of reproduction is more akin to the semelparous life cycle of species of *Agave* L., where a single massive inflorescence (1 – 5 m tall) takes place following long periods of vegetative growth (Arizaga & Ezcurra, 1995).

Inonotus obliquus will sporulate following host tree death, where defence mechanisms of decay are inactive, and any vegetative fungal growth in the host is saprotrophic (not parasitic). It is unknown if sporulation following death is ultimately triggered by depletion of resources during a saprotrophic stage or if other mechanisms are at play. It is generally stated that trees infected with *I. obliquus* can sustain the infection for 10 - 80 years before death, but this figure is likely not the full range of life cycle length. Life cycle length is determined by maximum tree age and host longevity under the pressures of *I. obliquus* colonization. The maximum tree age and longevity of a host tree are controlled by factors such as historical land use and past forest management; initial and current forest conditions; stand dynamics; soil, site, topography, and environmental conditions; biological stressors and disturbance regimes; weather/climate; genetics; and taxa (Hayek, 2019). In decay patterns of *I. obliquus*, the rot is typically restricted to the heartwood but can colonize sapwood at areas where the sterile conks or cankers form (Blanchette, 1982). Therefore, the sapwood and cambium are largely unaffected by decay where sterile conks are not produced, indicating that trees infected with *I. obliquus* can continue growing without a major reduction in cambium ability. As such, colonies of *I. obliquus* have the capability to continue rotting heartwood in relatively healthy trees for long periods of time before host death and semelparous sporulation.

The common host in the Thunder Bay region is *Betula papyrifera* Marshall, and has a longevity range of roughly 80 - 100 years (average 100 years), and maximum age range of 100 - 240 years (average 140) (Hayek, 2019). *Betula alleghaniensis* Britt. is the most commonly harvested host of chaga in North America, where sterile conks become much larger (personal communication with Cody Mcelrea of TruNorthNaturels in Northern-Ontario, and Garrett Kope of Birch Boys in USA). *Betula alleghaniensis* has a longevity range of 150-200 years (average 150), and a maximum age range of 309 – 387 years (average 300) (Hayek, 2019). These longevity and maximum age ranges and decay patterns indicate that *I. obliquus* can potentially have life cycles of well over 100 years in ideal conditions. This has serious implications for the conservation and management of this long-lived species in old-growth forests.

Now, how does the sterile conk fit into this unusual life cycle? At the moment, the most reasonable working theory is that it may be a storage sink of nutrients for growth and sporulation (Bunyard, 2015). This seems likely and will be elaborated upon, as well as additional theories provided.

As *I. obliquus* has a long-lived semelparous lifestyle, it is very likely that sterile conks are formed in preparation for its single sporulation event. From personal interactions with a wild basidioma, they produce an incredible amount of basidiospores, where their release can be viewed with the naked eye. The basidioma almost appears to release “smoke”. For this to occur, a high proportion of nutrients must be reallocated to fruit body formation and basidiospore production for this rare and crucial moment of sexual reproduction. Herman *et al.* (2020) showed that *Agaricus bisporus* (J.E. Lange) Imbach reallocates nutrients from older portions of hyphae to the young periphery of colonies, and switches allocation from this periphery to developing fruit bodies, where the production of nutrient-dense basidiospores takes place. Therefore, it is highly likely that the sterile conk is an external long-term storage structure for nutrients extracted from the decay of heartwood. In a life strategy like this one, it seems reasonable to create melanized resistant nutrient sinks which can stand the test of time and be utilized at the end of life for semelparous sporulation. Additionally, suitable Chaga is only harvested from living trees and is decayed and rotten on dead ones, indicating the sterile conks are depleted of nutrients after host death. As *Inonotus obliquus* is monomitic (i.e. does not produce skeletal hyphae), the corky interior of these structures is likely composed of modified setal hyphae as stated by Rivoire (2020). Sterile conk fragments can produce viable cultures of *I. obliquus*, elucidating that perhaps they may act as intermediary asexual propagules via mycophagy following the removal of the melanized exterior, where the corky, more supple, and nutrient-dense interior is exposed to insects (or birds/small mammals) and spread, but this is purely speculation. The infrequent sporulation of this species raises questions regarding gene flow and the genetics of populations.

Basidiospore dispersal

Once the basidiomata of *I. obliquus* are formed, they are quickly deteriorated by mycophagous insects and weathering (Gilbertson & Ryvarden, 1986). Adults and larvae of beetles belonging to the family Melandryidae were observed by Bunyard (2015) in September 2013 to be feeding on the rare and inconspicuous basidiomata of *Inonotus obliquus* appearing on a recently dead *Betula populifolia* Marsh. in New Hampshire, USA (Figure 1-7). Bunyard was the first to identify one of the insects responsible for mycophagy of the basidioma of *Inonotus obliquus* in North America. The beetles and larvae were observed to be *Orchesia cultriformis* Laliberté in the tribe Orchesiini. Twenty-three specimens were collected from the basidioma of *I. obliquus* over several days and stored in 95% ethanol. Upon dissection of their gut contents, they were found to be full of spores and basidioma tissue of *I. obliquus*. Genera in this tribe are generally considered mycophagous, thus playing an important role in spore dispersal of polyporoid fungi (Leschen 1990; Pollock 2002). Shiegel (2011) determined that in Finland, fruit bodies of *I. obliquus* are associated with mycophagous beetles and the commonest species collected was *Orchesia micans* Panzer. The beetle genus *Orchesia* seems to be implicated in the life cycle of *I. obliquus*. The fruit bodies are usually observed as nothing more than an unrecognizable assemblage of rough pores and beetle frass (Bondarstev, 1953).

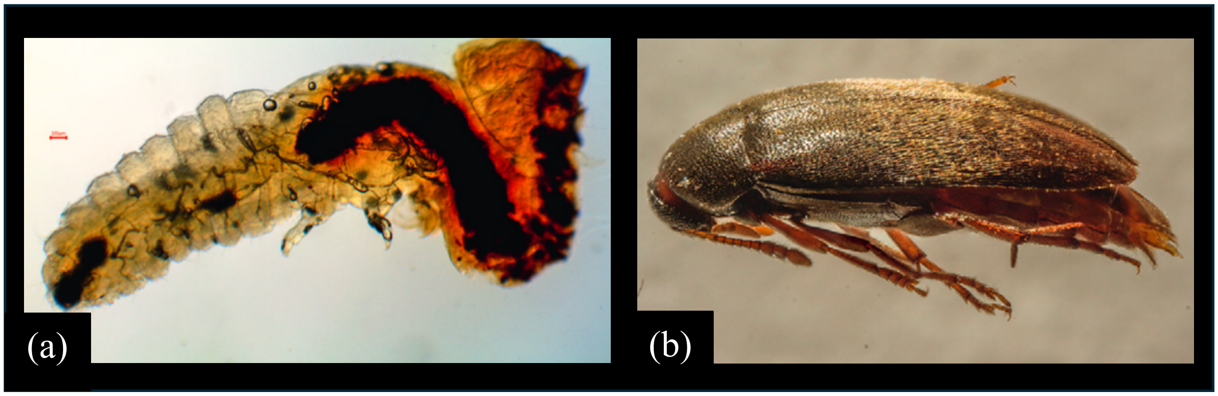

Figure 1-7. *Orchesia cultriformis* Laliberté found associated with basidiomata of *I. obliquus*. (a) larval form eating basidiomata. (b) adult form. Source: Bunyard (2015)

CHAGA IN MEDICINE

The sterile conk of *Inonotus obliquus is* regarded by many as the king of medicinal mushrooms. In recent years, a plethora of papers have been published on Chaga's medicinal use and health benefits. *Inonotus obliquus* is one of the most intensively researched medicinal mushrooms. The vast majority of research done on *I. obliquus* is with regard to the medicinal effects of secondary metabolites, therefore, it is important that some of these effects are reviewed. This is not the main focus of this document; thus, these examples only represent a portion of the researched medicinal effects.

A Summary of Medicinal Benefits

Anti-cancer

Approximately 700 species of medicinal mushrooms have been observed to inhibit the growth and development of a variety of cancers (Lemieszek *et al.* 2011). Of the medicinal benefits provided by the secondary metabolites of *I. obliquus*, the anti-cancer effects seem to be the most well-researched. Extracts from the sterile conk and cultivated hyphae of *I. obliquus* have been shown to significantly impact the growth and development of tumours both *in vivo* and *in vitro*. Kim *et* *al.* (2006) examined the *in vivo* and *in vitro* effects of endo-polysaccharides extracted from cultivated *I. obliquus* mycelium produced via submerged cultivation. Mice were inoculated with B16F10 melanoma cells and when treated with endo-polysaccharides, all mice demonstrated a prolonged survival rate in a dose-dependent manner. Tumour tissue was not observed whatsoever in mice which survived over 60 days. The cytotoxicity of mycelial endo-polysaccharides on cancer cell lines *in vitro* were analyzed. Even at high levels, endo-polysaccharide treatment was not cytotoxic to cancer cells. These observations by Kim *et al.* (2006) indicate that endo-polysaccharides produced from submerged fermentation activate the macrophage function of mouse immunocytes rather than having a direct effect on tumour growth. The immune-modulating effects of *I. obliquus* mycelial extracts impacting tumour development have also been observed by Kim *et al.* (2005). Lemieszek *et al.* 2011 examined how fraction IO4 isolated from the wild sterile conks of *I. obliquus* affect the proliferation, motility and viability of a variety of cancer cells *in vitro*. Human lung carcinoma (A549), colon adenocarcinoma (HT-29), and rat glioma (C6) cell cultures were analyzed. Fraction IO4 caused decreased tumour cell proliferation and motility and was found to not be toxic to normal cells.

Anti-viral

Extracts from the Chaga fungus have been observed to act deleteriously on biological mechanisms of a suite of viruses. Ichimura *et al.* (1999) reported that aqueous extracts of *I. obliquus* have an inhibitory effect against the protease of HIV-1. The water-soluble compound was identified as a lignin derivative with high molecular weight. This compound was observed to inhibit the propagation of HIV by effecting HIV reverse transcriptase. Recently, the potential of *I. obliquus* extracts to inhibit SARS-CoV-2 has been examined and has displayed promising results. A molecular docking study was completed by Basal *et al.* (2021) on how terpenoids from *I. obliquus* affect the SARS-CoV-2 virus. It was observed that many of the terpenoids interact with the receptor-binding domain of SARS-Cov2- spike glycoprotein with high affinity and thus may interfere with spike protein recognition of the host cell. Teplykova *et al.* (2022) observed that water extracts from *I. obliquus* inhibit the replication of SARS-CoV-2 in Vero E6 cells. Finally, Shibnev *et al.* (2011) examined the effect of aqueous extracts of *I. obliquus* on porcine embryo kidney cells infected with hepatitis C and they reduced the infective properties of the virus by 100 times.

Anti-diabetic

Polysaccharide extracts from both the sterile conk and liquid-fermented mycelia have shown hypoglycemic action in diabetic mice and rats (Chen *et al.* 2006; Wang *et al.* 2017; Cha *et al.* 2005).

The literature shows *I. obliquus* extracts have a significant effect on a variety of diseases; however, the majority of these studies were carried out *in vitro* and only *in vivo* within mice. For further development of Chaga as a commonplace drug, more research should be completed on producing drugs with specific actions from Chaga extracts and human testing of these drugs.

CHAGA AS A RESOURCE

Conservation

It is without a doubt that Chaga has attracted mass popularity among both consumers and the scientific community because of its reported medicinal benefits. In the last ten years, Google Trend analysis that the search term “Chaga” has increased by four times from 2009 to 2019 (Thomas *et* *al*, 2020) There have been a large number of products released to the consumer market made from the sterile conk itself or from fermented mycelia in the form of capsules, teas, and tinctures. Due to the rising interest in functional mushrooms and their wild harvest, the industry has caused a considerable ecological impact on other medicinally important mushrooms such as *Cordyceps* (Stone, 2015). In the paper titled *Chaga (Inonotus obliquus): A Medical Marvel but a Conservation Dilemma by* Thomas *et al* (2020), issues of the conservation and sustainability of Chaga as a resource are provided. There is minimal understanding of the ecological role of the sterile conk in the life cycle of *I. obliquus*. Collectors of this resource do not have a concept of the severity of the environmental impact caused by mass harvesting. More surveys must be completed with regard to sterile conk ecology as the popularity of Chaga rises to understand its resource potential, and more research must be completed regarding the true nature of the sterile conk. A better understanding of the ecology of Chaga will lead to the development of better management practices and harvest dynamics. Until then, a best practice for harvesting is to leave 30% to 50% of the sterile structure behind. Additionally, the sterile conk does regrow (Pilz, 2004). If the sterile conk is a storage sink of nutrients for semelparous sporulation, its removal will likely not impact the initiation of basidiomata after host death; however, such removal could greatly impact the size of basidiomata, host post-mortem bark removal capability, and the number of basidiospores released. As fruiting is rare, this reduction in fruiting capacity could have serious implications for basidiospore dispersal, population dynamics, and ecology of insects and fungi associated with the basidiomata and their substrate (Bunyard, 2015; Lõhmus & Lõhmus, 2024).

Harvest, exportation, and use of Chaga is very common in Russia. Martinmäki (2022) reports that Russia is the largest world producer of Chaga products of which the majority are exported to Asian countries. Pilz (2004) examined the sustainability of commercial Chaga harvest in Russia and found that significant harvesting pressure was observed. Brydon-Williams *et al*. (2021) completed a study examining the ecology, incidence, and harvest dynamics of Chaga in the White Mountain National Forest (WMNF) in New Hampshire, USA. A primary objective of the study was to determine if a special use permit should be required for the harvest of Chaga. Of the 2611 birch trees surveyed, only one displayed signs of prior harvest. At the time of the 2019 study, there was no large-quantity Chaga harvest occurring in the White Mountain National Forest. It was determined that there was very little risk of the exhaustion of Chaga as a forest resource, therefore, the development of Chaga harvesting permits was determined to be unnecessary. In the future, surveys must be completed to quantify the resource. Chaga is relatively scarce in the WMNF, and thus adds little value to harvest sites. With the 2017 value of Chaga estimated at $50 USD per pound by Carpenter *et al.* (2017), the Chaga surveyed in this project would only amount to $861 USD.

It is clear that there is a significant difference between scarcity of Chaga in North America and Russia. This may be due to Chaga being integrated significantly more into the culture of Russia and other European countries than in North America. Chaga was last surveyed in Russia in 2004 by Pilz (2004), thus more surveys are required. Also, there have been no surveys of Chaga in Canadian boreal forests and only a handful in the USA.

Cultivation

To date, only wild-harvested Chaga has been used for commercial use (Miina *et al*. 2021). Sterile conks typically amass harvestable size after 3-5 years and can be reharvested 3-10 years later from the same discrete infection area until the tree has died (Pilz, 2004). Due to the slow-growing nature of Chaga and the ever-increasing demand for its metabolites, many attempts have been made to cultivate mycelium of *I. obliquus* in large liquid fermentation bio-reactors (Kim *et al.* 2006; Bai *et al.* 2012; Chen *et al.* 2020) However, while cultivated mycelium does contain many of the important compounds found in the sterile conk, these compounds are chemically diverse, behave differently in medical experiments, and are often considered to be inferior to that isolated from the sterile conk (Kukulyanskaya *et al.* 2002; Zheng *et al.* 2010). These findings suggest that the superior form of *I. obliquus* is the sterile conk or Chaga. The scientific community has recognized that a means for consistently and successfully cultivating sterile conks to fulfill increasing demand and offset the ecological impacts of harvesting wild Chaga must be developed. A suite of researchers have examined the cultivation of Chaga on live birch:

Pietka & Grzywacz (2006) were one of the first to inoculate live birch stems with the mycelium of *I. obliquus* in an attempt to cultivate the sterile conk; however, they were unsuccessful potentially due to other unidentified basidiomycetous fungi. Ka *et al.* (2017) were able to successfully cultivate sterile conks on live *Betula platyphylla* var. *japonica* Sukaczev. Trees were initially inoculated by inserting saw dust spawn of *I. obliquus.* Trees were monitored over nine years for sterile conk formation. Conks grew approximately one cm per year and the largest “clinker” grew to a diameter of nine cm over the nine years of study. It was observed that birch trees of a larger diameter would facilitate the development of larger sterile conks. Park *et al.* (2010) were also successful in cultivating the sterile conk on live birch. Recently, companies in Finland have attempted to encourage forest owners to cultivate Chaga as a means to significantly increase forest value per hectare (Vanhanen *et al.* 2013; Martinmäki, 2022). Miina *et al.* (2021) examined the success of large-scale *I. obliquus* inoculations of birch stands in Finland. 679 birch trees across 24 stands were inoculated with *I. obliquus* mycelium. After 4-5 years, inoculation success varied widely from 53-100% across all stands. Approximately 79 ± 13% of trees showed signs of infection (bark bulging, bleeding, sterile conk formation) and approximately 6 ± 15% of trees bore one or more sterile conks (Figure 1-8). They concluded that the rate of development of cultivated sterile conks was much slower than anticipated; thus, it may be difficult to integrate the management of this resource in intensively managed stands of birch. However, sterile conk cultivation could increase the value of low-productivity birch stands.

At this point in time, Chaga cultivation seems to be much better suited to countries like Finland, where the resource is in high regard and forest areas are much smaller. Contrarily, forest areas in North America are much vaster and Chaga does not seem to be nearly as culturally important. However, with the steady rise of its popularity, this may change. If the cultivation of Chaga in Finland proves successful as a means to increase stand value per hectare over the next decade, these techniques could be transferred over to North America where there are a plethora of low-productivity birch stands. It is important to tread lightly with Chaga cultivation, as we are unaware of how the introduction of an aggressive fungal pathogen may affect the ecology of birch stands. (Thomas *et al.* 2020).

Figure 1-8. Bulging bark of *I. obliquus* inoculated birch. Source: Miina *et al.* (2021)

MATING IN AGARICOMYCETES

"Sexual reproduction implies the succession of haploid and diploid phases, transitions occurring by meiosis, where recombination and chromosomal segregation occur, and syngamy, where two haploids fuse" - Billiard *et al.* (2012). In mammals, sexual reproduction is anisogamous, whereby the fusion of compatible haploid gametes (syngamy) is regulated by their size differentiation: a large gamete (eggs produced by females) and a small gamete (sperm produced by males) (Billiard *et al.* 2012). This system is elegant, simple to comprehend, and is what comes to mind when most think of sexual reproduction in eukaryotes. This is a binary sex system, with clear distinctions between male and female, not only in their gametes, but also in their macromorphology.

In Agaricomycetes, this system is completely different, where the compatibility of haploid mating partners is not regulated by gamete morphology, but instead by small variations in mating loci that are termed **mating types (***MAT* loci). In the model agaricomycete *Schizophyllum commune* Fr., made "famous" by the crucial work of John Raper and colleagues on the sexuality of the higher fungi, it has been found to possess over **20,000** possible mating types (Fraser *et al.* 2007). In fungi, there are three main classes of **mating systems**: **heterothallism**, **homothallism**, and **pseudohomothallism.**

By broad definitions, **heterothallic** fungi require the cellular fusion and nuclear exchange of two genetically unique compatible mating partners for sexual reproduction. **Homothallic** fungi, which are self-fertile, do not require a mating partner for sexual reproduction. **Pseudohomothallic** fungi incorporate two meiotic nuclei of compatible mating type into a single basidiospore, which, upon germination, form a fertile mycelium that does not require a partner for sexual reproduction. As a result, pseudohomothallic fungi have reduced outcrossing (Kües *et al.* 2011). Whitehouse (1949) examined approximately 230 species of basidiomycetes and found that 90% displayed patterns of heterothallism while only 10% displayed patterns of homothallism.

Heterothallism in Agaricomycetes

This summary will go over the basic mushroom life cycle and generally be without embedded citations (Figure 1-9). This information can be found in introductory mycology textbooks such as Alexopoulos (1952).

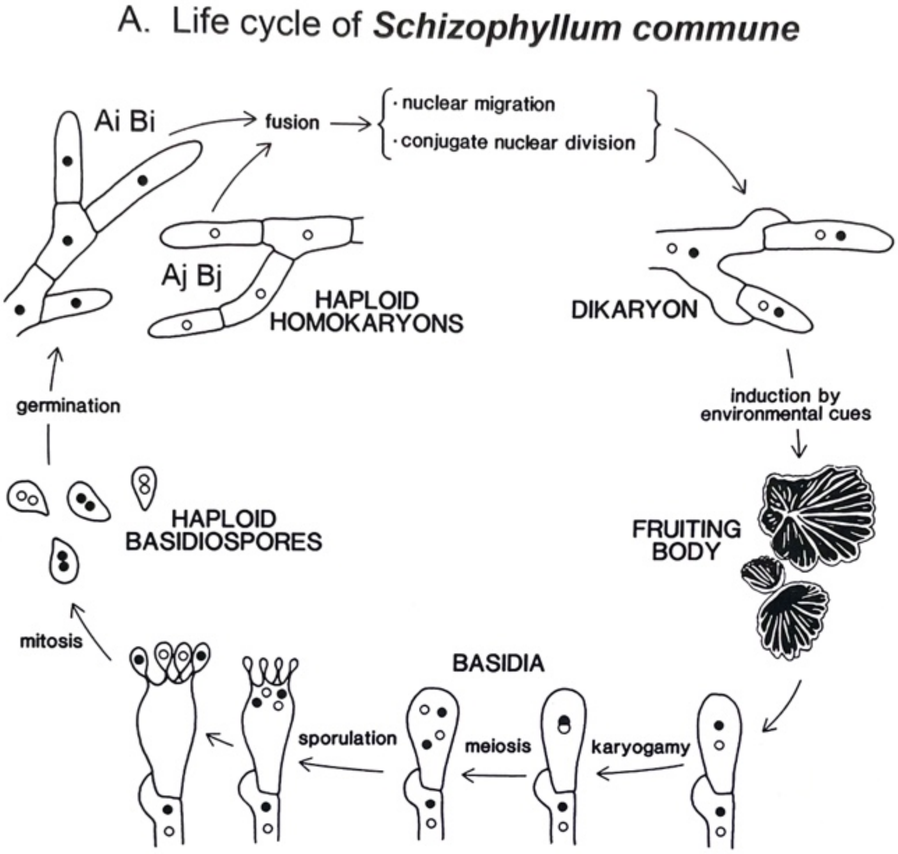

Figure 1-9. Basic mushroom life cycle in *Schizophyllum commune.*
Source: Stankis & Specht (2007)

In a broad sense, when a basidiospore lands in an environment of favourable condition, it germinates, forming a self-sterile haploid monokaryon (n), which possesses only half of the full genome. In textbook monokaryons, they contain a single haploid nucleus per hyphal cell. For sexual reproduction to occur, the monokaryon must come into contact with another monokaryon of compatible mating type. Compatible hyphae will fuse and exchange genetic material to form a dikaryon (n + n). In a textbook dikaryon, they contain two haploid nuclei per hyphal cell. The dikaryotic mycelium spends the majority of its life growing in a state that is not diploid, but can be viewed as being functionally diploid, whereby the other half of the genome is present in the same cell, but nuclear fusion (karyogamy) and meiosis do not take place immediately following exchange. Instead, the two genetically distinct nuclei divide in conjugation as the hypha expands from its tip. In most agaricomycetes, the dikaryon is associated with the formation of **clamp connections** or hook cells at each septum, which from a classical standpoint, ensure the equal segregation of daughter nuclei as they divide in conjugation. Currently, a proposed theory for clamp formation in the Basidiomycota is to check nuclear quality during somatic growth by briefly monokaryotizing dikaryotic hyphae during clamp cell formation, and continuously checking for fusion compatibility (Aanen *et al.* 2023).

These clamps can be easily viewed with a light microscope, which has made studying mating and compatibility in agaricomycetes with this character simple, whereas taxa that are clampless in a dikaryotic state (Hymenochaetaceae) are more problematic. In the dikaryon of Agaricomycetes, karyogamy, meiosis, and segregation of daughter nuclei only takes place in basidia, the basidiospore-producing structures. Agaricomycetes are only truly diploid (2n) for a brief moment during karyogamy in basidia. Following karyogamy and meiosis I and II, the four daughter nuclei migrate into one of the four sterigma and subsequently into one of the four developing basidiospores. In turn, the basidiospores are haploid and typically mononucleate. Once mature, the basidiospores are ejected from the sterigmata, and if they land in a favourable substrate, germinate to form a monokaryon, continuing the cycle.

Bipolar and tetrapolar heterothallism

While there exists an incredible amount of diversity in the exact function of heterothallism in Agaricomycetes, there are two basal paradigms: **bipolar heterothallism** and **tetrapolar heterothallism** (Fraser & Heitman, 2003). In bipolar Agaricomycetes, meiotic segregation results in basidiospores that are one of two mating types: A and B (or a and α). In this system, only a single locus is responsible for mating compatibility (Fraser *et al.* 2007). A compatible reaction occurs when monokaryotic partners are of opposite mating type at this locus, which results in the production of fertile dikaryotic mycelium. Half of all interactions (50%) of monokaryons from the same fruiting body will be compatible in bipolar fungi. While this system does exist in Agaricomycetes, it is much more common in the Ascomycota (Fraser *et al.* 2007). Tetrapolar heterothallism is the dominant system in Agaricomycetes (approximately 50 – 65%), where meiotic segregation results in basidiospores that are one of four mating types (i.e. A_1B_1, A_1B_2, A_2B_1, and A_2B_2) and compatibility is controlled by two unlinked loci (Fraser *et al.* 2007). A fully compatible reaction occurs when monokaryotic partners differ at both loci (Kothe, 1995). Raper (1965) proposed that the tetrapolar system is an ancestral form of the bipolar system, which is now supported by molecular evidence in *Coprinellus disseminates* (Pers.) Lange and *Pholiota nameko* (Berk.) Sacc. (Fraser *et al.* 2007). In bipolar agaricomycetes, the mating function of the B locus is typically lost (Coelho *et al.* 2017; Wang *et al.* 2023). The tetrapolar system promotes an incredible amount of genetic uncrossing, whereby only a quarter of reactions between monokaryons of the same fruiting body will be compatible. This review will focus on the genetic mechanisms of tetrapolar heterothallism in Agaricomycetes.

Mating Mechanisms and Compatibility in Tetrapolar Heterothallism

Compatibility and function of A and B *MAT* loci

Compatibility and phenotypic function

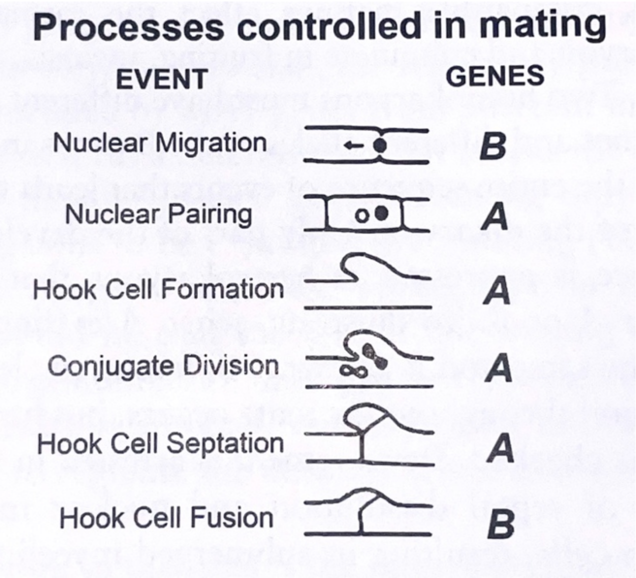

Figure 1-10. Functions of A and B *MAT* alleles in clamped Agaricomycetes. Source: Stankis & Specht (2007)

As stated above, tetrapolar heterothallism is controlled by two unlinked *MAT* loci: A and B; each serves unique and crucial roles in the mating process. Unlinked loci are those that exist in different portions of the genome (Heitman *et al.* 2007). Compatible mating of two monokaryons requires that they possess unlike loci at both the A and B mating factors. For example, monokaryon A_1B_1 is compatible with monokaryon A_2B_2 because they carry different alleles at both the A and B mating locus, resulting in a fertile dikaryon with clamp connections (Monokaryons: (A_1B_1) (n) + (A_2B_2) (n) = Fertile dikaryon: (A_1B_1 + A_2B_2) (n + n)). The A and B factors control different functions during dikaryon development; thus, their incompatibility results in various micro and macroscopic reactions. Stankis & Specht (2007) summarize the general functions of these factors: the A *MAT* locus controls nuclear pairing, clamp cell initiation, conjugate nuclear division, and clamp cell septation (Figure 1-10). The B *MAT* locus controls nuclear migration and clamp cell fusion (Figure 1-10). Other than a fully compatible reaction, where A and B factors are different ($A_1B_1 + A_2B_2$), there are intermediate reactions termed the pseudoclamp or "barrage" reaction, where A loci are different but B loci are the same ($A_1\mathbf{B_2} + A_2\mathbf{B_2}$), the "flat" reaction, where A loci are the same and B loci are different ($\mathbf{A_2}B_1 + \mathbf{A_2}B_2$), and completely incompatible reaction where both A and B loci are the same ($\mathbf{A_2B_2} + \mathbf{A_2B_2}$) (Kothe, 1995).

Genetic function

The A and B loci utilize a dual "lock and key" system of sexual compatibility that is complex but incredibly elegant. The A locus controls compatibility through the production of homeodomain proteins (HD1/HD2), where the heterodimerization of compatible proteins is required (Kothe, 1995; Fraser *et al.* 2007). In a general sense, each A sublocus ($A\alpha$ and $A\beta$) produces pairs of HD1 and HD2 proteins (Fraser *et al.* 2007). In an A-locus reaction between two monokaryons both possessing compatible homeodomain protein pairs at their A subloci: HD1 ($A\alpha1$) will heterodimerize with HD2 ($A\alpha2$), and HD2 ($A\alpha1$) will heterodimerize with HD1 ($A\alpha2$) to form a protein complex (heterodimer). But if the A loci are not compatible (alike), no heterodimerization will occur between homeodomain proteins, and mating will not occur (Fraser *et al.* 2007; Kothe, 1995).

The B locus controls compatibility through a pheromone-sensing/production system whereby genes encode G protein-coupled receptors, and separate genes encode small lipopeptide pheromones that require significant post-translational modification. (Horn *et al.* 2003; Fraser *et al.* 2007). When B loci are different, they encode unique pheromone receptors and pheromones precursors that allow hyphal fusion and sexual development, but do not if they are the same. In the model, *Ustilago maydis* (DC.) Corda pheromone production and reception are an extracellular check for sexual compatibility before cell fusion, followed by the intracellular homeodomain protein heterodimer system (Fraser *et al.* 2007). In the model Agaricomycetes *Schizophyllum commune* and *Coprinopsis cinerea* (Schaeff.) Redhead, Vilgalys & Moncalvo, however, they practice promiscuous hyphal fusion regardless of pheromone signature, where nuclear mating type is only important post-fusion and the B locus is primarily responsible for dikaryon maintenance and basidiomata formation (Casselton & Olesnicky, 1998; Fraser *et al.* 2007). The dispensed extracellular pheromone system in Agaricomycetes bypasses the first mating compatibility check and allows free and efficient monokaryon fusion. As the B locus controls nuclear migration within the thallus, incompatible nuclei are restricted to the interaction zone.

Homothallism in Agaricomycetes

In a broad sense, homothallism is the ability for colonies arising from a single spore to reproduce sexually in complete isolation. This is the historical definition provided by Blakeslee (1904). Over the last 100 years of fungal mating, homothallism *sensu* Blakeslee (1904) has been found to be caused by a wide array of unique mechanisms such as **primary homothallism**, **mating type switching**, **unisexual reproduction**, **monokaryotic fruiting**, and **pseudohomothallism** (Lin & Heitman, 2007; Wilson *et al.* 2015). Currently, a combination of molecular, cytological, and phenotypic variation is utilized to differentiate between these systems.

Primary homothallism *sensu stricto*

Primary homothallism is the modern term to describe a specific system of homothallism where sexual reproduction occurs in a haploid monokaryon that contains a full complement of active *MAT* genes (Lin & Heitman, 2007; Wilson *et al.* 2015). In heterothallic fungi, a monokaryon typically only holds one set of *MAT* genes and requires the fusion of another compatible monokaryon to form a full set of heteroallelic *MAT* genes for sexual reproduction. A primarily homothallic fungus has all the genes required for sexual reproduction in a single thallus and does not need a mate. David-Palma *et al.* (2016) described primary homothallism *sensu stricto* in the basidiomyceteous yeast *Phaffia rhodozyma* Mill. Yoneyama & Soneda*,* where all molecular components for sexual reproduction existed in a single haploid genome, insinuating primary homothallism *sensu stricto*.

Unisexual Reproduction

Unisexual reproduction is a relatively newly described system of homothallism in haploid monokaryotic basidiomycetes where only one set of *MAT* genes is required for sexual reproduction (Wilson *et al.* 2015). This concept was elucidated in the model basidiomyceteous yeast *Cryptococcus neoformans* (San Felice) Vuill. (Lin *et al.* 2005). In haploid monokaryons, basidia form, where meiosis takes place, followed subsequently by basidiospore formation, which all possess the same mating type (Lin *et al.* 2005). The only well-documented case of unisexuality in Agaricomycetes is demonstrated in the invasive California death cap *Amanita phalloides* Link (Wang *et al.* 2023). Basidiomata in California, USA were found to be heterokaryotic and homokaryotic. *Amanita phalloides* was discovered to be bipolar heterothallic, where sexual compatibility is controlled by a single mating type locus. This agaric can reproduce unisexually, *sensu Cryptococcus neoformans,* and form homokaryotic fruit bodies through the germination of haploid homokaryotic basidiospores that form basidia, where haploid nuclei likely endoduplicate.

Mating Type Switching

Mating type switching was a phenomenon first described in the model ascomyceteous yeast *Saccharomyces cerevisiae* (Desm.) Meyen ex E.C. Hans. (Lin & Heitman, 2007). The molecular basis for mating type switching was described by Herskowitz & Oshima (1981), where silent copies of the alternative *MAT* locus are stored as silent cassettes such that only a single mating type is expressed at a given time (Lin & Heitman, 2007). In Agaricomycetes, mating type switching has been described in the predominantly tetrapolar heterothallic *Agrocybe aegerita* (V. Briganti) Singer (Labarère & Noel, 1992). In this system, haploid monokaryotic basidiospores germinate and give rise to a homokaryotic mycelium, which quickly dikaryotizes. This is caused by certain nuclei in the homokaryon expressing alternate A and B mating types; thus, dikaryon formation, basidium formation, karyogamy, meiosis, and sporulation occur (Labarère & Noel, 1992). They hypothesize that silent copies of mating type genes are stored in the genome of *A. aegerita*, analogous to silent cassettes in *S. cerevisiae*.

Monokaryotic/Homokaryotic Fruiting

Monokaryotic fruiting occurs when haploid basidiospores give rise to a monokaryotic mycelium that spontaneously forms sexual fruit bodies without evidence of dikaryotization as found in heterothallic species (Lin & Heitman, 2007). Often, homokaryotic fruiting bodies are associated with morphologically diverse fruit bodies that are different from heterokaryotic fruit bodies, where macroscopic characteristics such as suppressed gills and elongated stipes occur, as well as microscopic characters such as variation in the number of basidiospores per basidium (Esser *et al.* 1979; Labarère & Noel, 1992; Elders & Hennicke, 2021). Labarère & Noel (1992) and Elders & Hennicke (2021) described two varieties of homokaryotic fruiting in *Agrocybe aegerita* (syn. *Cyclocybe aegerita* (V. Brig.) Vizz.) and *Cyclocybe parasitica* (G. Stev.) Vizz., respectively. First, they displayed true homokaryotic fruiting (THF), where fruiting bodies formed two-spored basidia that are predicted to possess uninucleate mitotic basidiospores. Second, abortive homokaryotic fruiting (AHF) was displayed, where fruitbodies showed partially or completely suppressed gill formation and did not produce any basidiospores.

Pseudohomothallism

Physiologically, pseudohomothallism (secondary homothallism) functions identically to homothallism *sensu* Blakeslee (1904): single-spored colonies can be self-fertile and complete sexual reproduction. However, this system is functionally completely different from any of the homothallic systems described above. In this case, self-fertility of single-spored colonies is caused by the packaging of two mating-compatible meiotic nuclei into a single spore during meiosporangial (basidial) development, such that the resulting colonies are immediately di/heterokaryotic (Elliott & Challen, 1983; Lin & Heitman, 2007; Wilson *et al.* 2015). This system is functionally identical to heterothallism, where two unique mating-compatible nuclei are required for di/heterokaryon formation (Wilson *et al.* 2015). In pseudohomothallic species, mating is confined to a single thallus and does not require the fusion of two unlike homo/monokaryons and can be referred to as functional heterothallism. Pseudohomothallism is akin to diploid selfing through automixis as described by Billiard *et al.* (2012).

The occurrence of pseudohomothallism is inherently a karyological (meiotic division, post-meiotic mitosis, spindle alignment, etc.) and microscopic (number of sterigma per basidium) process dependent on the segregation of mating-compatible meiotic nuclei into a single basidiospore, caused by a variety of different mechanisms (Elliott & Challen, 1983; Tommerup *et al.* 1991; Kerrigan *et al*. 1993; Kamzolkina *et al.* 2006). Before examining the karyological development of basidia and basidiospores to elucidate pseudohomothallism, the number of sterigma per basidium can be an important indicator to predict basidiospore nuclear status. Elliot & Challen (1983) explained that pseudohomothallism can occur in both bi- and tetra-sterigmate basidia (two or four-spored basidia). In bi-sterigmate species, the four meiotic products must segregate into two basidiospores instead of the typical four; thus, two meiotic binucleate spores result as opposed to four haploid ones in textbook spore development (e.g. Alexopoulos, 1952). In tetra-sterigmate species, a post-meiotic mitosis must occur in the basidium so that the number of meiotic daughter nuclei is doubled from four to eight; therefore, four meiotic binucleate spores result. The sorting of two mating compatible nuclei into basidiospores has been suggested to occur through one of two functions: (1) the random migration of mating compatible nuclei into a single spore that results in a high ratio of mating compatible heterokaryotic spores (Challen & Elliott, 1989) (2) non-random migration of mating compatible nuclei into a single spore possibly mediated through spindle alignment in meiosis (Evans, 1959; Summerbell *et al.* 1989; Kamzolkina *et al.* 2006). The mechanisms of non-random migration in Agaricomycetes are not well understood (Grognet & Silar, 2015).

Many pseudohomothallic fungi display a system of homothallism *sensu* Blakeslee (1904) (single spore self-fertility) and heterothallism (single spore self-sterility) that are described as amphithallic

(Lange, 1952). Amphithallism is not uncommon in the Agaricomycetes; approximately 9% of agarics display this system (Kamzolkina *et al.* 2006; Lin & Heitman, 2007).

POST-MEIOTIC EVENTS IN AGARICOMYCETES

In total six patterns of post-meiotic nuclear events have been formalized in the agaricomycetes based on the criteria of (i) the location of the post-meiotic division and (ii) the fate of the nuclei following these events: Pattern A, Pattern B, Pattern C, Pattern D, Pattern E, and Pattern F (Duncan & Galbraith, 1972; Arita, 1979; Tommerup *et al.* 1991). These patterns are incredibly important in dictating the mating system of a species (Figure 1-11). Patterns A – D were described as follows: Pattern A: a post-meiotic mitosis occurs in the club portion of the basidium (8 nuclei), four nuclei then migrate into basidiospores while the others remain in the basidium and degenerate. Pattern B: a post-meiotic mitosis occurs in sterigmata (transterigmate division), where four continue to migrate while the remaining four degenerate. Four haploid spores are the result. Pattern C: post-meiotic mitosis occurs in the basidium, and all eight nuclei migrate into basidiospores, then four of the eight nuclei back-migrate into the basidium and degenerate, resulting in four haploid basidiospores. Pattern D: post-meiotic mitosis occurs in the basidium, and the eight nuclei migrate into basidiospores, forming four binucleate homokaryotic basidiospores. Arita (1979) described Pattern E: no post-meiotic mitosis occurs, and the four daughter nuclei migrate into four haploid monokaryotic spores. This pattern is often taught as the classical segregation of mushroom-forming fungi, but it is a rarity (Kuhner, 1945). Tommerup *et al.* 1991 described Pattern F: post-meiotic mitosis occurs in the club portion of the basidium, which all migrate into basidiospores and form four binucleate dikaryotic spores. Pattern F is the classic pattern of pseudohomothallism. Hibbett and Thorn (2001) claimed that no sufficient investigation of post-meiotic events has occurred in the hymenochaetoid clade; which contains the Hymenochaetaceae and *Inonotus obliquus*.

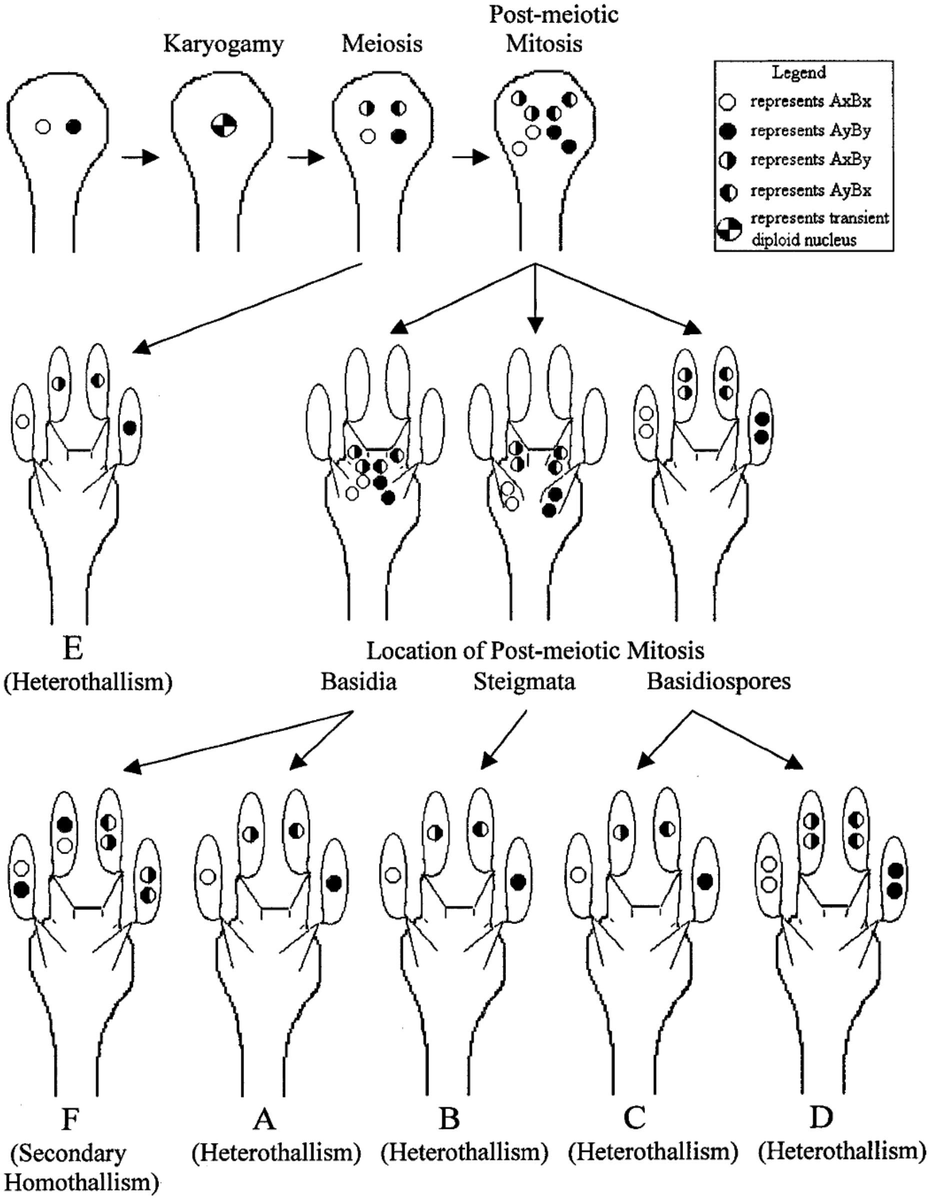

Figure 1-11. Examples of Patterns A, B, C, D, E, and F post-meiotic events in relation to resulting mating system. Source: Price (2006)

MATING IN INONOTUS OBLIQUUS

Difficulty of Studying the Mating System

Inonotus obliquus is in the family Hymenochaetceae (detailed in the taxonomy section), in which mating types have barely been elucidated because the lack of clamp connections complicates the examination of classical mating compatibility reactions between homokaryons (Rajchenberg *et al.* 2015). To make matters more complicated, homo and heterokaryons are often indistinguishable in cultural characters and essentially all possess multinucleate hyphae (Goldstein & Gilbertson, 1981; Mallett & Myrholm, 1995; Rajchenberg, 2011). Classical *in vitro* pairings, such as in *Phellinus tremulae* by Mallett & Myrholm, (1995), where compatibility/incompatibility reactions are influenced by media, have been refuted. Not only does *I. obliquus* possess all the characters, but its basidiomata are extremely difficult to find reliably. Therefore, studying mating in this fungus has largely been seen as unfavourable by mycologists. In order to study mating in this family, the use of molecular techniques is vital (Kauserud & Schumacher, 2001).

Summary of Current Research on the Mating System of *Inonotus obliquus*

The work of Sun *et al.* (2023) (in Mandarin) examined laboratory sporulation, basidiospore behaviour, and *MAT* of *I. obliquus*. Chapter 3 focuses on a similar topic and draws many comparisons to this work; thus, it is summarized.

Sun *et al.* (2023) reported for the first time, that *I. obliquus* primarily displays a pseudohomothallic (secondary homothallic) mating system. It was found to produce anucleate, uninucleate, binucleate, trinucleate, and tetranucleate basidiospores. This was achieved through laboratory cultivation of basidiomata. They examined the development of 96 single spore isolates (SSI) from

I. obliquus basidiomata and found that 85 (88.5%) were able to form spore-producing basidiomata. Of the remaining eleven SSI's, nine (9.4%) formed sporeless basidiomata and two (2.1%) were completely self-sterile and did not form basidiomata of any kind. The formation of sporeless fruiting bodies is a common trait of a type of homokaryotic fruiting in agaricomycetes known as abortive homokaryotic fruiting (AHF) (Labarère & Noel. 1992; Elders & Hennicke. 2021). The eleven strains that did not form sterile basidiomata were crossed in all combinations to reveal classical characteristics indicative of heterothallism such as fertile fruiting body formation, hyphal knots, mycelial fusion, and antagonism. These characters led Sun *et al.* (2023) to suggest that *I. obliquus* is primarily pseudohomothallic with tetrapolar heterothallic tendencies. A fungus that displays a system of homothallism *sensu* Blakeslee (1904) (single spore self-fertility) and heterothallism (single spore self-sterility) is described as amphithallic; therefore*, I. obliquus* is an amphithallic agaricomycete. (Lange, 1952).

Sun *et al.* (2023) sequenced the *MAT* region of *I. obliquus* (Figure 1-12). In the reviewed literature, it appears no members of the Hymenochaetaceae have had their *MAT* regions sequenced and annotated, making this the first putative examination of the *MAT* locus in this family. Sun *et al.* (2023) found the *MAT* region of *I. obliquus* was relatively similar to a typical agaricomyceteous *MAT* structure, which contains two unlinked *MAT* A and *MAT* B that encode pairs of homeodomain proteins (HD1/HD2) and complements of pheromone receptor and pheromone precursor genes, respectively (Fraser *et al.* 2007). However, the B (pheromone) locus structure was unusual, as it possessed three putative distantly linked pheromone receptor genes on the same scaffold annotated as STE3-1, STE3-2, and STE3-3, and only one putative pheromone precursor (PP1) that is closely linked to STE3-2. STE3-1 is 111 kb downstream from STE3-2, and STE3-3 is 679 kb upstream from STE3-2.

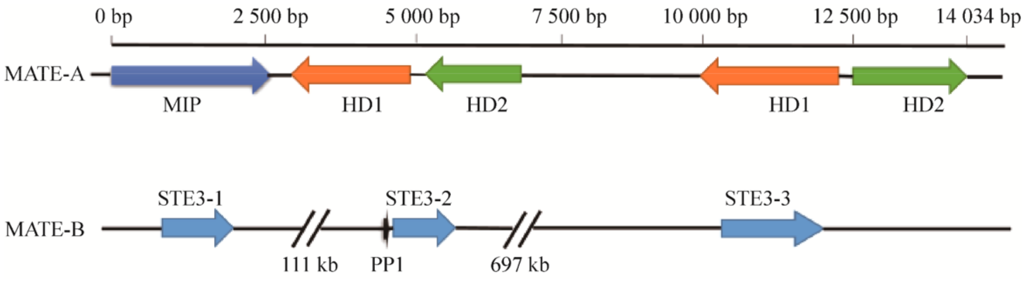

Figure 12-1. Structure of the *MAT* locus in *I. obliquus*. Source: Sun *et al.* (2023)

In *Schizophyllum commune*, the B locus encodes two pheremone receptors that are only spaced by 8kb; the first receptor is closely linked with three pheromone precursor genes, and the second is closely linked with 1 pheromone precursor gene (Fraser *et al.* 2007). In the case of *I. obliquus,* two putative pheromone receptor genes (STE3-1 and STE3-3) lack close association with any pheromone precursor genes. Moore *et al*. (2021) indicate that one of the key features of non-mating-type-specific pheromone receptors is that they lack any pheromone precursor genes nearby. Under that logic, the flanking non-pheromone-associated STE3-1 and STE3-3 genes of the pheromone-associated gene STE3-2, are likely not involved in the mating process. Moore *et al.* (2021) suggest that non-mating-type-specific pheromone receptors may play a role in monokaryotic fruiting or communication within vegetative mycelium. If STE3-1 and STE3-3 are not involved in mating, then *I. obliquus* likely possesses a single mating-type-specific pheromone receptor and is associated with a single pheromone precursor gene. This is speculation and requires further investigation. As presented, the preliminary *MAT* analysis of *I. obliquus* is indicative of a bifactorial (controlled by two *MAT* loci) tetrapolar heterothallic system including a classic agaricomyceteous homeodomain (A) locus and a pheremone (B) locus containing a pheromone receptor that is closely linked to a pheromone precursor gene. Molecular studies of the mating type locus in *I. obliquus* are vital for understanding mating in this species and in the family Hymenochaetaceae.

OBJECTIVES AND HYPOTHESES

In the following two chapters, the primary objectives are to (i): develop a reliable protocol to fruit the basidiomata of *I. obliquus in vitro* and to optimize linear growth using different media, (ii): examine the basidiospore nuclear type variability (uni, bi, tri and tetranucleate) as basidiomata mature.

It is hypothesized that *in vitro* fruiting of *I. obliquus* should be relatively straight forward as it has been completed by Campbell and Davidson (1938) and Sun *et al.* (2023) with relative ease. Sun *et al.* (2023) observed that the proportion of basidiospores with different nuclear types varies with maturity, where basidiospores containing more than a single nucleus predominate in young basidiomata, and uni and anucleate basidiospores predominate in maturity. It is hypothesized that basisidopores in this study may form a similar trend; however, it is likely to deviate from the ratios they observed.

LITERATURE CITED

Aanen, D. K., van ’t Padje, A., Auxier, B. 2023. Longevity of fungal mycelia and nuclear quality checks: a new hypothesis for the role of clamp connections in dikaryons. *Microbiology and Molecular Biology Reviews*, *87*(3), e00022-21.

Alexopoulos, C. J. 1952. Introductory mycology. Wiley & Sons, Inc. New York, USA. 481 pp.

Arita, I. 1979. Cytological studies on *Pholiota*. *Rep Tottori Mycol Inst*, 17:1-118

Arizaga, S., & Ezcurra, E. 1995. Insurance against reproductive failure in a semelparous plant: Bulbil formation in *Agave macroacantha* flowering stalks. *Oecologia*, *101*(3), 329–334.

Bai, Yan-Hon, Yong-Qiang Feng, Duo-Bin Mao, and Chun-Ping Xu. 2012. Optimization for betulin production from mycelial culture of inonotus obliquus by orthogonal design and evaluation of its antioxidant activity. *Journal of the Taiwan Institute of Chemical Engineers* 43(5):663–69.

Basal, Wesam Taha, Abdo Elfiky, and Jehane Eid. 2021. Chaga medicinal mushroom *Inonotus obliquus* (Agaricomycetes) terpenoids may interfere with sars-cov-2 spike protein recognition of the host cell: a molecular docking study. *International Journal of Medicinal Mushrooms* 23(3). 1-14.

Balandaykin, M. E., & Zmitrovich, I. V. 2015. Review on chaga medicinal mushroom, *Inonotus obliquus* (higher basidiomycetes): realm of medicinal applications and approaches on estimating its resource potential. *International Journal of Medicinal Mushrooms*, *17*(2). 95-104.

Billiard, S., López-Villavicencio, M., Hood, M. E., & Giraud, T. 2012. Sex, outcrossing and mating types: unsolved questions in fungi and beyond. *Journal of Evolutionary Biology*, *25*(6), 1020–1038.

Blakeslee A. F. 1904. Sexual reproduction in the Mucorineae. *Proceedings of the American Academy of Arts and Sciences,* 40:205-319.

Blanchette, R. A. 1982. Progressive stages of discoloration and decay associated with the canker-rot fungus, *Inonotus obliquus*, in birch. *Phytopathology*, *72*(10), 1272–1277.

Bondartsev A.S. 1912. The fungi collected on stems of forest trees in Bryansk experimental forestry Trudy po lesnomu opytnomu delu v Rossii. 1912;37:1–56 (in Russian).

Bondartsev, A.S. 1953. The Polyporaceae of European part of USSR and Caucasus. Moscow–Leningrad:AN SSR; (in Russian)

Brydon-Williams, R., I. A. Munck, and H. Asbjornsen. 2021. Incidence and ecology of the chaga fungus (*Inonotus obliquus*) in hardwood New England--Acadian forests. *Canadian Journal of Forest Research* 51(1):122–32.

Bunyard, B. A. 2015. First record of insect mycophagy of the commercially-important "chaga" fungus *Inonotus obliquus* (Ach. ex Pers.) Pilát (Hymenochaetales: Hymenochaetaceae) in North America. *Proceedings of the Entomological Society of Washington*, *117*(4), 452–457.

Campbell, W. A. 1938. The cultural characteristics of the species of *Fomes*. *Bull. Torrey Club*. 65: 31-69.

Campbell, W. A., & Davidson, R. W. 1938. A *Poria* as the fruiting stage of the fungus causing the sterile conks on birch. *Mycologia*, *30*(5), 553–560.

Carpenter, C., & R. Crawford. 2017. Chaga birch canker assessment conducted by Northeastern Area State and Private Forestry. Staff in cooperation with University of New Hampshire for the National Forest System (NFS). Received by J.S. Barresi, K. Atkinson.

Casselton, L. A., & N. S. Olesnicky. 1998. Molecular genetics of mating recognition in basidiomycete fungi. *Microbiol. Mol. Biol. Rev*. 62:55-70.

Černý A. 1976. Lesnická fytopatologie. *Státni zemědělské nakladatelstvi*, Praha. (in Czech)

Cha, J. Y., S. Y. Lee, S. Y. Lee, &, K. W. Chun. 2011. Basidiocarp formation by *Inonotus obliquus* on a living paper birch tree." *Forest Pathology* 41(2):163–64.

Cha, J. Y., Jun, B. S., Lee, C. H., Yooi, K. S., Moon, J. C., & Cho, Y. S. 2005. Hypoglycemic and antioxidative effects of fermented chaga mushroom (*Inonotus obliquus*) on streptozotocin-induced diabetic rats. *Journal of Life Science*, *15*(5), 809-818.

Chen, Y. Q., Zhou, L. J., & Li, Y. 2006. Study on experimental comparison of hypoglycemic effect of polysaccharides of cultured mycelia, sclerotia and wild sclerotia from *Inonotus obliquus*. *Edible Fungi (Chin)*, *28*, 52-54.

Chen, H.-J., Chen, Y.-S., Liu, S.-L., Liou, B.-K., & Chen, C.-S. 2020. The influence of submerged fermentation of *Inonotus obliquus* with control atmosphere treatment on enhancing bioactive ingredient contents. *Applied Biochemistry and Biotechnology*, *191*(1), 412–425.

Coelho, M. A., Bakkeren, G., Sun, S., Hood, M. E., & Giraud, T. 2017. Fungal sex: the Basidiomycota. *Microbiology Spectrum*, *5*(3), 5.3.12.

Dai, Y. C. 2010. Hymenochaetaceae (Basidiomycota) in China. *Fungal Diversity*, *45*(1), 131–343.

David-Palma, M., Sampaio, J. P., & Gonçalves, P. 2016. Genetic dissection of sexual reproduction in a primary homothallic basidiomycete. *PLoS Genetics*, *12*(6), e1006110.

Domański, S. 1965. Flora Polska. Grzyby (Fungi) 2: Basidiomycetes. Aphyllophorales. Polyporaceae I. Mucronoporaceae I, *PWN*, Warszawa. (in Polish)

Donk, M. 1948. Notes on Malesian fungi I. - *Bull. Bot. Gard.* Buitenzorg III 17: 473-482.

Duncan, E. G., & Galbraith, M. H. 1972. Post-meiotic events in the Homobasidiomycetidae. *Transactions of the British Mycological Society*, *58*(3), 387–392.

Elders, H., & Hennicke, F. 2021. The Pacific tree-parasitic fungus *Cyclocybe parasitica* exhibits monokaryotic fruiting, showing phenotypes known from bracket fungi and from *Cyclocybe aegerita*. *Journal of Fungi*, *7*(5), 394.

Elliott, T. J., & Challen, M. P. 1983. Genetic ratios in secondarily homothallic basidiomycetes. *Experimental Mycology*, *7*(2), 170–174.

Evans, H. J. 1959. Nuclear behaviour in the cultivated mushroom. *Chromosoma*, *10*(1), 115–135.

Fact.MR. 2024. *Chaga mushroom market to reach $2.1 billion by 2034, driven by rising health awareness & supplement demand*. Global Banking & Finance Review. https://www.factmr.com/report/chaga-mushroom-market

Fiasson, J. L., & Niemelä, T. 1984. The Hymenochaetales: A revision of the European poroid taxa. *Karstenia*, *24*(1), 14–28.

Fraser, J. A., Heitman, J. 2003. Fungal mating-type loci. *Curr. Biol.* 13;R792-R795

Fraser, J. A., Hsueh, Y., Findley, K. M., Heitman, J. 2007. Evolution of the mating-type locus: the Basidiomycetes. In *Sex in Fungi: Molecular Determination and Evolutionary Implications* (J. Heitman, J. W. Kronstad, J. W. Taylor & L. A. Casselton, Eds.), Chapter 2, pp. 19–34. *ASM Press*.

Gammerman A. F., Kadaev G. N., Šupinskaja M. D., Jacenko-Chmelevskij A. A. 1975. Lekarstvennye rastenija. *Vysšaja Škola*, Moskva. (in Russian)

Germain, H., Bergeron, M. -J., Bernier, L., Laflamme, G., & Hamelin, R. C. 2009. Patterns of colonization and spread in the fungal spruce pathogen *Onnia tomentosa*. *Molecular Ecology*, *18*(21), 4422–4433.

Ghobad-Nejhad, M., Zhou, L., Tomšovský, M., Angelini, P., Cusumano, G., Angeles Flores, G., Venanzoni, R., Wang, X., Chaharmiri-Dokhaharani, S., Moridi Farimani, M., Pärtel, K., Dai, Y., & Wu, F. 2024. Unlocking nature's pharmacy: Diversity of medicinal properties and mycochemicals in the family Hymenochaetaceae (Agaricomycetes, Basidiomycota). *Mycosphere*, *15*(1), 6347–6438.

Gilbertson, R. L., & Ryvarden, L. 1986. North American polypores. Vol. I. *Abortiporus-Lindtneria*. *Fungiflora.* Norway. 433 pp.

Grognet, P., & Silar, P. 2015. Maintaining heterokaryosis in pseudo-homothallic fungi. *Communicative & Integrative Biology*, *8*(4), e994382.

Goldstein, D., & Gilbertson, R. L. 1981. Cultural morphology and sexuality of *Inonotus arizonicus*. *Mycologia*, *73*(1), 167–180.

Hayek, J.C. 2019. Maximum Tree Age & Longevity. *Illinois Extension. Technical Forestry Bulletin – NRES-502.* 6pp.

He, M.-Q., Zhao, R.-L., Hyde, K. D., Begerow, D., Kemler, M., Yurkov, A., McKenzie, E. H. C., Raspé, O., Kakishima, M., Sánchez-Ramírez, S., Vellinga, E. C., Halling, R., Papp, V., Zmitrovich, I. V., Buyck, B., Ertz, D., Wijayawardene, N. N., Cui, B.-K., Schoutteten, N., Kirk, P. M. 2019. Notes, outline and divergence times of Basidiomycota. *Fungal Diversity*, *99*(1), 105–367.

Heitman, J., Kronstad, J. W., Taylor, J. W., & Casselton, L. A. 2007. Sex in fungi: molecular determination and evolutionary implications. *ASM Press.*

Herman, K. C., Wösten, H. A. B., Fricker, M. D., & Bleichrodt, R. -J. 2020. Growth induced translocation effectively directs an amino acid analogue to developing zones in *Agaricus bisporus*. *Fungal Biology*, *124*(12), 1013–1023.

Herskowitz, I., & Y. Oshima. 1981. Control of cell type in *Saccharomyces cerevisiae*: mating type and mating-type interconversion, p. 181-209. In J. N. Strathern, E. W. Jones, and J. R. Broach (ed.), *The Molecular Biology of the Yeast Saccharomyces, Life Cycle and Inheritance*. Cold Spring Harbor Laboratory, Cold Spring Harbor, NY.

Hibbett, D. S., Bauer, R., Binder, M., Giachini, A. J., Hosaka, K., Justo, A., Larsson, E., Larsson, K. H., Lawrey, J. D., Miettinen, O., Nagy, L. G., Nilsson, R. H., Weiss, M., & Thorn, R. G. 2014. In *The Mycota. 14 Agaricomycetes*. D. J. McLaughlin & J. W. Spatafora (Eds.), *Systematics and Evolution* (pp. 373–429). Springer Berlin Heidelberg.

Hibbett, D. S., & Donoghue, M. J. 1998. Integrating phylogenetic analysis and classification in fungi. *Mycologia*, *90*(3), 347-356.

Hibbett, D. S., & Thorn, R. G. 2001. Basidiomycota: Homobasidiomycetes. In D. J. McLaughlin, E. G. McLaughlin, & P. A. Lemke (Eds.), *Systematics and Evolution* (pp. 121–168). Springer.

Horn, F., E. Bettler, L. Oliveira, F. Campagne, F. E. Cohen, and G. Vriend. 2003. GPCRDB information system for G protein-coupled receptors. Nucleic Acids Res. 31:294-297

Ichimura, T., Otake, T., Mori, H., & Maruyama, S. 1999. HIV-1 protease inhibition and anti-HIV effect of natural and synthetic water-soluble lignin-like substances. *Bioscience, Biotechnology, and Biochemistry* 63(12):2202–4.

Ka, K.-H., Jeon, S.-M., Park, H., Lee, B.-H., & Ryu, S.-R. 2017. Growth of chaga mushroom *(Inonotus obliquus*) on *Betula platyphylla* var. *japonica*. *The Korean Journal of Mycology*, *45*(3), 241–245.

Kamzolkina, O. V., Volkova, V. N., Kozlova, M. V., Pancheva, E. V., Dyakov, Y. T., & Callac, P. 2006. Karyological evidence for meiosis in the three different types of life cycles existing in *Agaricus bisporus*. *Mycologia*, *98*(5), 763–770.

Katayevskaya, H. T. 1928. "Tchaga ": Contribution to the study of tree rots (In Russia). Mitt. Aus dem Forst. Versuchsw. Omsk. 6, 12 pp. Abstr. in *Rev. Appl. Mcy*. 8: 345-346. 1929.

Kauserud, H., & Schumacher, T. 2001. Outcrossing or inbreeding: DNA markers provide evidence for type of reproductive mode in *Phellinus nigrolimitatus* (Basidiomycota). *Mycological Research*, *105*(6), 676–683.

Kerrigan, R. W., Royer, J. C., Baller, L. M., Kohli, Y., Horgen, P. A., & Anderson, J. B. 1993. Meiotic behavior and linkage relationships in the secondarily homothallic fungus *Agaricus bisporus*. *Genetics*, *133*(2), 225–236.

Kim, Yong Ook, Sang Bae Han, Hong Woen Lee, Hyo Jung Ahn, Yeo Dae Yoon, Joon Ki Jung, Hwan Mook Kim, and Chul Soo Shin. 2005. Immunostimulating effect of the endo-polysaccharide produced by submerged culture of *Inonotus obliquus*. *Life Sciences* 77(19):2438–56.

Kim, Yong Ook, Hae Woong Park, Jong Hoon Kim, Jae Young Lee, Seong Hoon Moon, and Chul Soo Shin. 2006. Anti-cancer effect and structural characterization of endo-polysaccharide from cultivated mycelia of *Inonotus obliquus*. *Life Sciences* 79(1):72–80.

Kothe, E. 1996. Tetrapolar fungal mating types: sexes by the thousands. *FEMS Microbiology Reviews*, *18*(1), 65–87.

Korotkin, H. 2017. Stable isotopes, phylogenetics, and experimental data indicate a unique nutritional mode for *Rickenella fibula*, a bryophyte-associate in the Hymenochaetales. Master's thesis. *Tennessee research and creative exchange*. https://trace.tennessee.edu/utk_gradthes/4886

Kües, U., James, T. Y., & Heitman, J. 2011. 6 mating type in Basidiomycetes: unipolar, bipolar, and tetrapolar patterns of sexuality. In S. Pöggeler & J. Wöstemeyer (Eds.), *Evolution of Fungi and Fungal-Like Organisms* (pp. 97–160). Springer. Berlin.

Kuhner, R. 1945. Nouvelles recherches sur les divisions nucleares dans la baside et les spores des Agaricales, *CSeTanc, Acad, Sci, Paris*, 220. 618-620.

Kukulyanskaya, T. A., N. V. Kurchenko, V. P. Kurchenko, and V. G. Babitskaya. 2002. Physicochemical properties of melanins produced by the sterile form of *Inonotus obliquus* ('Chagi') in natural and cultivated fungus. *Applied Biochemistry and Microbiology* 38(1):58–61.

Kuz'michev, E. P. 2001. Common fungal diseases of Russian forests (Vol. 279). US Department of Agriculture, Forest Service, Northeastern Research Station.

Kuznetsova-Zarudnaya T. N. 1955. To the problem of chaga affinity. Botanicheskie materialy Otdela sporovykn rastenii *Botanicheskogo instituta* AN SSSR. 10:196–209 (in Russian).

Labarère, J., & Noel, T. 1992. Mating type switching in the tetrapolar Basidiomycete *Agrocybe aegerita*. *Genetics*, *131*(2), 307–319.

Lange, M. 1952. Species concept in the genus *Coprinus*. A Study on the significance of intersterility. *Dansk Bot. Arkiv*. 14(6): 1-164.

Larsen M. J., Cobb-Poulle L. A. 1990. *Phellinus* (Hymenochaetaceae). A survey of the world taxa. *Fungiflora*. Oslo, Norway. 206 pp.

Larsson, K.-H., Parmasto , E., Fischer, M., Langer , E., Nakasone, K., & Redhead, S. A. 2006. Hymenochaetales: A molecular phylogeny for the hymenochaetoid clade. *Mycologia*, *98*(6), 926–936.

Lee, Min-Woong, Hyeon-Hur, Kwang-Choon Chang, Tae-Soo Lee, Kang-Hyeon Ka, and L. Jankovsky. 2008. Introduction to distribution and ecology of sterile conks of *Inonotus obliquus*. *Mycobiology* 36(4):199–202.

Lemieszek, Marta Kinga, Ewa Langner, Jozef Kaczor, Martyna Kandefer-Szerszen, Bozena Sanecka, Witold Mazurkiewicz, and Wojciech Rzeski. 2011. Anticancer effects of fraction isolated from fruiting bodies of chaga medicinal mushroom, *Inonotus obliquus* (Aphyllophoromycetideae): *in vitro* studies. *International Journal of Medicinal Mushrooms* 13(2).

Leschen, R. A. B. 1990. Tenebrionid-basidiomycete relationships with comments on feeding ecology and the evolution of fungal monophagy (Coleoptera/Hymenomycetes). *University of Kansas Science Bulletin* 54(5): 165–177.

Lin, X. & Heitman, J. 2007. Chapter 3: Mechanisms of homothallism in fungi and transitions between heterothallism and homothallism. J. Heitman, J. W. Kronstad, J. W. Taylor, & L. A. Casselton (Eds.), *Sex in fungi: Molecular determination and evolutionary implications* (pp. 267–282). Washington, DC: *ASM Press*.

Lin, X., Hull, C. M., Heitman, J. 2005. Sexual reproduction between partners of the same mating type in *Cryptococcus neoformans*. *Nature,* 434: 1017-1021.

Lindroth, J. I. 1904. Beitrage zur Kentniss der Zersetzungserscheinungen des Birkenholzes. Naturw.-Zeits. Land- Forstwiss. 2: 393-406.

Lõhmus, A., & Lõhmus, P. 2024. A heart-rot fungus, *Inonotus obliquus* (chaga), mediates microhabitat creation in birch snags and contributes to forest fungal diversity. *Global Ecology and Conservation*, *56*, e03319.

Maine Forest Service. 2023. *Chaga and Forest Health FAQ (Inonotus obliquus)*.

Mallett, K. I., & Myrholm, C. L. 1995. The mating system of *Phellinus tremulae*. *Mycologia*, *87*(5), 597–603.

Martinmäki, M. 2022. Pakuri Venäjällä: kirjallisuuskatsaus pakurin asemaan Venäjällä.

Miina, J., Peltola, R., Veteli, P., Linnakoski, R., Escribano, M. C., Haveri-Heikkilä, J., Mattila, P., Marnila, P., Pihlava, J.-M., Hellström, J., Sarjala, T., Silvan, N., Kurttila, M., & Vanhanen, H. 2021. Inoculation success of *Inonotus obliquus* in living birch (*Betula* spp.). *Forest Ecology and Management*, *492*, 119244.

Millman, L. 2012. Chaga's significant other. *Fungi* 5(3): 10–12.

Minter, D. W., and G. S. Soliman. 2022. *Inonotus obliquus*. [Descriptions of Fungi and Bacteria]. *Descriptions of Fungi and Bacteria* 2296-Sheet 2296.

Moncalvo, J.-M., Vilgalys, R., Redhead, S. A., Johnson, J. E., James, T. Y., Aime, M. C., Hofstetter, V., Verduin, S. J., Larsson, E., & Baroni, T. J. 2002. One hundred and seventeen clades of euagarics. *Molecular Phylogenetics and Evolution*, *23*(3), 357–400.

Moore, D., Robson, G. D., Trinci, A. P. J. 2021. *Mating types in Basidiomycota*. In *21st Century Guidebook to Fungi – Chapter 8.5* (Section 8.5: "Mating types in Basidiomycota"). Retrieved from https://www.davidmoore.org.uk

Myasoedov, A. N. 1896. Album of the most harmful wood-parasitic fungi. St. Petersburg: *Petroff P. Marx Publ. House* 1896 (in Russian).

Nobles, M. K. 1965. Identification of cultures of wood-inhabiting Hymenomycetes. *Canadian Journal of Botany*, *43*(9), 1097–1139.

Oberwinkler F. 1977. Das neue System der Basidiomyceten. In: Frey W, Hurka H, Oberwinkler F, eds. Beitra¨ge zur Biologie der niederen Pflanzen. Stuttgart, New York: Gustav Fischer Verlag. p 59–104.

Park, Hyun, Bong-Hun Lee, and Won-Chull Bak. 2005. Cultural characteristics of *Inonotus obliquus* isolated from *Betula costata* at Mt. Jumbong in Korea. *Journal of Mushroom* 3(2):71–74.

Parmasto, E., Saar, I., Larsson, E., & Rummo, S. 2014. Phylogenetic taxonomy of *Hymenochaete* and related genera (Hymenochaetales). *Mycological Progress*, *13*(1), 55–64.

Patouillard, N. 1900. Essai taxonomique sur les familles et les genres des Hyménomycètes. *Université de Paris: École supérieure de Pharmacie, Année 1900-1901, No. 2*.

Pietka, J & Grzywacz, A. 2006. Attempts at active protection of *Inonotus obliquus* by inoculating birches with its mycelium. *Acta Mycologica*, *41*(2).

Pilz, D. 2004. Chaga and other fungal resources: assessment of sustainable commercial harvesting in Khabarovsk and Primorsky Krais, Russia. *Report Prepared for Winrock International, Morrilton, Arkansas and the FOREST Project, Khabarovsk, Russia*.

Pollock, D. A. 2002. Melandryidae Leach 1815. In: R. H. Arnett, Jr., M. C. Thomas, P. E. Skelley, and J. H. Frank, eds. American Beetles, *Volume 2: Polyphaga: Scarabaeoidea through Curculionoidea. CRC Press*, Boca Raton, USA. pp. 417–422.

Price, S. H. 2006. Selection for multinucleate basidiospores in Pleurotus ostreatus (Jacq.:Fr.) Kummer as a means for selecting for secondary homothallism by inbreeding large basidiospores. *PhD thesis*. University of New Brunswick. 436 pp.

Pringle, A., & Taylor, J. 2002. The fitness of filamentous fungi. *Trends in Microbiology*, *10*(10), 474–481.

Rajchenberg, M. 2011. Nuclear behavior of the mycelium and the phylogeny of Polypores (Basidiomycota). *Mycologia*, *103*(4), 677–702

Rajchenberg, M., Pildain, M. B., Bianchinotti, M. V., & Barroetaveña, C. 2015. The phylogenetic position of poroid Hymenochaetaceae (Hymenochaetales, Basidiomycota) from Patagonia, Argentina. *Mycologia*, *107*(4), 754–767.

Raper, J. R. 1966. Genetics of sexuality in higher fungi. Ronald Press Company. USA. 283 pp.

Redhead, S. A. 2002. Phylogeny of agarics: partial systematics solutions for bryophilous omphalinoid agarics outside of the Agaricales (euagarics). *Mycotaxon*, *82*, 151-168.

Rivoire, B. 2020. Polypores de France et d'Europe. *Orilénas, Mycopolydev*. 874 p.

Rogers, R. D. 2012. The true tinder conk: First Nation's use. *Fungi*, *5*(3), 56–57.

Ryvarden, L. 2005. *The genus Inonotus: A synopsis*. *Index fungorum*.

Saar, M. 1991. Fungi in Khanty Folk Medicine. *Journal of Ethnopharmacology* 31(2):175–79.

Schiegel, D. S. 2011. Polypore-beetle associations in Finland. *Annales Zoologici Fennici* 48: 319–348.

Shibnev, V. A., D. V. Mishin, T. M. Garaev, N. P. Finogenova, A. G. Botikov, and P. G. Deryabin. 2011. Antiviral activity of *Inonotus obliquus* fungus extract towards infection caused by hepatitis C virus in cell cultures. *Bulletin of Experimental Biology and Medicine* 151(5):612.

Shigo, A. L. 1965. The Pattern of Decays and Discolorations in Northern Hardwoods. *Phytopathology*, 55: 648-652

Shigo, A. L. 1969. How *Poria obliqua* and *Polyporus glomeratus* incite cankers. *Phytopathology* 59:1164-1165.

Shigo, A. L. 1984. Compartmentalization: a conceptual framework for understanding how trees grow and defend themselves. *Annual Review of Phytopathology* 22(1):189–214.

Sinadskij, J. V. 1973. Bereza eë vrediteli i bolezni. Izdatel ́stvo Nauka, Moskva.

Sinclair, W.A., & H.H. Lyon. 2005. Diseases of trees and shrubs. 2nd ed., *Cornell University Press*, 680 pp.

Stone, N. 2015. The himalayan gold rush: the untold consequences of yartsa gunbu in the Tarap valley. Independent Study Project (ISP) Collection. 2088

Stalpers, J. A. 1978. Identification of wood-inhabiting fungi in pure culture. *Studies in Mycology*, *16*. 1-248.

Stankis, M.M. & Specht, C.A. 2007. Chapter 2: The origin of multiple mating types in the basidiomycetes. In J. Heitman, J. W. Kronstad, J. W. Taylor, & L. A. Casselton (Eds.), *Sex in fungi: Molecular determination and evolutionary implications* (pp. 267–282). Washington, DC: ASM Press.

Summerbell, R. C., Castle, A. J., Horgen, P. A., & Anderson, J. B. 1989. Inheritance of restriction fragment length polymorphisms in *Agaricus brunnescens*. *Genetics*, *123*(2), 293–300.

Sun, Y., Zhang, Y., Cao, X., Zhou, J., & Jiang, J. 2023. Characteristics related to sexual reproduction and mating type locus of *Inonotus obliquus*. *Mycosystema*, 42(2), 520–529.

Tedersoo, L., Suvi, T., Beaver, K., & Saar, I. 2007. Ectomycorrhizas of *Coltricia* and *Coltriciella* (Hymenochaetales, Basidiomycota) on Caesalpiniaceae, Dipterocarpaceae and Myrtaceae in Seychelles. *Mycological Progress*, *6*(2), 101–107.

Teplyakova, T. V., Oleg V. Pyankov, Alexandr S. Safatov, Alena S. Ovchinnikova, Tatiana A. Kosogova, Maxim O. Skarnovich, Ekaterina I. Filippova, and Alevtina L. Poteshkina. 2022. Water extract of the chaga medicinal mushroom, *Inonotus obliquus* (Agaricomycetes), inhibits SARS-CoV-2 replication in vero E6 and vero cell culture experiments. *International Journal of Medicinal Mushrooms* 24(2).

Thomas, P. W., Elkhateeb, W. A., & Daba, G. M. 2020. Chaga (*Inonotus obliquus*): a medical marvel but a conservation dilemma. *Sydowia*, *72*, 123–130.

Tommerup, I. C., Bougher, N. L., & Malajczuk, N. 1991. *Laccaria fraterna*, a common ectomycorrhizal fungus with mono- and bi-sporic basidia and multinucleate spores: comparison with the quadristerigmate, binucleate spored *L. laccata* and the hypogeous relative *Hydnangium carneum*. *Mycological Research*, *95*(6), 689–698.

Tumanova, I.V., Arzamastseva, A.P., Kosyreva, N. S., Levushkina, L.V., Kiseleva, V. F., Zybova, L. A. 1989. State pharmacopeia URSS XI. Issue 2. General methods of analysis. Drug plant material. Moscow, 400 p. (in Russian).

Vanhanen, He., Peltola, R., Pappinen, A., & Ahtikoski, A. 2013. Cultivation of pakuri (*Inonotus obliquus*)-potential for new income source for forest owners. https://www.researchgate.net/publication/271585149_Cultivation_of_Pakuri_Inonotus_obliquus_-_potential_for_new_income_source_for_forest_owners

Verrall, A. F. 1937. Variation in *Fomes igniarius* (L.*) Gill. Tech. Bull*. 117, Univ. Minnesota, Agr. Exp. Sta.

Wagner, T., & Fischer, M. 2002. Proceedings towards a natural classification of the worldwide taxa *Phellinus s.l.* and *Inonotus s.l*., and phylogenetic relationships of allied genera. *Mycologia*, *94*(6), 998–1016.

Wang, J., Hu, W., Li, L., Huang, X., Liu, Y., Wang, D., & Teng, L. 2017. Antidiabetic activities of polysaccharides separated from *Inonotus obliquus* via the modulation of oxidative stress in mice with streptozotocin-induced diabetes. *PLoS One*, *12*(6), e0180476.

Wang, Y.-W., McKeon, M. C., Elmore, H., Hess, J., Golan, J., Gage, H., Mao, W., Harrow, L., Gonçalves, S. C., & Hull, C. M. 2023. Invasive Californian death caps develop mushrooms unisexually and bisexually. *bioRxiv*, 2023–01.

Weir, J. R. 1915. Some observations on abortive sporophores of wood-destroying fungi. *Phytopathology* 5: 48-50.

Wilson, A. M., Wilken, P. M., van der Nest, M. A., Steenkamp, E. T., Wingfield, M. J., & Wingfield, B. D. 2015. Homothallism: an umbrella term for describing diverse sexual behaviours. *IMA Fungus*, *6*(1), Article 1.

Whitehouse, H. L. K. 1949. Heterothallism and sex in the fungi. *Biological Reviews*, *24*(4), 411-447.

Wu, F., Zhou, L.-W., Vlasák, J., & Dai, Y.-C. 2022. Global diversity and systematics of Hymenochaetaceae with poroid hymenophore. *Fungal Diversity*, *113*(1), 1–192.

Yachevskii A.A. 1913. Key-book of fungi. T. I. St. Petersburg: *Kind's Typ*. (in Russian).

Zabel R.A. 1947. *Poria obliqua* on dying beech. *Phytopathology*, 37:189–90.

Zhao, H., Wu , Fang, Maurice, Sundy, Pavlov, Igor N., Krutovsky, Konstantin V., Liu, Hong-Gao, Yuan, Yuan, & Dai, Y.-C. 2024. Large-scale phylogenomic insights into the evolution of the Hymenochaetales. *Mycology*, *16*(2), 1–18.

Zheng, Weifa, Kangjie Miao, Yubing Liu, Yanxia Zhao, Meimei Zhang, Shenyuan Pan, and Yucheng Dai. 2010. Chemical diversity of biologically active metabolites in the sclerotia of *Inonotus obliquus* and submerged culture strategies for up-regulating their production. *Applied Microbiology and Biotechnology* 87(4):1237–54.

CHAPTER 2:

PRELIMINARY INVESTIGATIONS OF *IN VITRO* SPORULATION AND LINEAR GROWTH OF *INONOTUS OBLIQUUS* (HYMENOCHAETACEAE)

ABSTRACT

Inonotus obliquus (Ach. ex Pers.) Pilàt is a white heart rot fungus parasitic on members of the genus *Betula* L. and possesses a circumboreal distribution. It is typically recognized by the production of charcoal-like sterile conks on living hosts, which have been reported to have medicinal benefits. Following host death, a resupinate poroid basidioma develops underneath the bark only once during an infection cycle lasting 10–80 years. Due to its rarity, it has been difficult to study. Therefore, a series of experiments were done to optimize *in vitro* sporulation and linear growth of *I. obliquus.* Laboratory sporulation was highly strain dependent, as only one (IOB2) of the four (IOB1, IOB2, IOB3, IOB5) formed fruit bodies reliably and consistently. 2% modified malt extract agar (MEA) was the ideal fruiting medium relative to the other media tested and fruit bodies formed optimally at room temperature under blue light stimulation and in complete darkness. Additionally, carrot agar was found to stimulate vigorous, dense colony growth and was the ideal medium for culturing in this experiment. This report aims to develop a protocol for isolation, culturing, and reliable *in vitro* fruiting of *I. obliquus*. This will enable future study of the basidiomata of this unusual but popular fungus.

INTRODUCTION

Inonotus obliquus (Ach. ex Pers.) Pilàt is a circumboreal white heart rot fungus belonging to the Hymenochaetaceae, a family of the Phylum Basidiomycota that primarily parasitizes trees of the genus *Betula* L. (Gilbertson & Ryvarden, 1986; Lee *et al.* 2008). This fungus produces melanized charcoal-like sterile conks (chaga) with a corky yellowish-brown interior on living host trees (Gilbertson & Ryvarden, 1986; Rivoire, 2020). These sterile conks have been a historic folk medicine used since the 16th and 17th centuries in Northern Europe (Lee *et al.* 2008). Studies have elucidated that chaga has potential medicinal properties such as anti-cancer, anti-diabetes, and anti-viral effects (Ern *et al.* 2023). Chaga is becoming an increasingly popular consumer product and non-timber forest resource that is wild-harvested and cultivated (Thomas *et al.* 2020; Miina *et al.* 2021). Once the host dies, the short-lived reddish-brown resupinate poroid fertile basidioma ruptures the bark once in an infection cycle of approximately 10 – 80 years (Shigo, 1965; Černý, 1976; Bunyard, 2015). The bark-removing quality of this life cycle has been recently found to create microhabitat for species of fungi and lichen (Lõhmus & Lõhmus, 2024). This fruiting body is incredibly rare and difficult to find; thus, its cryptic ecology has made study of the basidiomata difficult.

Sun *et al.* (2023) (in Mandarin) recently examined the laboratory sporulation and mating of *I. obliquus* and were successful in forming the basidioma on bagged supplemented soybean hull substrate. For this chapter, a protocol for the wild isolation, axenic culturing and *in vitro* sporulation of *I. obliquus* was developed using 9 cm Petri dishes. Four strains of *I. obliquus* were grown using eight media types, light conditions, and gravity stimuli to examine fruiting capacity and linear growth differences under different treatments.

MATERIALS AND METHODS

ISOLATION OF *INONOTUS OBLIQUUS* STRAINS

A total of four strains were collected from the field in a variety of locations in the Thunder Bay District from *Betula papyrifera* Marshall. Collections were made in the City of Thunder Bay and the townships of Lappe, Ontario and Dorian, Ontario. These strains were labelled as IOB1, IOB2, IOB3 and IOB5 (Table 2-1). IOB4 was not included as the isolate was misidentified in early stages and not used in this study. When IOB1, IOB2, and IOB5 were encountered, small to medium portions of their sterile conk were pried off by hand and placed in a collection bag. These specimens were dated, labelled and stored in a standard consumer freezer until biopsy, isolation, and cultivation occurred. When examining a sterile conk in cross-section, one may observe a mottled corky interior of colour ranging from dark rusty brown to light yellow. Within this matrix are pockets of whitish-yellow mycelium, which appear more vigorous for isolation. These portions were aseptically removed using a flame-sterilized scalpel from freshly exposed sections of the sterile conk, cut into 3-6mm pieces, surface sterilized with a light spray of 70% ethanol, and left to dry under a flow hood (Figure 2-1). The sterile conk of IOB3 was not collected. Instead, a wood cookie from a white birch tree infected with *I. obliquus* was cut following its removal from private property by Rutter Urban Forestry. The wood cookie was placed in a consumer freezer. For isolation, 3-6mm sections of infected heartwood from freshly exposed portions of the cookie were aseptically removed using a flame-sterilized scalpel.

The sterile conk and wood fragments were placed on 2% modified malt extract agar (20g malt extract, 20g agar powder, 1g yeast extract, 1L distilled water) with the addition of a very small amount of powdered antibiotic no larger than the tip of a ballpoint pen (1:1 of penicillin G and streptomycin sulphate). These were reproduced in triplicate for each attempt and left to incubate in the dark at room temperature (20 ºC ± 2º C). After about a week to two weeks (strain dependent), a slow-growing mycelium would begin to colonize the agar surface or form aerially on the surface of the inoculation fragments (Figure 2-2). Occasionally, axenic culture would arise from all pieces placed on the agar surface. More often than not, these cultures would require serial transfers. Contamination by various ascomycetes and some basidiomycetous wood decay fungi was relatively common in this technique.

Table 2-1. Strain location and isolation method

Strain	Location	Coordinates	Isolation Method
IOB1	Dorian, Ontario	48.47004° N, 88.41471° W	Sterile conk biopsy
IOB2	Dorian, Ontario	48.46376° N, 88.41399° W	Sterile conk biopsy
IOB3	Lappe, Ontario	48.67477° N, 89.32907° W	Infected wood isolation
IOB5	Thunder Bay, Ontario	48.25588° N, 89.15317° W	Sterile conk biopsy

Figure 2-1. Sterile conk fragments

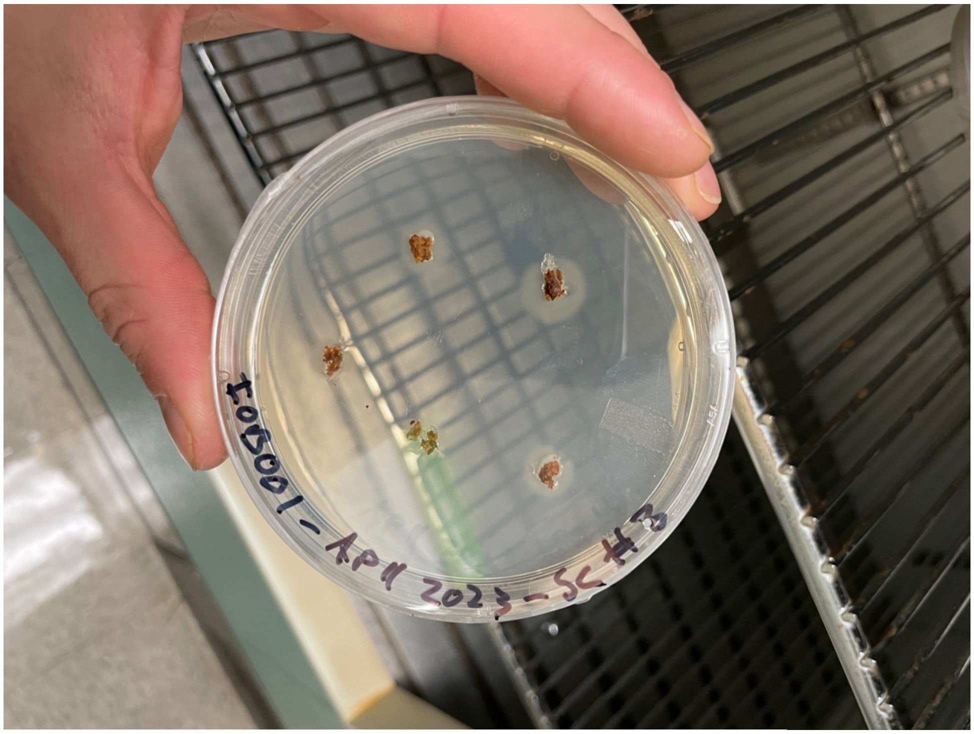

Figure 2-2. Culture from sterile conk fragments

STRAIN SPECIES IDENTIFICATION

Each strain had the Internal Transcribed Spacer (ITS) region sequenced by Ohio Mushroom DNA Lab (OMDL) using high-throughput Oxford Nanopore technology (Canan *et al.* 2024). OMDL is a community-based lab working in parallel with the Fungal Diversity Survey (FUNDIS) and Mycota Labs to provide free and affordable fungal sequencing for the public and to explore fungal diversity while also setting the stage for descriptions of novel taxa through high-throughput ITS barcoding (Canan *et al.* 2024). Dehydrated tissue biopsies of strains IOB1, IOB2, IOB3, and IOB5 were sent to OMDL in sealed centrifuge tubes placed in labelled plastic bags following the sample protocol outlined in Canan *et al*. (2024). All strains were associated with an iNaturalist observation number for organization in the tagged primer workflow, where posted ITS sequences can be viewed (Table 2-2). OMDL completed DNA extraction, indexed PCR, Nanopore ITS barcode sequencing, and sequence validation through GenBank/MycoMap using the MycoBLAST and NCBI BLAST tools (Canan *et al.* 2024). They followed the protocol developed by Russell (2023), founder of Mycota Labs. Therefore, see Canan *et al.* (2024) and Russell (2023) for these protocols. All strains (IOB1, IOB2, IOB3, and IOB5) were 99-100% matches to *I. obliquus* sequences available on the NCBI database, confirming their identity (Table 2-2).

Table 2-2. Strain confirmation

Strain	Identified Species	iNaturalist Observation No.	Closest GenBank Accession No.	Similarity (%)
IOB1	*Inonotus obliquus*	229513477	KT693232	99.70
IOB2	*Inonotus obliquus*	229513540	KT693232	100.00
IOB3	*Inonotus obliquus*	229513598	KT693232	99.85
IOB5	*Inonotus obliquus*	229513640	OR122500	99.50

MEDIA RECIPES

Four different core media types were utilized where each had a full nutrition and a starved nutrition variant, resulting in eight total media types: modified 2% malt extract agar (full nutrition and starved) (MEF/MES), carrot agar (full nutrition and starved) (CAF/CAS), birch agar (full nutrition and starved) (BAF/BAS), and chaga agar (full nutrition and starved) (CAF/CAS). The starved media had half the carbon of the full media. The following are recipes for these media:

Malt Extract Agar (MEA)

MEA full (MEF)

20g malt extract
15g agar powder
1g yeast extract
1 L distilled water

MEA starved (MES)

10g malt extract
15g agar powder
1g yeast extract
1 L distilled water

Instructions for MEA media

All ingredients were added to a 2 L flask, the mouth was covered with aluminum foil, and autoclaved. Once autoclaved and cooled, the mixture was poured into 9 cm Petri dishes.

Carrot Agar

Carrot agar full (CAF)

Flask 1:
300g chopped carrots
400ml distilled water

Flask 2:
14g agar powder
400ml distilled water

Carrot agar starved (CAS)

Flask 1:
150g chopped carrots

400ml distilled water

Flask 2:
14g agar powder
400ml distilled water

Instructions for carrot media

For Flask 1, 300g or 150g of chopped carrots and 400ml of distilled water were added to a blender and blended until homogenous and smooth. The carrot mixture was added to a 1 L flask, the mouth was covered with aluminum foil, and autoclaved. For Flask 2, all ingredients all ingredients were added to a 1 L flask, the mouth was covered with aluminum foil, and autoclaved. Once both flasks were substantially cooled, the contents of Flask 2 were poured into Flask 1. The flask with the combined ingredients was swirled until the contents were homogeneous and was poured into 9cm Petri dishes.

Birch Agar

Birch agar full (BAF)

100g white birch sawdust
20g malt extract
15g agar powder
1 L distilled water

Birch agar starved (BAS)

100g white birch sawdust
10g malt extract
15g agar powder
1 L distilled water

Instructions for birch media

100g of birch sawdust and 1 L of distilled water was added to a 2 L flask and placed on a laboratory-grade hot plate. The hot plate did not have an exact temperature gauge, but was set to a medium-low setting. The 2 L flask with distilled water and birch sawdust was simmered for 3 hours to extract from the birch sawdust and left to cool overnight at room temperature. The following day, distilled water was added to the 2 L flask until the total contents measured 1 L to partially account for water lost during extraction. Then, the malt extract and agar powder were added to the 2 L flask, stirred, the mouth was wrapped with aluminum foil, and autoclaved. Once cooled, the contents were poured into 9mm Petri dishes. One must ensure that the flask is frequently agitated while pouring to keep the birch sawdust in suspension as it settles to the bottom of the flask when left to rest.

Chaga Agar

Chaga agar full (CHF)

75g medium-sized sterile conk fragments (chaga)
20g malt extract
15g agar powder
1 L distilled water

Chaga agar starved (CHS)

75g medium-sized sterile conk fragments (chaga)
10g malt extract
15g agar powder
1 L distilled water

Instructions for chaga media

75g of sterile conk fragments and 1 L of distilled water was added to a 2 L flask and placed on a laboratory-grade hot plate. The hot plate did not have an exact temperature gauge, but was set to a medium-low setting. The 2 L flask with distilled water and sterile conk fragments was simmered for 3 hours to extract from the sterile conk fragments and left to cool overnight at room temperature. The following day, the extraction was strained to remove large fragments of sterile conk. Distilled water was added to the 2 L flask until the total contents measured 1 L to partially account for water lost during extraction. Then, the malt extract and agar powder were added to the 2 L flask, stirred, the mouth was wrapped with aluminum foil, and autoclaved. Once cooled, the contents were poured into 9mm Petri dishes. In the future, Millipore filtration could be used to avoid autoclaving the chaga infusion, which can destroy heat sensitive stimulatory compunds.

LINEAR GROWTH AND LONG-TERM FRUITING OF *INONOTUS OBLIQUUS* ON DIFFERENT MEDIA

The linear growth (colony diameter (cm)) and fruiting capacity of the four isolated strains of *I. obliquus* (IOB1, IOB2, IOB3, and IOB5) were tested on eight different media (MEF, MES, CAF, CAS, BAF, BAS, CHF, and CHS). Additionally, half of all Petri dishes were oriented either vertically (V) or horizontally (H) to examine if varying gravity stimuli would affect fruiting body initiation. In total, this experiment used 320 9cm Petri dishes with five replicates per treatment combination (4 strains x 8 media x 2 plate orientations x 5 replicates = 320). The 320 plates were inoculated with four different strains of *I. obliquus* equally over 36 hours. The inoculum for each strain was grown on carrot agar (CAF) in complete darkness at room temperature (20°C ± 2) for 2-3 weeks. A 7mm cork borer was used to aseptically cut agar plugs from the colony margin of each respective strain and transferred into the centre of a sterile Petri dish of one of the eight media. The inoculated dishes were incubated at room temperature (20°C ± 2) in complete darkness for 40 days. For the first four weeks, measurements of colony linear growth diameter (cm) were taken with a graduated ruler every week in four directions. Two lines were drawn on the lid of each Petri dish that intersected perpendicularly at their inoculation points. This ensured that measurements would always be taken in the same direction and angle. The radius of colony growth was taken from the margin of the 7mm agar plug to the margin of the growing colony in all four directions, averaged, and multiplied by two to get an accurate measurement of colony diameter. A fully grown colony was considered to be 8 cm, as opposed to 9 cm, since the colonizable agar surface is approximately 8.7 cm, minus the diameter of the 7 mm inoculation plug, which was not included in the measurements. Thus, this accurately represented colony linear growth diameter.

After 40 days of incubation in complete darkness at room temperature (20 ºC ± 2 ºC), all plates of *I. obliquus* mycelium were fully or nearly fully colonized and placed into a fruiting chamber that was modulated randomly between 15 ºC and 20 °C over six months. This chamber contained a series of blue light LED strips (KUNOVA 5V USB Powered LED) set to turn on and off every 12 hours (12/12 light cycle). Four sets of 1m blue LED strips were placed at different positions in the incubator (Figure 2-3). Plates were frequently shuffled to ensure that light was evenly distributed for each replicate. Colonies were scored for fruiting body formation after three and six months of incubation. Petri dishes were given a fruiting score of "0" to represent no fruiting and "1" to describe that a fertile poroid fruiting body had formed.

Figure 2-3. Blue light incubator

SHORT-TERM FRUITING OF *INONOTUS OBLIQUUS* ON MEA IN DIFFERENT LIGHT CONDITIONS

A total of 180 2% modified MEA (MEF) Petri dishes were aseptically inoculated with four strains (IOB1, IOB2, IOB3, IOB5) of *I. obliquus* in equal proportion. Three different light conditions were tested for fruiting body stimulation: blue light (BL) (12/12), white light (WL) (12/12), and complete darkness (DK). Additionally, plates were oriented in three different directions, face-up (UP), face-down (DW) or vertical (VR). There were five replicates for all possible combinations of the above treatments. Inoculum was also sourced from 7mm diameter agar plugs cut from the margin of colonies growing on carrot agar (CAF) at room temperature (20 ºC ± 2 ºC) for 2-3 weeks in complete darkness. Agar plugs were aseptically transferred into the centre of all 180 plates on the same day. Following inoculation, the colonies were incubated in complete darkness at room temperature (20 ºC ± 2 ºC) for 40 days. After incubation, a third of all plates remained in complete darkness, a third was placed in an incubator with a single blue light LED strip (KUNOVA 5V USB Powered LED), and the other third was placed in an incubator with a single white light LED strip (UVTaoYuan 5V 6000K USB Powered LED). All incubators were maintained at room temperature (20 ºC ± 2 ºC). Cultures were examined weekly for fruiting body formation over 11 weeks. Petri dishes were given a fruiting score of "0" to represent no fruiting and "1" to describe that a fertile poroid fruiting body had formed.

PHOTOGRAPHY AND MICROSCOPY

Photographs of colonies and fruitbodies were taken with an iPhone 12 or a Fujifilm XT-1. A Nikon Eclipse e400 or an Olympus IX51 were used for brightfield or phase contrast microscopy. For fruiting body microscopy, basidiomata were cut from the agar surface and dehydrated. Sections of fruitbodies were cut as thin as possible by hand using a fresh razor blade (Figure 2-4). The small sections were transferred onto a slide with a moistened insect pin and mounted in water or 2% KOH (Figure 2-5). A typical workflow would consist of taking microscopic images with the Fujifilm-XT1 and measuring structures with ImageJ. Photos on the iPhone 12 could not be measured digitally accurately, as it was held up to the eyepiece at an unfixed position. Unfortunately, many of the photos on the Fujifilm-XT1 were corrupted, meaning they could not be measured in the typical workflow. As a result, most microscope images were taken with an iPhone 12 and were not measured. Therefore, many images do not have scale bars associated with them, but microscopic characters matched those in the description in Chapter 1 during preliminary analysis (not shown). For publication, microscopy will be redone on the stored dehydrated fruit bodies, but for this thesis, these photos will suffice.

Figure 2-4. Razor blade and dried fruit body

Figure 2-5. Fruiting body fragments (insect pin for scale)

STATISTICAL ANALYSIS

RStudio (Version 2024.12.0+467) was the primary software used for statistical analysis in combination with Microsoft Excel Version 16.89. To analyze the linear growth diameter (cm) of *I. obliquus* on different media, a linear mixed-effects model (LMM) was run using the lme4 package in RStudio. The response was continuous **Diameter** (cm), the fixed effects were **Strain**, **Week**, **Media**, and **Gravity** and the random effect was for the replicates of all combined treatments **(1 | Replicate)**, such that they could be tracked over four weeks of growth by having random intercepts. This was chosen because a standard generalized linear model (GLM) assumes that growth measurements of the same plate at different weeks are independent (Nimon, 2012). Long-term fruiting (6 months) on these different media had very obvious results and were presented as a summary of means. To analyze the effects of different light conditions and strain on MEA, a binomial logit GLM was run. The response was binomial **Fruited** (0 = no FB, 1 = FB formation), the fixed effects were **Light**, **Strain,** and **Gravity.** There were thousands of data points for these models; thus, the data were not included in Appendix I. The raw data can be accessed at: https://drive.google.com/drive/folders/1VLlqVjnD_PMogZcO8XQ2MCgppRHfiZrJ?usp=drive_link

RESULTS

LINEAR GROWTH EXPERIMENTATION ON DIFFERENT MEDIA

Through a series of likelihood ratio tests (LRT) and AIC comparisons, it was found that a model with a full 3-way interaction between predictors had the best fit. LRTs are widely used in biological research for model selection (Lewis *et al.* 2011). These tests compared full models and reduced models that did not contain the predictor factor of interest. The effect of **Gravity** (plate orientation) was negligible and not included as a fixed effect. A Wald Chi-square ANOVA (Table 2-3) on the 3-way interaction linear mixed effects model (LMM) revealed that the main effects of Media, Strain, Week, all their two-way interactions (Week:Media, Week:Strain, and Media:Strain), and their three-way interaction (Week:Media:Strain) all had statistically significant effects on colony growth diameter (cm) ($p < 0.05$) (Table 2-3). A Post-hoc analysis of the main effects and their interactions was completed through the use of the emmeans()function from the emmeans package, followed by their summary to extract estimated colony diameter, a Tukey-adjusted pairwise comparison using pairs(), and a summarization of significant pairwise contrasts using a compact letter display (CLD) generated from the cld() function from the emmeans package. As there are over 8000 three-way interaction pairwise contrasts (Media * Week * Strain), it was simplified for interpretation.

It was known that the diameter means would differ week to week (through linear growth); thus, those interactions were analyzed by completing analyses by week or overall. Many interactions in the full 3-way framework (Media * Week * Strain) were partially redundant, as changes in growth over time were expected. Therefore, the response of media was analyzed by week and strain (Media | Strain * Week). Any analyses, such as the main effects of media (Media), strain (Strain), or interactions between media and strain (Media: Strain), are averaged over every week. Many figures and tables of this analysis are included in Appendix I. The most meaningful results are presented here for simplification of outputs.

Table 2-3. Wald-Chi-Square ANOVA

Effect	Chisq	df	p-value
(Intercept)	153.159	1	< 0.0001
Week	2271.753	3	< 0.0001
Media	226.822	7	< 0.0001
Strain	16.949	3	0.0007
Week:Media	1009.466	21	< 0.0001
Week:Strain	110.191	9	< 0.0001
Media:Strain	89.008	21	< 0.0001
Week:Media:Strain	1250.031	63	< 0.0001

The Effect of Media by Week and Strain

The modified 3-way comparison (Media | Week * Strain) analyzed the effects of different media on colony diameter (cm) by the interaction of week and strain. This yielded a more interpretable and reduced output, which had 287 significant contrasts of 560 total contrasts ($p < 0.05$) (See https://drive.google.com/drive/folders/1VLlqVjnD_PMogZcO8XQ2MCgppRHfiZrJ?usp=drive_link for significant contrasts). The most meaningful and informative results are in this analysis, as we can identify exactly under what conditions media differed. Significant contrasts were summarized as a compact letter display (CLD). Each plot is a bar graph representing a week (1-4) and is grouped by strain to represent how media types differ under these conditions (Figures 2-6 to 2-9). The estimated diameter means of these conditions, along with a CLD, are displayed (Tables 2-4 to 2-7).

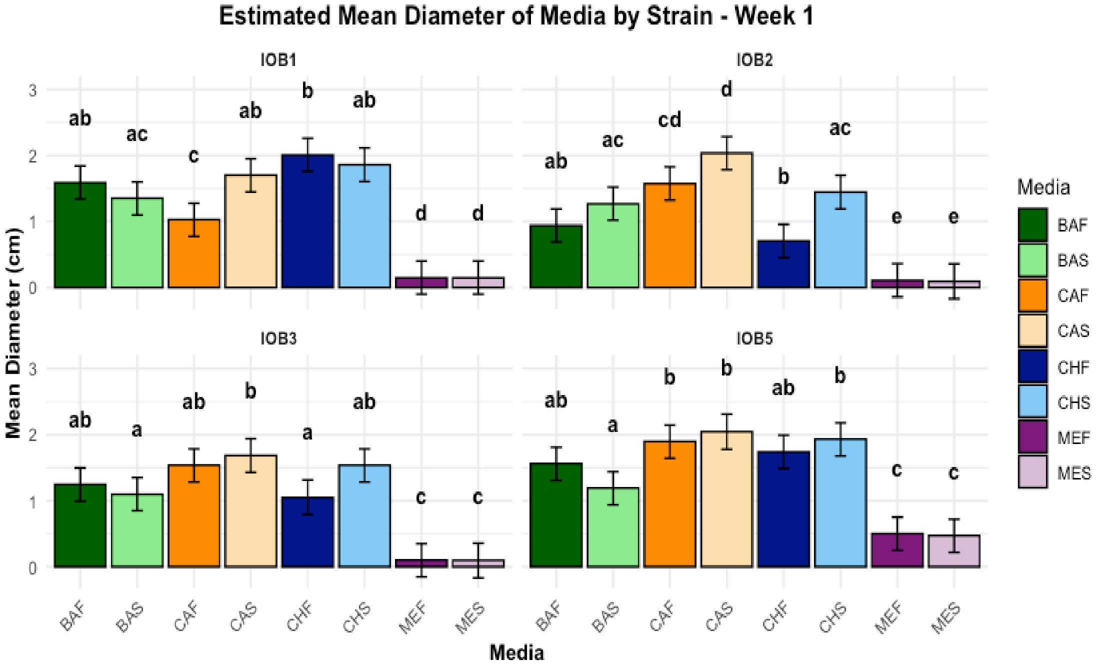

Figure 2-6. Estimated mean diameter of media by strain – week 1.
Error bar: 95% confidence interval

Table 2-4. Estimated mean diameter of media by strain – week 1

Media	Strain	Week	Estimated Diameter (cm)	SE	df	95% CoI: L	95% CoI: U	CLD
BAF	IOB1	1	1.59	0.13	924.02	1.34	1.84	ab
BAS	IOB1	1	1.35	0.13	924.02	1.10	1.60	ac
CAF	IOB1	1	1.03	0.13	924.02	0.78	1.28	c
CAS	IOB1	1	1.70	0.13	924.02	1.45	1.95	ab
CHF	IOB1	1	2.01	0.13	924.02	1.76	2.26	b
CHS	IOB1	1	1.86	0.13	924.02	1.61	2.11	ab
MEF	IOB1	1	0.15	0.13	924.02	-0.10	0.40	d
MES	IOB1	1	0.15	0.13	924.02	-0.10	0.40	d
BAF	IOB2	1	0.94	0.13	924.02	0.69	1.19	ab
BAS	IOB2	1	1.27	0.13	924.02	1.02	1.52	ac
CAF	IOB2	1	1.58	0.13	924.02	1.32	1.83	cd
CAS	IOB2	1	2.04	0.13	924.02	1.78	2.29	d
CHF	IOB2	1	0.70	0.13	924.02	0.45	0.96	b
CHS	IOB2	1	1.45	0.13	924.02	1.19	1.70	ac
MEF	IOB2	1	0.11	0.13	924.02	-0.14	0.36	e
MES	IOB2	1	0.09	0.13	972.03	-0.17	0.36	e

Table 2-4. cont'd

BAF	IOB3	1	1.24	0.13	924.02	0.99	1.50	ab
BAS	IOB3	1	1.10	0.13	924.02	0.85	1.35	a
CAF	IOB3	1	1.54	0.13	924.02	1.28	1.79	ab
CAS	IOB3	1	1.69	0.13	924.02	1.43	1.94	b
CHF	IOB3	1	1.05	0.13	972.03	0.79	1.32	a
CHS	IOB3	1	1.54	0.13	924.02	1.28	1.79	ab
MEF	IOB3	1	0.10	0.13	924.02	-0.15	0.35	c
MES	IOB3	1	0.10	0.13	972.03	-0.17	0.36	c
BAF	IOB5	1	1.56	0.13	924.02	1.31	1.81	ab
BAS	IOB5	1	1.19	0.13	924.02	0.94	1.44	a
CAF	IOB5	1	1.90	0.13	924.02	1.64	2.15	b
CAS	IOB5	1	2.05	0.13	972.03	1.78	2.31	b
CHF	IOB5	1	1.74	0.13	924.02	1.49	1.99	ab
CHS	IOB5	1	1.93	0.13	924.02	1.68	2.18	b
MEF	IOB5	1	0.50	0.13	924.02	0.25	0.75	c
MES	IOB5	1	0.47	0.13	924.02	0.22	0.72	c

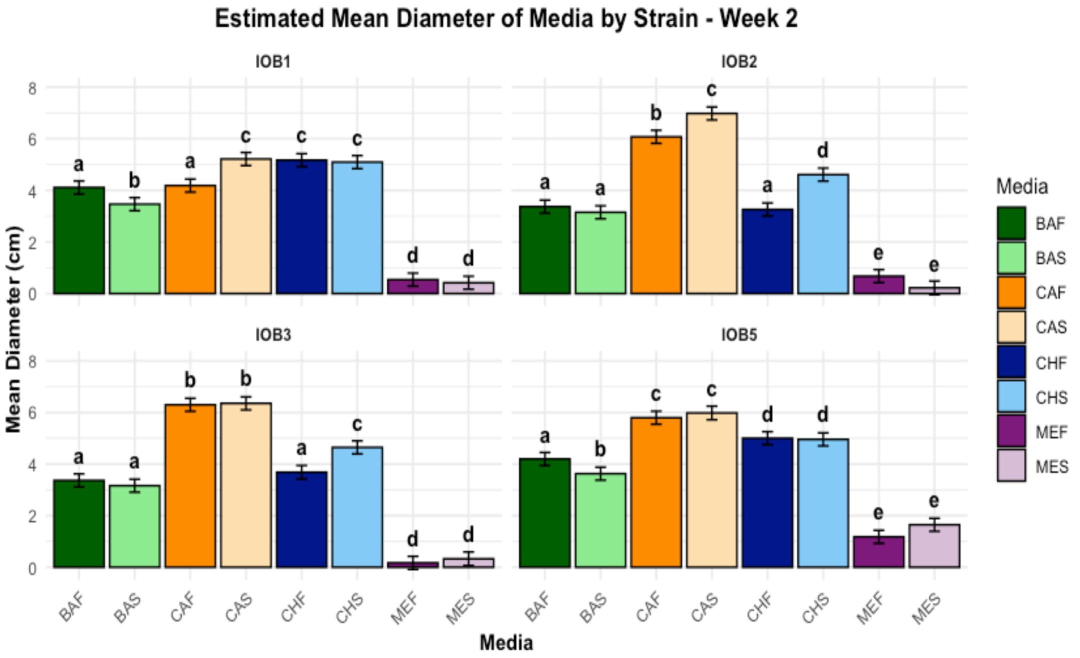

Figure 2-7. Estimated mean diameter of media by strain – week 2. Error bar: 95% confidence interval

Table 2-5. Estimated mean diameter of media by strain – week 2

Media	Strain	Week	Estimated Diameter (cm)	SE	df	95% CoI: L	95% CoI: U	CLD
BAF	IOB1	2	4.11	0.13	924.02	3.86	4.36	a
BAS	IOB1	2	3.47	0.13	924.02	3.21	3.72	b
CAF	IOB1	2	4.18	0.13	924.02	3.93	4.44	a
CAS	IOB1	2	5.21	0.13	924.02	4.96	5.47	c
CHF	IOB1	2	5.17	0.13	924.02	4.92	5.42	c
CHS	IOB1	2	5.09	0.13	924.02	4.84	5.35	c
MEF	IOB1	2	0.54	0.13	924.02	0.29	0.79	d
MES	IOB1	2	0.42	0.13	924.02	0.17	0.67	d
BAF	IOB2	2	3.37	0.13	924.02	3.12	3.62	a
BAS	IOB2	2	3.15	0.13	924.02	2.90	3.40	a
CAF	IOB2	2	6.08	0.13	924.02	5.82	6.33	b
CAS	IOB2	2	6.98	0.13	924.02	6.73	7.23	c
CHF	IOB2	2	3.26	0.13	924.02	3.01	3.51	a
CHS	IOB2	2	4.61	0.13	924.02	4.36	4.86	d
MEF	IOB2	2	0.67	0.13	924.02	0.42	0.93	e
MES	IOB2	2	0.22	0.13	972.03	-0.04	0.49	e
BAF	IOB3	2	3.36	0.13	924.02	3.11	3.62	a
BAS	IOB3	2	3.16	0.13	924.02	2.91	3.41	a
CAF	IOB3	2	6.30	0.13	924.02	6.04	6.55	b
CAS	IOB3	2	6.35	0.13	924.02	6.10	6.60	b
CHF	IOB3	2	3.68	0.13	972.03	3.42	3.94	a
CHS	IOB3	2	4.65	0.13	924.02	4.39	4.90	c
MEF	IOB3	2	0.17	0.13	924.02	-0.08	0.42	d
MES	IOB3	2	0.33	0.13	972.03	0.06	0.59	d
BAF	IOB5	2	4.20	0.13	924.02	3.94	4.45	a
BAS	IOB5	2	3.63	0.13	924.02	3.37	3.88	b
CAF	IOB5	2	5.80	0.13	924.02	5.54	6.05	c
CAS	IOB5	2	5.98	0.13	972.03	5.71	6.24	c
CHF	IOB5	2	5.00	0.13	924.02	4.75	5.25	d
CHS	IOB5	2	4.96	0.13	924.02	4.70	5.21	d
MEF	IOB5	2	1.18	0.13	924.02	0.93	1.43	e
MES	IOB5	2	1.65	0.13	924.02	1.39	1.90	e

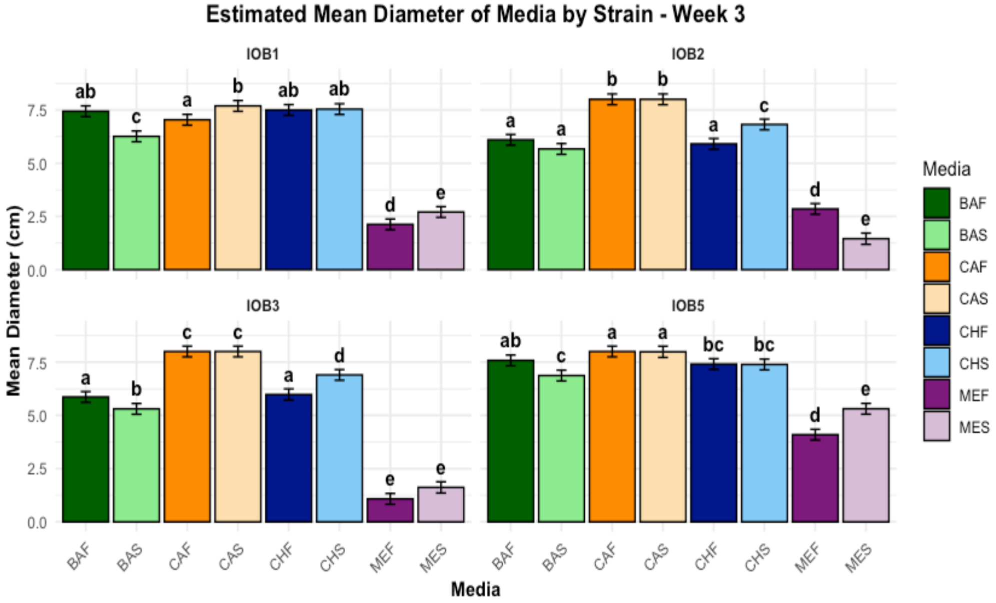

Figure 2-8. Estimated mean diameter of media by strain – week 3.
Error bar: 95% confidence interval

Table 2-6. Estimated mean diameter of media by strain – week 3

Media	Strain	Week	Estimated Diameter (cm)	SE	df	95% CoI: L	95% CoI: U	CLD
BAF	IOB1	3	7.44	0.13	924.02	7.19	7.69	ab
BAS	IOB1	3	6.26	0.13	924.02	6.01	6.51	c
CAF	IOB1	3	7.04	0.13	924.02	6.79	7.29	a
CAS	IOB1	3	7.69	0.13	924.02	7.44	7.94	b
CHF	IOB1	3	7.50	0.13	924.02	7.25	7.75	ab
CHS	IOB1	3	7.54	0.13	924.02	7.29	7.79	ab
MEF	IOB1	3	2.13	0.13	924.02	1.88	2.38	d
MES	IOB1	3	2.71	0.13	924.02	2.46	2.96	e
BAF	IOB2	3	6.10	0.13	924.02	5.85	6.35	a
BAS	IOB2	3	5.67	0.13	924.02	5.42	5.92	a
CAF	IOB2	3	8.00	0.13	924.02	7.75	8.25	b
CAS	IOB2	3	8.00	0.13	924.02	7.75	8.25	b
CHF	IOB2	3	5.91	0.13	924.02	5.66	6.16	a
CHS	IOB2	3	6.82	0.13	924.02	6.57	7.07	c
MEF	IOB2	3	2.86	0.13	924.02	2.60	3.11	d
MES	IOB2	3	1.46	0.13	972.03	1.19	1.72	e

Table 2-6. cont'd

BAF	IOB3	3	5.86	0.13	924.02	5.61	6.12	a
BAS	IOB3	3	5.31	0.13	924.02	5.05	5.56	b
CAF	IOB3	3	8.00	0.13	924.02	7.75	8.25	c
CAS	IOB3	3	8.00	0.13	924.02	7.75	8.25	c
CHF	IOB3	3	5.98	0.13	972.03	5.72	6.25	a
CHS	IOB3	3	6.90	0.13	924.02	6.65	7.15	d
MEF	IOB3	3	1.08	0.13	924.02	0.83	1.33	e
MES	IOB3	3	1.62	0.13	972.03	1.36	1.88	e
BAF	IOB5	3	7.58	0.13	924.02	7.33	7.83	ab
BAS	IOB5	3	6.87	0.13	924.02	6.62	7.12	c
CAF	IOB5	3	8.00	0.13	924.02	7.75	8.25	a
CAS	IOB5	3	7.98	0.13	972.03	7.72	8.25	a
CHF	IOB5	3	7.41	0.13	924.02	7.16	7.66	bc
CHS	IOB5	3	7.39	0.13	924.02	7.14	7.64	bc
MEF	IOB5	3	4.10	0.13	924.02	3.84	4.35	d
MES	IOB5	3	5.31	0.13	924.02	5.06	5.56	e

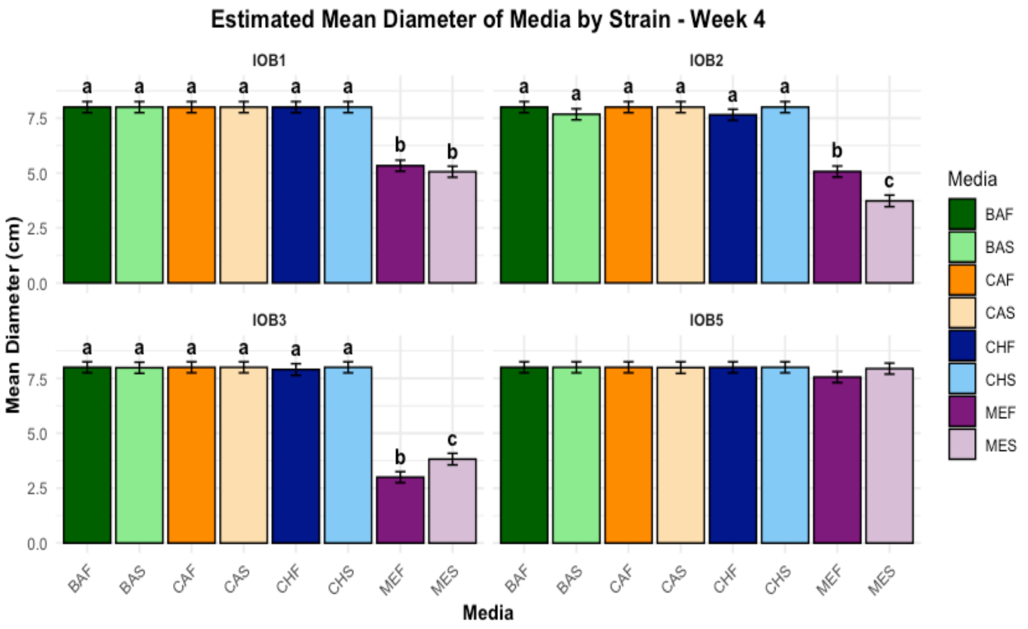

Figure 2-9. Estimated mean diameter of media by strain – week 4.
Error bar: 95% confidence interval

Table 2-7. Estimated mean diameter of media by strain – week 4

Media	Strain	Week	Estimated Diameter (cm)	SE	df	95% CoI: L	95% CoI: U	CLD
BAF	IOB1	4	8.00	0.13	924.02	7.75	8.25	a
BAS	IOB1	4	8.00	0.13	924.02	7.75	8.25	a
CAF	IOB1	4	8.00	0.13	924.02	7.75	8.25	a
CAS	IOB1	4	8.00	0.13	924.02	7.75	8.25	a
CHF	IOB1	4	8.00	0.13	924.02	7.75	8.25	a
CHS	IOB1	4	8.00	0.13	924.02	7.75	8.25	a
MEF	IOB1	4	5.34	0.13	924.02	5.08	5.59	b
MES	IOB1	4	5.06	0.13	924.02	4.81	5.31	b
BAF	IOB2	4	8.00	0.13	924.02	7.75	8.25	a
BAS	IOB2	4	7.68	0.13	924.02	7.42	7.93	a
CAF	IOB2	4	8.00	0.13	924.02	7.75	8.25	a
CAS	IOB2	4	8.00	0.13	924.02	7.75	8.25	a
CHF	IOB2	4	7.66	0.13	924.02	7.40	7.91	a
CHS	IOB2	4	8.00	0.13	924.02	7.75	8.25	a
MEF	IOB2	4	5.07	0.13	924.02	4.82	5.32	b
MES	IOB2	4	3.73	0.13	972.03	3.47	4.00	c
BAF	IOB3	4	8.00	0.13	924.02	7.75	8.25	a
BAS	IOB3	4	7.98	0.13	924.02	7.73	8.23	a
CAF	IOB3	4	8.00	0.13	924.02	7.75	8.25	a
CAS	IOB3	4	8.00	0.13	924.02	7.75	8.25	a
CHF	IOB3	4	7.90	0.13	972.03	7.64	8.16	a
CHS	IOB3	4	8.00	0.13	924.02	7.75	8.25	a
MEF	IOB3	4	3.00	0.13	924.02	2.75	3.25	b
MES	IOB3	4	3.82	0.13	972.03	3.56	4.08	c
BAF	IOB5	4	8.00	0.13	924.02	7.75	8.25	a
BAS	IOB5	4	8.00	0.13	924.02	7.75	8.25	a
CAF	IOB5	4	8.00	0.13	924.02	7.75	8.25	a
CAS	IOB5	4	7.99	0.13	972.03	7.72	8.25	a
CHF	IOB5	4	8.00	0.13	924.02	7.75	8.25	a
CHS	IOB5	4	8.00	0.13	924.02	7.75	8.25	a
MEF	IOB5	4	7.56	0.13	924.02	7.30	7.81	a
MES	IOB5	4	7.94	0.13	924.02	7.69	8.19	a

Summary of the effect of media on diameter by week and strain

It was found that depending on when (week 1, 2 , 3 or 4) and which strain was inoculated (IOB1, IOB2, IOB3, and IOB5), there is relatively high variability of the performance of media types. The most consistent result across all weeks and strains is that the malt extract media (MEF and MES) greatly underperformed relative to all media at all time frames. The only time this was not true is for IOB5 in the fourth week, where it was not seen as statistically significant from other media (Figure 2-9). Malt-extract-based media performed best for IOB5 (Figures 2-6 to 2-9). In the fourth week for all strains, there is the greatest homogeneity of media as they approach a fully colonized state (Figure 2-9). Generally, carrot-based media (CAF and CAS) are significantly better performers for colony diameter in weeks 2 and 3 (Figures 2-7 and 2-8). Overall, the first week shows a great level of heterogeneity during the early colonization stage, the second week shows a clearer stratification of media performance, the third week shows slightly clearer stratification and occasionally more homogeneity between non-malt-extract-based media, and the fourth week shows clear homogeneity of non-malt-extract-based media at full colonization (Figures 2-6 to 2-9). This analysis aims to visualize significant differences at fine-level interactions. More broad analyses of these trends will follow.

The Effect of Media Averaged over Strain - Overall

This analysis examines how different media affect colony diameter overall (across all weeks), averaged over strain. See Appendix I for week-to-week results. This analysis will show broader media difference trends and be represented graphically (Figure 2-10), through tabulation (Table 2-8), and summarized. Significant pairwise contrasts are presented in Appendix I. In total, 26 of 28 media contrasts were significant when averaged across weeks.

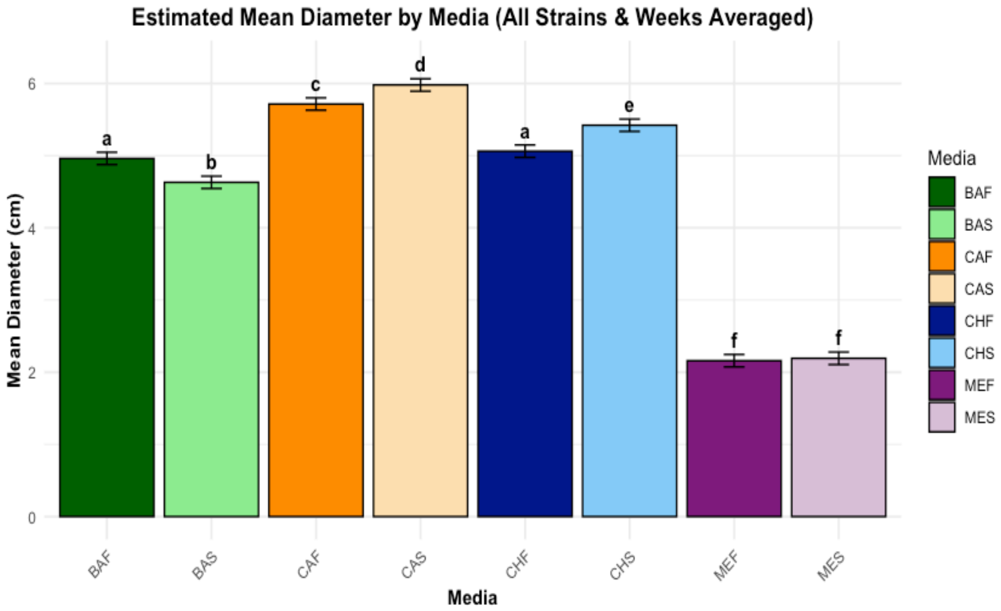

Figure 2-10. Estimated mean diameter by media – averaged.
Error bar: 95% confidence interval

Table 2-8. Estimated mean diameter by media - overall

Media	Estimated Diameter (cm)	SE	df	95% CoI: L	95% CoI: U	CLD
BAF	4.96	0.04	284.49	4.87	5.05	a
BAS	4.63	0.04	284.49	4.54	4.72	b
CAF	5.71	0.04	284.49	5.63	5.80	c
CAS	5.98	0.04	290.93	5.89	6.06	d
CHF	5.06	0.04	290.93	4.97	5.15	a
CHS	5.42	0.04	284.49	5.33	5.51	e
MEF	2.16	0.04	284.49	2.07	2.24	f
MES	2.19	0.04	297.40	2.11	2.28	f

Overall – summary

Averaged across weeks and strain, BAF, BAS, CAF, CAS, CHF, CHS, MEF, and MES had estimated diameters (cm) of 4.96 (4.87 – 5.05), 4.63 (4.54 – 4.72), 5.71 (5.63 -5.80), 5.98 (5.89 – 6.06), 5.06 (4.97 – 5.15), 5.42 (5.33 – 5.51), 2.16 (2.07 – 2.24), and 2.19 (2.11 -2.28) respectively. Malt-extract-based media (MEF-MES) (f) performed the worst and were significantly different (SigD) from all media, but were not significantly different (NSigD) from each other (f). BAF (a) and CHS (a) were SigD from all media, but were NSigD from each other. BAS (b), CAF (c), CAS (d), and CHS (e) were SigD from all media and were SigD from each other. Overall, CAS (d) performed best, followed by CAF (c), CHS (e), CHF (a) + BAF (a), BAS (b), and finally MEF (f) + MES (f).

The Effects of Strain Averaged over Media - Overall

This analysis examines how different strains affect colony diameter overall, averaged over media and weeks. See Appendix I for week-to-week results. This analysis will show broader strain difference trends and be represented graphically (Figure 2-11), through tabulation (Table 2-9), and summarized. Additionally, how each strain responded to the different media, averaged over weeks, is summarized in Appendix I. Significant pairwise contrasts are presented in Appendix I. Overall, 5 of 6 pairwise contrasts were SigD when averaged across strains.

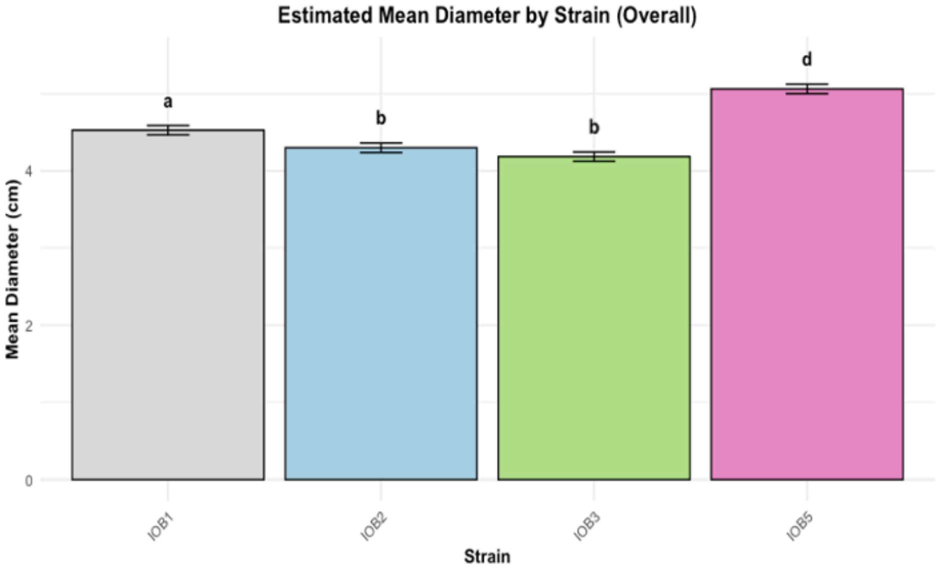

Figure 2-11. Estimated mean diameter by strain – overall.

Error bar: 95% confidence interval

Table 2-9. Estimated mean diameter by strain - overall

Strain	Estimated Diameter (cm)	SE	df	95% CoI: L	95% CoI: U	CLD
IOB1	4.52	0.03	284.49	4.46	4.58	a
IOB2	4.30	0.03	287.70	4.23	4.36	b
IOB3	4.18	0.03	290.93	4.12	4.24	b
IOB5	5.06	0.03	287.70	5.00	5.12	d

Overall – Summary

Overall, IOB1, IOB2, IOB3, and IOB5 had estimated diameters (cm) of 4.52 (4.46 – 4.58), 4.30 (4.23 – 4.36), 4.18 (4.12 – 4.24), and 5.06 (5.00 – 5.12), respectively. IOB1 (a) was SigD from all media and performed second best, IOB2 (b) and IOB3 (b) were SigD from all media, but were NSigD from each other and performed worst, IOB5 (c) was SigD from all media and performed best.

Notable Colony Characteristics

Unfortunately, many detailed photos of colony development and microscopy were corrupted and lost. Therefore, a comparison of the general colony density characteristics of IOB5 at week 2 and notable observations will be discussed; the best saved photos. CAF (Figure 2-12), CAS (Figure 2-12), BAF (Figure 2-14), BAS (Figure 2-14), CHF (Figure 2-15), and CHS (Figure 2-15) were relatively similar in linear growth diameter relative to MEF (Figure 2-13) and MES (Figure 2-13); the worst-performing media. However, the density of colonies was wildly different. Carrot media (CAF and CAS) by far grew with the most vigour, and produced thick cottony aerial mycelium. On the contrary, birch media (BAF and BAS) and chaga media (CHF and CHS) both produced relatively diffuse submerged colonies, which sometimes could barely be seen in certain cases. However, thin colonies still had reasonable diameters; therefore, linear growth diameter (cm) was still similar to CAF and CAS. Generally, colonies began growing hyaline and matured to mottled yellowish-brown (Figure 2-16) (see Chapter 1 for details on colony development). The prevalence of hyphal setae (Figure 2-17) seemed to be more common in mature colonies growing on carrot agar in thick aerial mats (Figure 2-16). These mats often became lacerate (leathery) in maturity. Typically, characteristics of hyphae, such as kinks, hyphal swellings, and anastomoses, changed when colonies were mature, and varied between media types, but no formal examination was made of these characters.

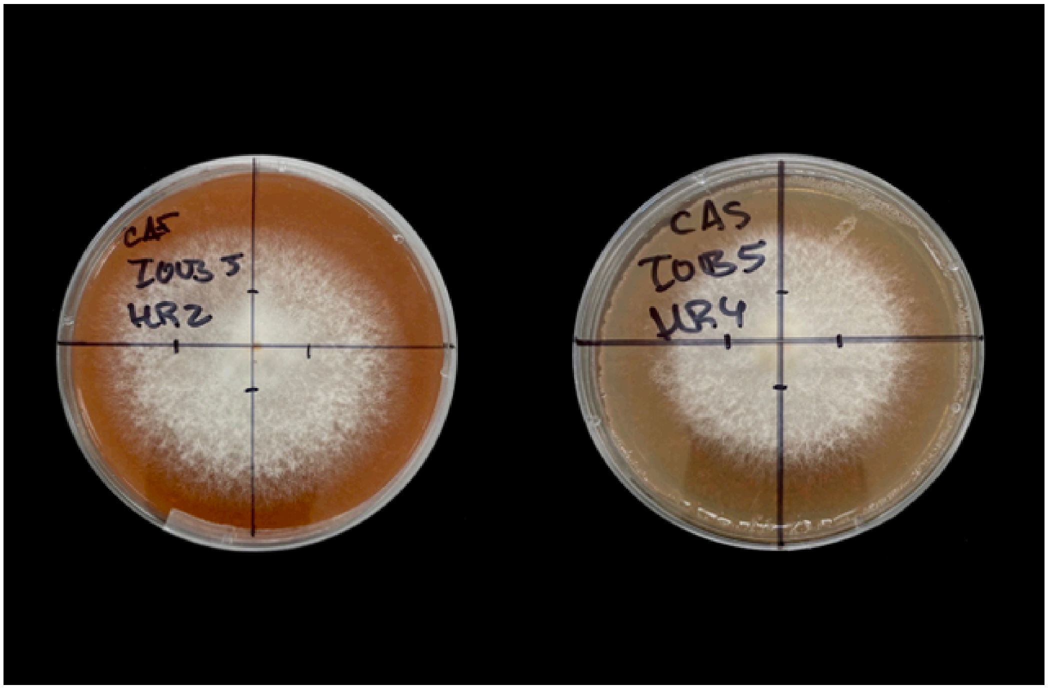

Figure 2-12. Culture characters of CAF – CAS (IOB5 – Week 2)

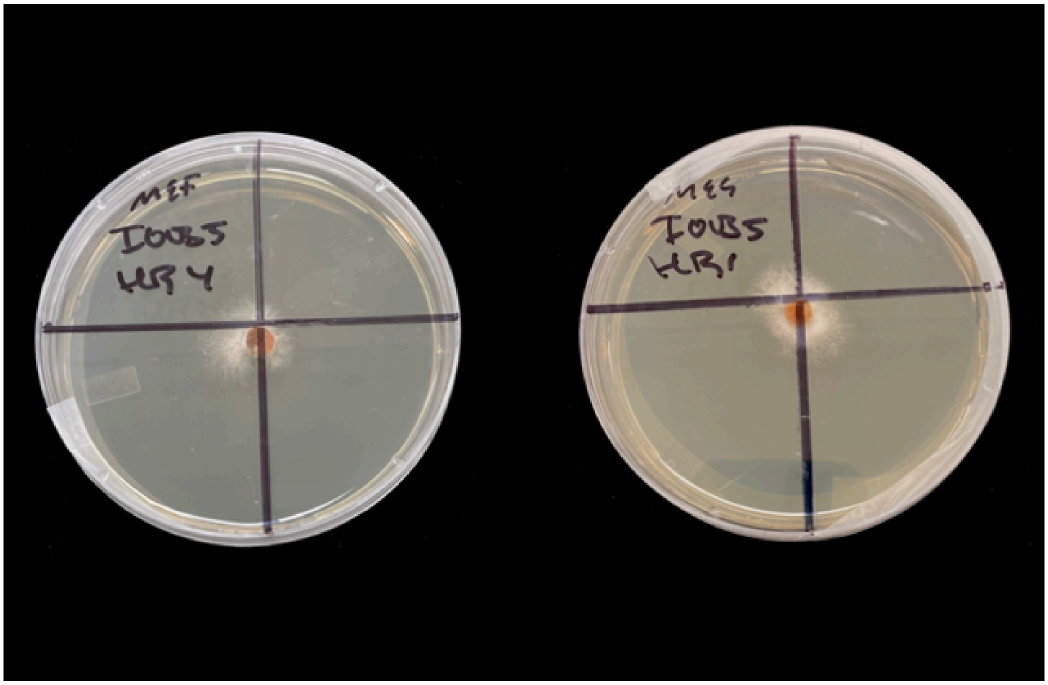

Figure 2-13. Culture characters of MEF – MES (IOB5 – Week 2)

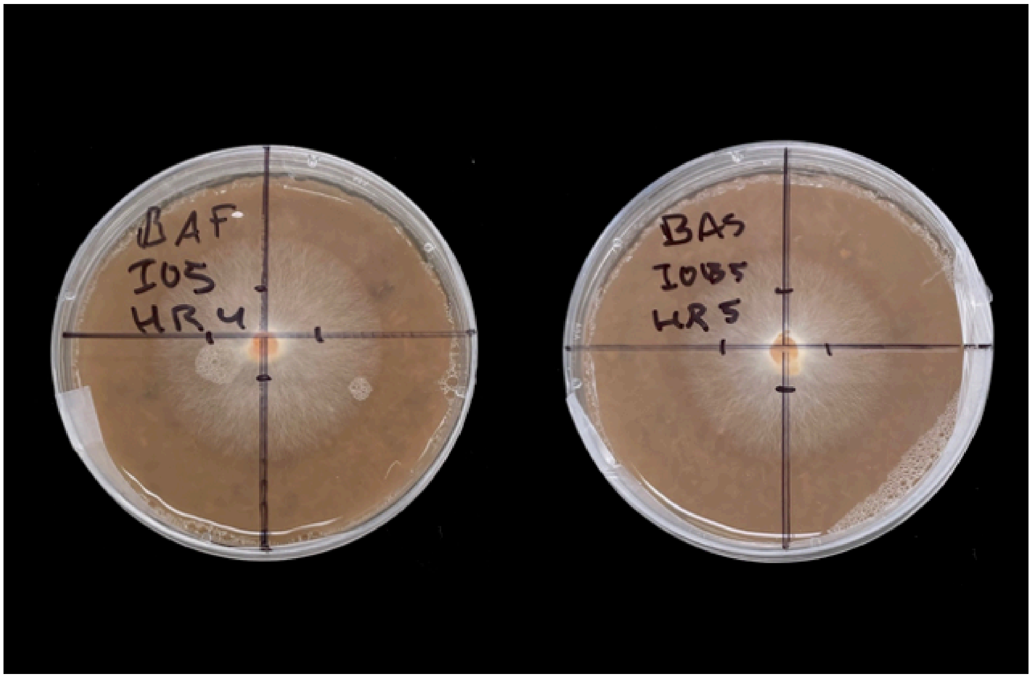

Figure 2-14. Culture characters of BAF – BAS (IOB5 – Week 2)

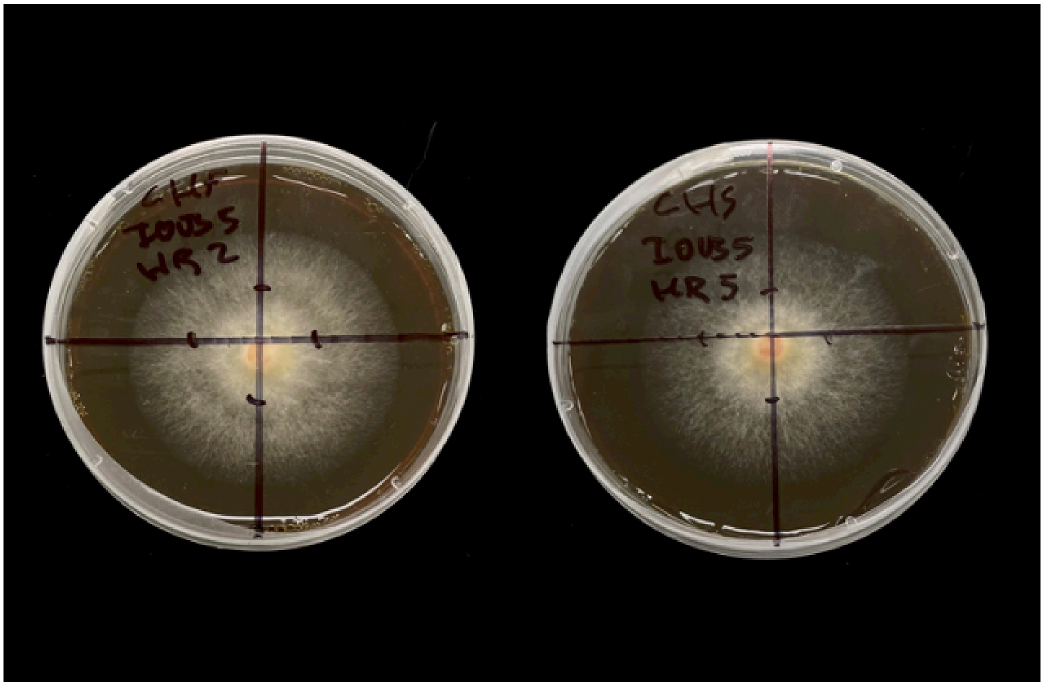

Figure 2-15. Culture characters of CHF – CHS (IOB5 – Week 2)

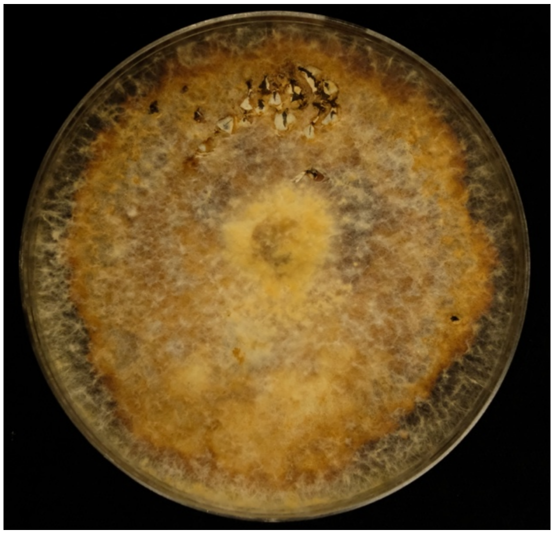

Figure 2-16. Mature culture on carrot agar (IOB2 – week 6)

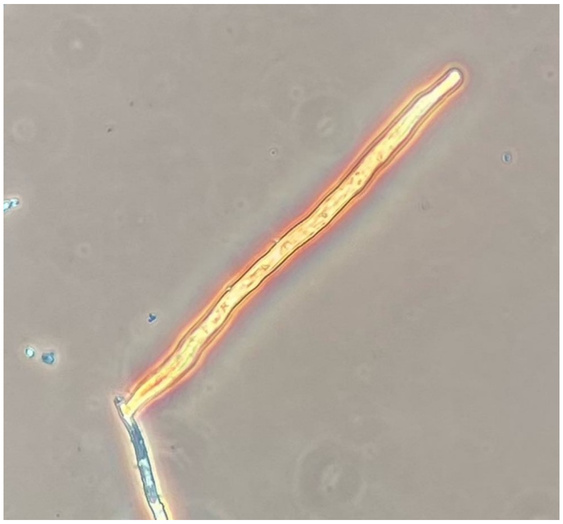

Figure 2-17. Hyphal setae in mature culture (IOB2 – Week 6)

FRUITING EXPERIMENTATION

Media Selection

This analysis will focus on fruiting data collected at six months to assess broad media performance. The fruiting capability of each strain is assessed in the short-term fruiting experiment following this. Half of the 320 plates were placed horizontally face-up, and the other half were placed vertically. Plate orientation did not appear to meaningfully impact fruiting body formation. Almost all media, except for MEF and MES, formed minimal fruit bodies across all strains (Table 2-10). As the results were evident in showing which media encouraged fruiting body formation, no formal statistical analysis is presented; only a summary of counts of fruited replicates by strain and averaged across strains is provided. This sufficed for media selection in these experiments.

Of the 320 plates, 51(15.94%) formed fruiting bodies after long-term 12/12 blue light incubation. Across all strains, cultures on BAF formed 0, BAS formed 1 (0.31% of 320, 2.50% of 40 replicates), CAF formed 1 (0.31% of 320, 2.50% of 40 replicates), CAS formed 0, CHF formed 2 (0.63% of 320, 5.00% of 40 replicates), CHS formed 3 (0.94% of 320, 7.50% of 40 replicates), MEF formed 27 (8.44% of 320, 67.50% of 40 replicates), and MES formed 17 (5.32% of 320, 42.50% of 40 replicates) (Table 2-10).

Table 2-10. All fruited plates after 6 months of light stimulation

Media	# of Fruited Plates	# of Total Plates	Fruited Plates (%)
BAF	0	40	0.00
BAS	1	40	2.50
CAF	1	40	2.50
CAS	0	40	0.00
CHF	2	40	5.00
CHS	3	40	7.50
MEF	27	40	67.50
MES	17	40	42.50

Each strain had a total of 80 plates. For IOB1, cultures on BAF, BAS, CAF, CAS, CHF, and CHS formed 0. Cultures on MEF formed 3 (3.75% of 80, 3.00% of 10 replicates), and MES formed 2 (2.5% of 80, 2.00% of 10 replicates) (Table 2-11). For IOB2, cultures on BAF, BAS, CAF, CAS, CHF, and CHS formed 0. Cultures on MEF formed 8 (10.00% of 80, 80.00% of 10 replicates), and MES formed 9 (11.25% of 80, 90.00% of 10 replicates) (Table 2-12). For IOB3, cultures on BAF, CAF, and CAS formed 0. Cultures on BAS formed 1 (1.25% of 80, 10.00% of 10 replicates), CHF formed 2 (2.5% of 80, 2.00% of 10 replicates), CHS formed 3 (3.75% of 80, 3.00% of 10 replicates), MEF formed 6 (7.50% of 80, 60.00% of 10 replicates), and MES formed 5 (6.25% of 100, 50.00% of 10 replicates) (Table 2-13). For IOB5, cultures on BAF, BAS, CAS, CHF, and CHS formed 0. Cultures on CAF formed 1 (1.25% of 80, 10.00% of 10 replicates), MEF formed 10 (10.00% of 80, 100.00% of 10 replicates), and MES formed 1 (1.25% of 80, 10.00% of 10 replicates) (Table 2-14).

Table 2-11. IOB1 fruited plates after 6 months of light stimulation

Strain	Media	# of Fruited Plates	# of Total Plates	Fruited Plates (%)
IOB1	BAF	0	10	0.00
IOB1	BAS	0	10	0.00
IOB1	CAF	0	10	0.00
IOB1	CAS	0	10	0.00
IOB1	CHF	0	10	0.00
IOB1	CHS	0	10	0.00
IOB1	MEF	3	10	30.00
IOB1	MES	2	10	20.00

Table 2-12. IOB2 fruited plates after 6 months of light stimulation

Strain	Media	# of Fruited Plates	# of Total Plates	Fruited Plates (%)
IOB2	BAF	0	10	0.00
IOB2	BAS	0	10	0.00
IOB2	CAF	0	10	0.00
IOB2	CAS	0	10	0.00
IOB2	CHF	0	10	0.00
IOB2	CHS	0	10	0.00
IOB2	MEF	8	10	80.00
IOB2	MES	9	10	90.00

Table 2-13. IOB3 fruited plates after 6 months of light stimulation

Strain	Media	# of Fruited Plates	# of Total Plates	Fruited Plates (%)
IOB3	BAF	0	10	0.00
IOB3	BAS	1	10	10.00
IOB3	CAF	0	10	0.00
IOB3	CAS	0	10	0.00
IOB3	CHF	2	10	20.00
IOB3	CHS	3	10	30.00
IOB3	MEF	6	10	60.00
IOB3	MES	5	10	50.00

Table 2-14. IOB5 fruited plates after 6 months of light stimulation

Strain	Media	# of Fruited Plates	# of Total Plates	Fruited Plates (%)
IOB5	BAF	0	10	0.00
IOB5	BAS	0	10	0.00
IOB5	CAF	1	10	10.00
IOB5	CAS	0	10	0.00
IOB5	CHF	0	10	0.00
IOB5	CHS	0	10	0.00
IOB5	MEF	10	10	100.00
IOB5	MES	1	10	10.00

By far, cultures on malt-extract-based media formed the most fruiting bodies and were the ideal fruiting media in this experiment (13.75% of 320, 55.00% of 80 replicates) (Table 2-10). MEF performed slightly better and is readily available in our laboratory; thus, it was chosen as the fruiting medium.

Short-term Fruiting on MEA in Different Light Conditions

For the short-term MEA fruiting analysis, it was decided to focus on fruiting data collected in the final week of the experiment (week 11) as this week represents the culmination of total fruited Petri dishes across different strains, light and gravity conditions. A series of likelihood ratio tests (LRTs) on nested binomial generalized linear models (GLM) were completed to assess whether the inclusion or exclusion of predictor factors of light condition (**Light**), plate orientation (**Gravity**), and strain type (**Strain**) significantly affected model fitness. Plate orientation was first examined and was found to not have a significant effect on model fit (p = 0.34), suggesting that **Gravity** does not meaningfully affect fruiting. Contrasting these results, strain type (**Strain**) (p = 2.31e-13) and light condition (**Light**) (p = 0.014) were found to individually improve model fitness, indicating a significant effect on fruiting. Because plate orientation did not improve model fitness, it was not included as a factor in any further analyses. GLM outputs revealed that there were no significant interactions found between light condition, strain, and gravity; thus, only main effects were analyzed. For post-hoc analysis, the emmeans R package was utilized to calculate estimated marginal means on the response scale, as well as Tukey-adjusted pairwise comparisons.

In total, 38 of the examined 180 Petri dishes developed mature basidiomata over the eleven-week fruiting period (Table 2-15) (Figure 2-18). Meaning only 21.11% of all Petri dishes formed fruiting bodies. Of the 38, one was IOB1 (2.63%), twenty-eight were IOB2 (73.68%), six were IOB3 (15.79%), and three were IOB5 (7.89%) (Table 2-15). In terms of light conditions, of the 38, seventeen plates formed fruitbodies in BL (44.74%), fourteen in DK (36.84%), and seven in WL (18.42%) (Table 2-16). The rate of fructification of these strains over the eleven weeks is visualized (Figure 2-18).

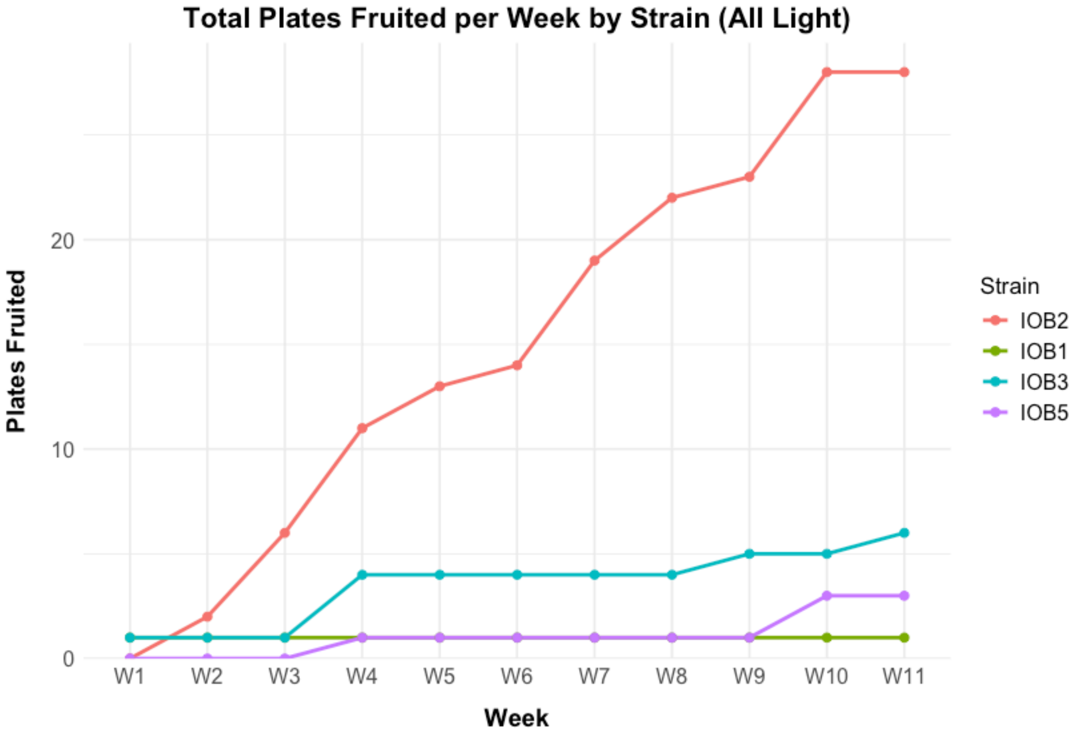

Figure 2-18. Total plates fruited per week by strain (all light)

Table 2-15. Total fruited plates by strain – 11 weeks

Strain	# of Fruited Plates	# of Total Plates	Fruited Plates (%)
IOB1	1	45	2.22
IOB2	28	45	62.22
IOB3	6	45	13.33
IOB5	3	45	6.66

Table 2-16. Total fruited plates by light– 11 weeks

Light Condition	# of Fruited Plates	# of Total Plates	Fruited Plates (%)
BL	17	60	28.33
DK	14	60	23.33
WL	7	60	11.66

The final binomial GLM examined the main effects of light condition and strain, and revealed significant differences in fruiting probability between strains and light conditions ($p < 0.05$) (Table 2-17). This model set IOB2 as the reference strain, and blue light (BL) as the reference light condition with an intercept log-odds estimate of 1.27. Based on these model assumptions, significant differences were found in both light conditions and strain. IOB1, IOB3, and IOB5 all have negative log-odds estimates (-4.55, - 2.59, and – 3,38, respectively), $p < 0.001$ for all, and low SE (Table 2-17). The compared strains appear to have significantly reduced odds of fruiting in comparison to IOB2. The significant difference found for light was present, but far more reduced, where only white light (WL) was found to differ significantly from BL (- 1.71, $p = 0.006$), while complete darkness (DK) did not differ significantly from BL (Table 2-17). These results suggest that colonies exposed to BL have higher odds of fruiting than those in WL, but no difference was found between colonies in DK.

Table 2-17. GLM output

Predictor	Estimate	SE	z-value	p-value
Intercept	1.27	0.49	2.58	0.009
Strain: IOB1	- 4.55	1.08	- 4.21	<0.001
Strain: IOB3	- 2.59	0.57	- 4.52	<0.001
Strain: IOB5	- 3.38	0.71	- 4.79	<0.001
Light: DK	- 0.45	0.55	- 0.82	0.415
Light: WL	- 1.71	0.63	- 2.70	0.007

The inverse logit function was applied to GLM log-odds estimates using emmeans(). Across all light conditions, IOB1, IOB2, IOB3, and IOB5 had predicted fruiting probabilities of 1.81% (0.25 – 12.00), 63.40% (47.62 – 76.80) 11.44% (4.96 – 24.30), and 5.54% (1.72 – 16.50), respectively (Figure 2-19) (Table 2-18). In Tukey adjusted pairwise comparisons using pairs(), IOB1, IOB3, and IOB5 all differed significantly from IOB2, but did not significantly differ from each other (Table 2-19). Due to an observed reduced fruiting capacity in strains IOB1, IOB3, and IOB5, their predicted fruiting probabilities have high standard error (SE) and wide confidence intervals (CoI:95%), thus should be interpreted with caution (Table 2-18). IOB2, however, had the highest predicted probability of fruiting and relatively low SE and narrow CoI; thus, is a more statistically robust observation.

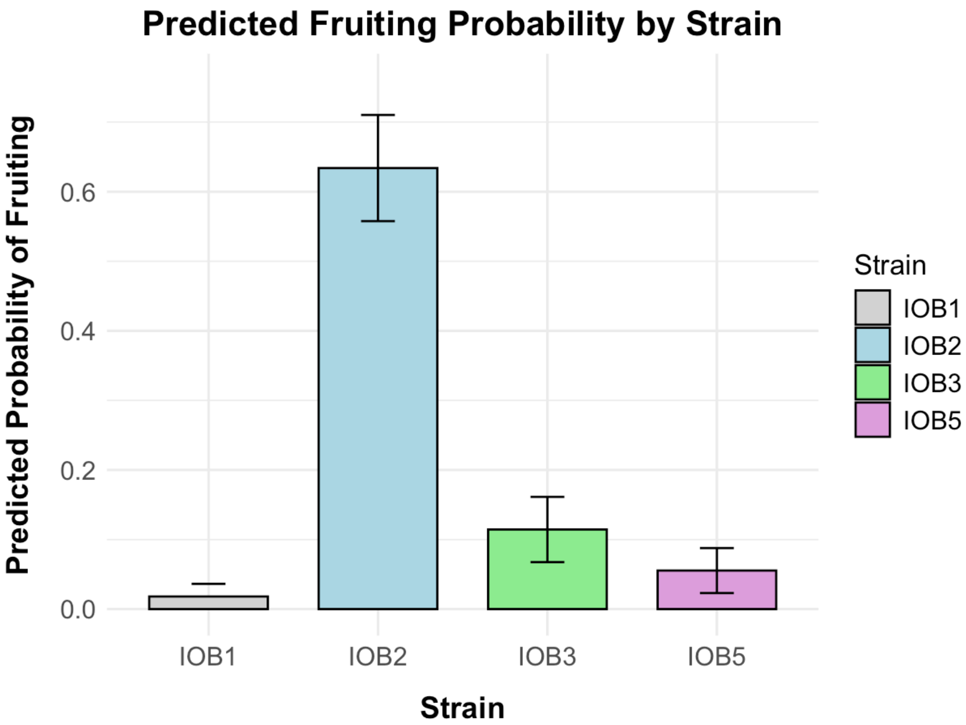

Figure 2-19. Predicted probability of fruiting by strain – week 11.
Error bar: Standard error

Table 2-18. Predicted probability of fruiting by strain – week 11

Strain	Pred. Prob. (%)	SE (%)	CoI:95% (%)
IOB1	1.81	1.82	0.25 – 12.00
IOB2	63.40	7.63	47.62 – 76.80
IOB3	11.44	4.69	4.96 – 24.30
IOB5	5.54	3.23	1.72 – 16.50

Table 2-19. Pairwise contrasts of strains – fruiting week 11

Comparison	Odds Ratio	SE	z ratio	p-value
IOB2/IOB1	94.16	102.00	4.21	0.002
IOB2/IOB3	13.41	7.71	4.52	< 0.0001
IOB2/IOB5	29.54	20.90	4.79	< 0.0001
IOB1/IOB3	0.14	0.16	- 1.76	0.294
IOB1/IOB5	0.37	0.37	- 0.98	0.759
IOB3/IOB5	2.21	1.66	1.05	0.719

Across all strains, light conditions BL, DK, and WL had predicted fruiting probabilities of 20.35% (10.03 – 36.90), 14.03% (6.25 – 28.50), and 4.44% (1.51 – 12.30), respectively (Figure 2-20) (Table 2-20). Tukey-adjusted pairwise comparisons revealed statistical significance between BL and WL (p = 0.019), but none for BL/DK or DK/WL (p < 0.05) (Table 2-21).

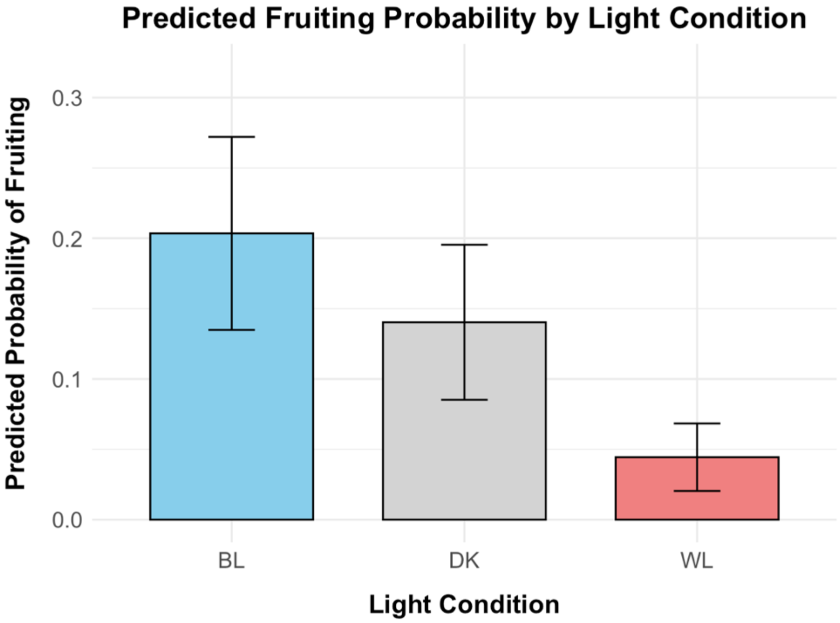

Figure 2-20. Predicted probability of fruiting by light – week 11.
Error bar: Standard error

Table 2-20. Predicted probability of fruiting by light – week 11

Strain	Pred. Prob. (%)	SE (%)	CoI: 95% (%)
BL	20.35	6.86	10.03 – 36.90
DK	14.03	5.55	6.25 – 28.50
WL	4.44	2.40	1.51 – 12.30

Table 2-21. Pairwise contrasts of light– fruiting week 11

Comparison	Odds Ratio	SE	z ratio	p-value
BL/DK	1.57	0.86	0.82	0.694
BL/WL	5.50	3.47	2.71	0.019
DK/WL	3.51	2.19	2.01	0.109

Overall, IOB2 was the highest fruiting strain and SigD from IOB1, IOB3, and IOB5, which were NSigD from each other and barely formed fruiting bodies. BL was SigD from WL, but was NSigD from DK. DK was NSigD from WL. As BL is similar to DK, they are the best conditions for fruiting body formation in this experiment.

Development and Microscopy of *in vitro Inonotus obliquus* Basidiomata

All the following examinations of fruiting body development were carried out on those which developed on malt extract agar (MEF). Fruiting bodies matched wild basidiomata descriptions for general macromorphology (colour, poroid) (Figures 2-21 & 2-22) and micromorphology (basidiospores, hymenial setae, basidia) (Figures 2-23 to 2-25) (see Chapter 1 for description). Detailed basidiospore measurements were taken for IOB2: n = 75, (5.06) 5.27 – 9.32 (9.86) x (3.26) 3.33 – 6.46 (6.53) µm; Me = 7.04 x 4.81 µm; Q = 1.22 – 1.86; Qe = 1.48 (Figure 2-24).

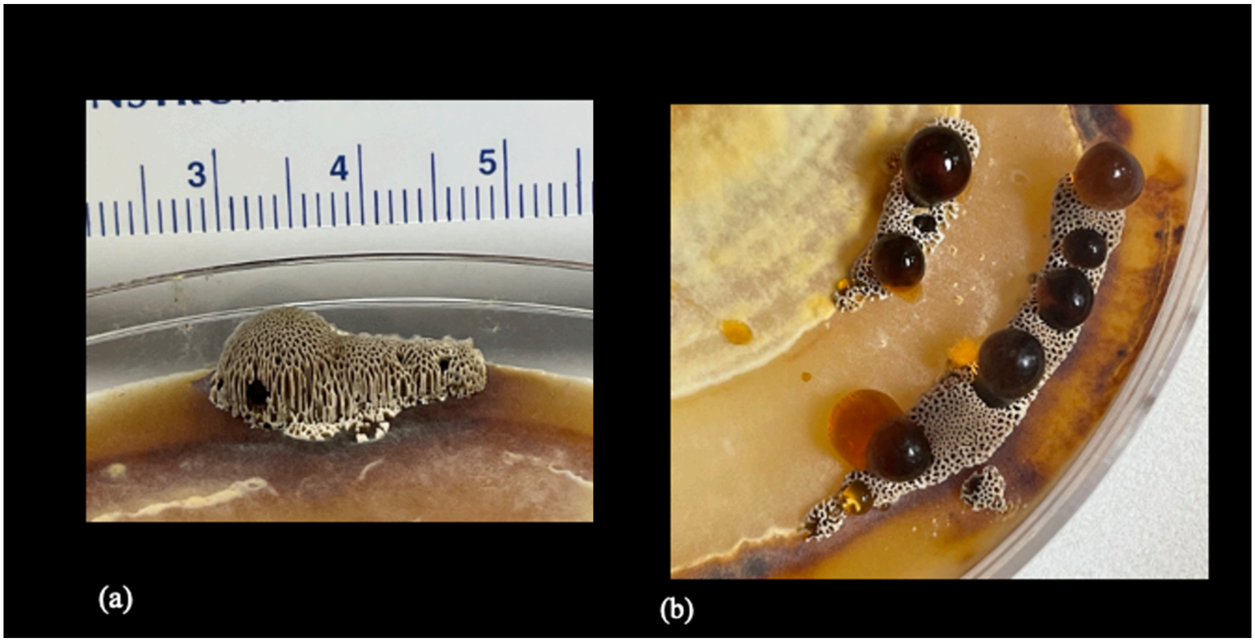

Figure 2-21. Examples of fruiting bodies – close up (a) basidiomata with ruler for scale (cm). (b) basidiomata with intense guttation (IOB2)

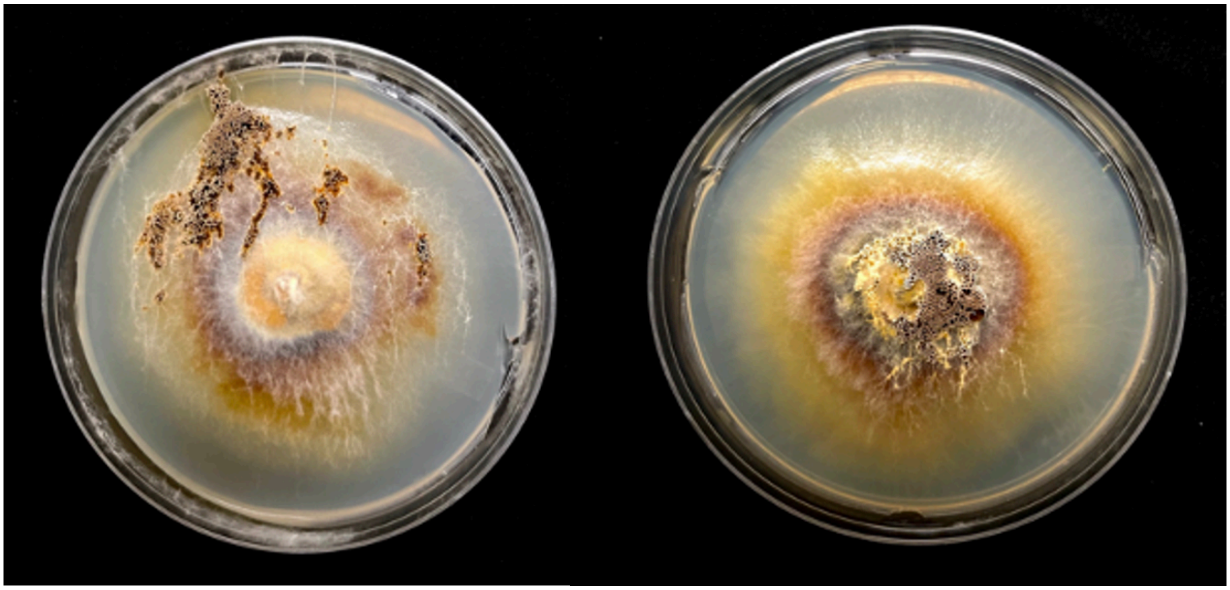

Figure 2-22. Examples of fruiting bodies – whole dish (IOB2)

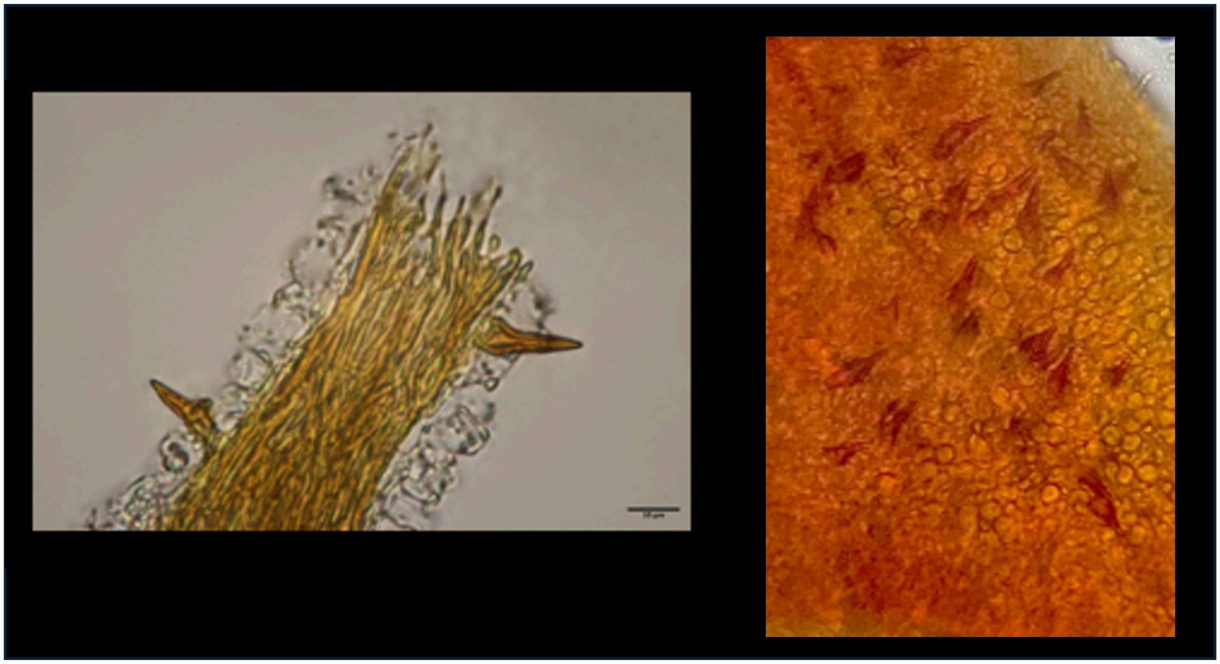

Figure 2-23 . Hymenial setae (IOB2)

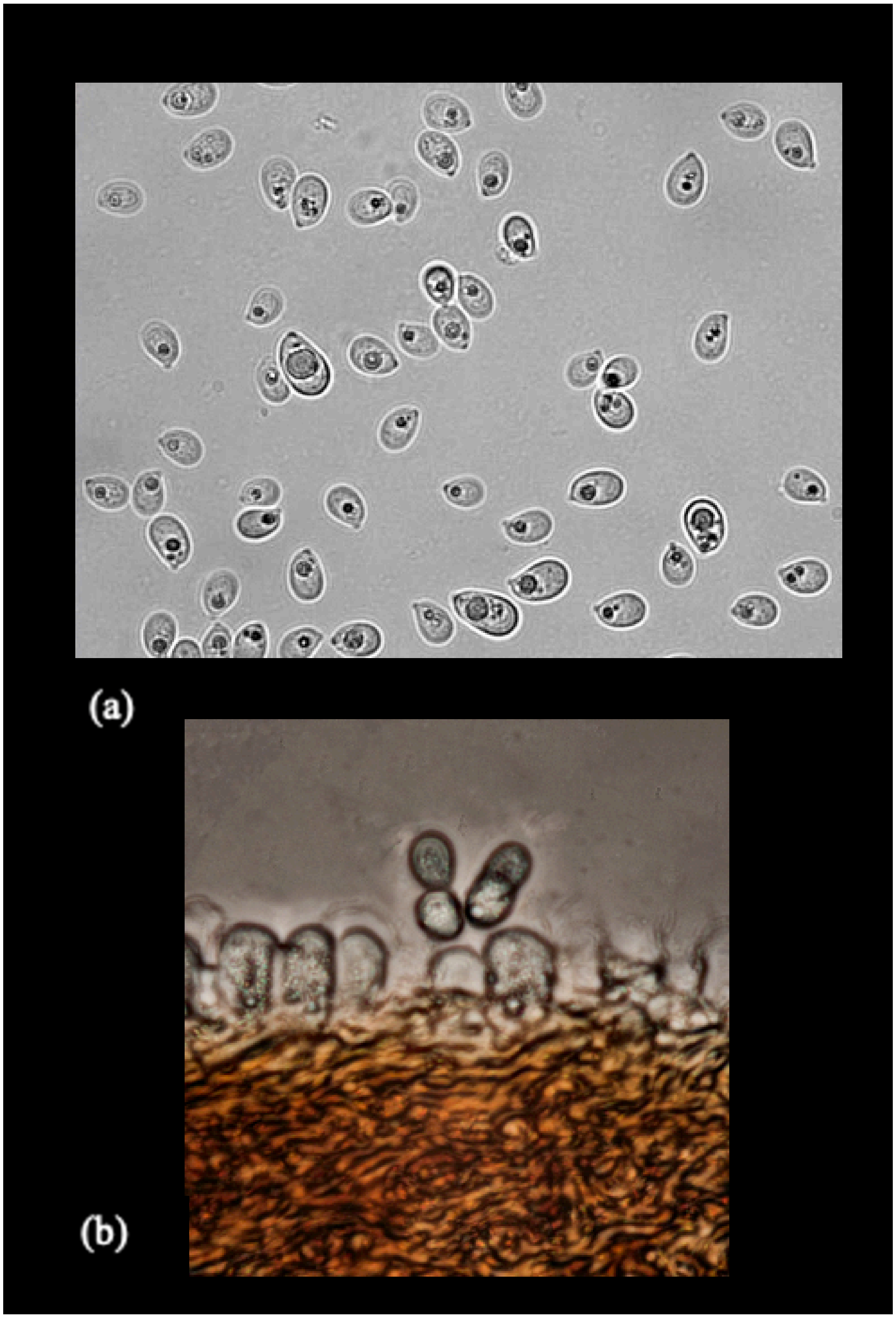

Figure 2-24. Basidiospores and basidia (IOB2). (a) basidiospores of variable size displaying prominent guttules. (b) basidia with four basidiospores attached

Figure 2-25. Cross-section of a pore showing agglutinated trama, setae, basidia, and basidiospores (IOB2)

The size, shape, and position of *in vitro* fruiting bodies were highly variable. Fruitbodies were sometimes only a few mm across or multiple centimetres across. Basidiomata shape was unique for each Petri dish and could be round/nearly round, elongate, or irregular. Sometimes the basidiomata would produce prolific guttation, other times they would not (Figure 2-21). Fruitbodies would initiate at different positions in the Petri dish: on the agar surface, the margin of the dish, and rarely on the lid of the dish (Figures 2-21 & 2-27)

The development of fruit bodies was closely examined (Figures 2-26 & 2-27). For fruiting bodies that formed on the agar surface, primordia were easily missed as cultures sometimes formed many sterile hyphal knots. However, primordial basidiomata were occasionally associated with a dark yellowish-brown guttation and could be separated from sterile hyphal knots (Figure 2-26a). Over nine days of development from the observation of small guttate primordia, photographs were taken every three days to observe development (scale bar 3mm) (Figure 2-26). On day one (Figure 2-26a), a hyaline scattered cluster of guttate hyphal aggregates formed, indicating fruiting body development. On day two (Figure 2-26b), the scattered hyphal aggregates coalesced, guttation increased and became slightly more pigmented, and primordial pores (sunken tissue) began to form in the lower right portion of the fruit body. On day six (Figure 2-26c), the fruit body greatly increased in size, pores with a dark pigmented hymenium formed all over its surface, small guttation coalesced into larger, more pigmented droplets, and the context between pores was hyaline. On day nine (Figure 2-26d), the fruiting body was fully mature; it greatly increased in size, guttation coalesced into one large droplet, and the context between pores was greyish-brown/red. From this point onward, the fruitbody continues to get slightly larger, and the pores elongate. The primordium takes less than 10 days to become fully mature and begins to produce basidiospores as soon as primordial pores form; thus, it begins to lightly sporulate very quickly.

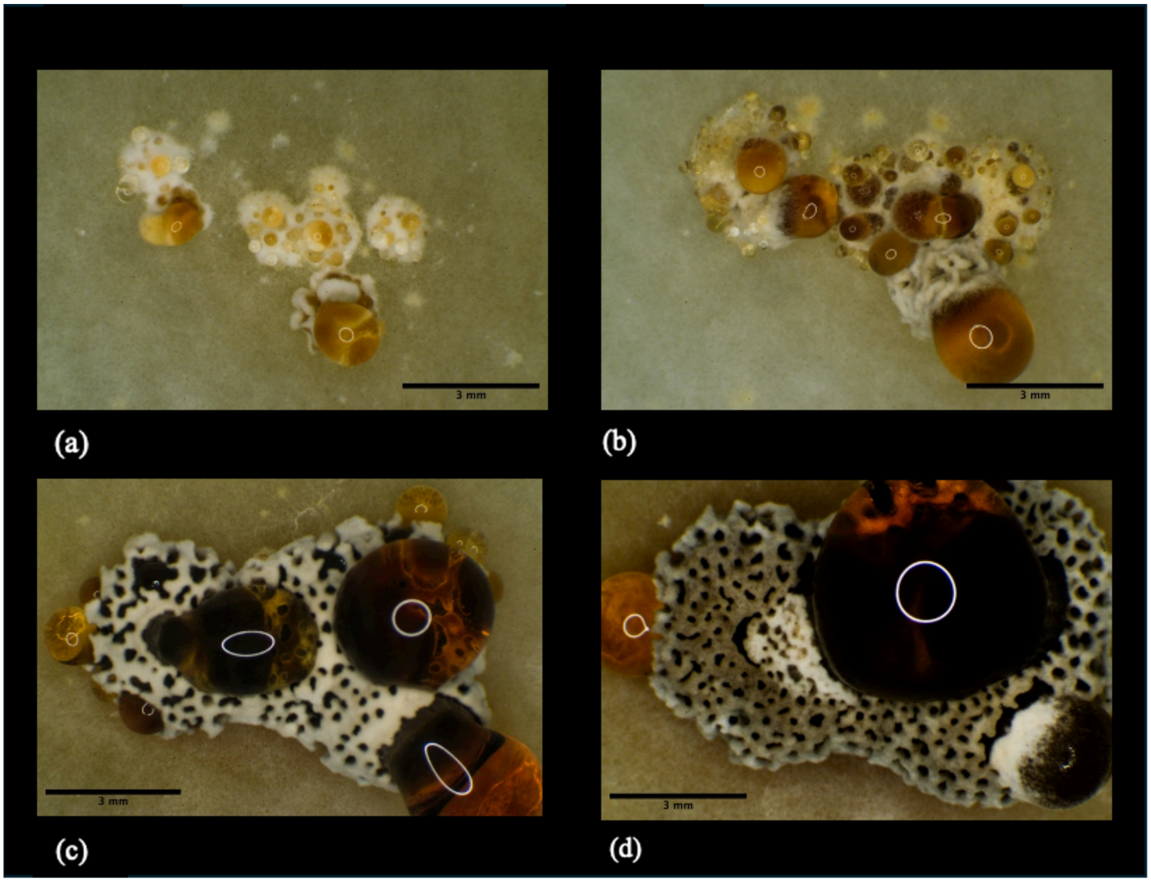

Figure 26-2. Fruiting body development over 9 days – agar (IOB2). (a) 1 day old. (b) 3 days old. (c) 6 days old. (d) 9 days old

For fruiting bodies that formed on the margin, development was different and not as closely photographed as in the example above, but was still observed twice over 20 days (Figure 2-27). In the margin-type fruiting bodies, aerial hyphae colonized the plastic margin and formed cotton candy-like hyphal aggregates (Figure 2-27a). This step typically took longer, as the mycelium had to form a substrate on the plastic to anchor the developing fruit body. After 20 days (Figure 2-27b), another photo was taken showing a highly matured basidioma with elongated pores and a robust constructed substrate. Fruit bodies easily separate from the petri dish margin. Additionally, while plate orientation (**Gravity**) did not meaningfully affect fruiting body initiation, it did impact the direction of pore elongation (Figure 2-27).

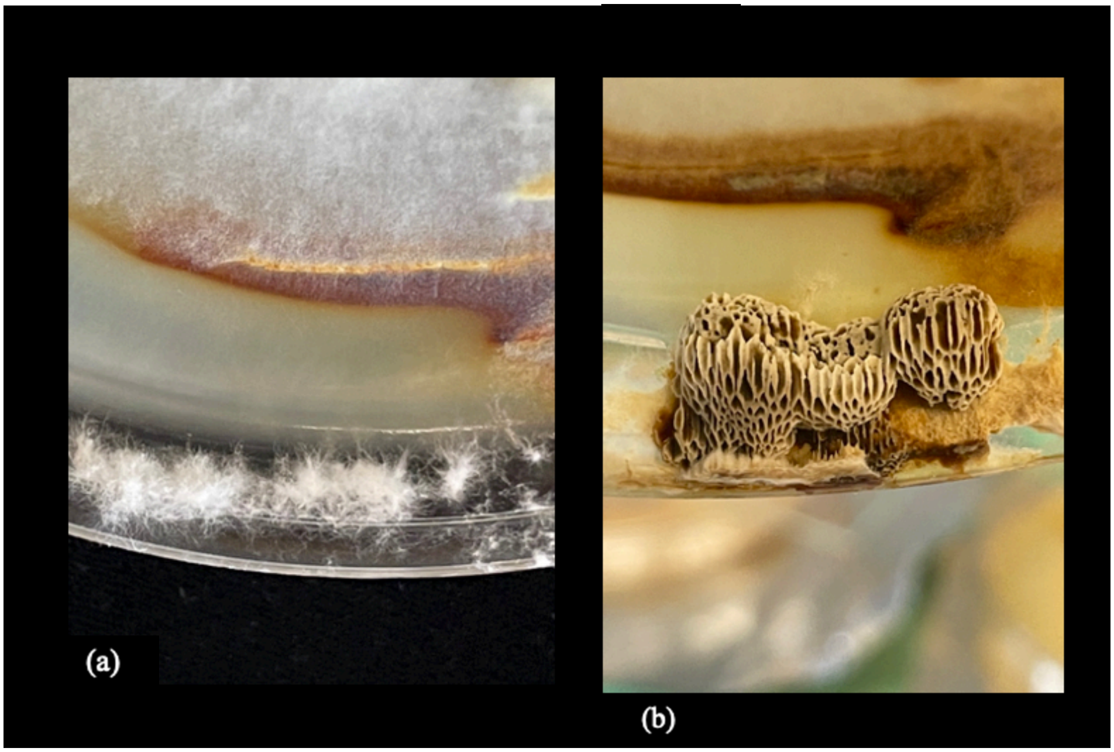

Figure 2-27. Fruiting body development over 20 days – margin (IOB2). (a) early development (1 day old). (b) 20 days of development

DISCUSSION

Through experimentation of the fruiting and growth capacity of varying strains of *I. obliquus* on unique media under different light and gravity conditions, a protocol for isolation, rapid culturing, and fruiting body production has been developed for future study.

MEDIA EXPERIMENTATION – LINEAR GROWTH AND FRUITING

In total, 320 plates of eight different media (MEF, MES, CAF, CAS, BAF, BAS, CHF, and CHS) and four strains (IOB1, IOB2, IOB3, and IOB5) were tested for their ability to induce sporulation and their capacity to induce or supress colony growth. Linear growth diameter (cm) was examined weekly over four weeks with colonies incubated at room temperature (20 ºC ± 2 ºC) in complete darkness. Significant three-way interactions were found between different strains, media, and when they were measured over a temporal scale (Figures 2-6 to 2-9). The four strains were found to behave slightly differently in linear growth in response (Figure 2-11). This was especially the case in malt extract-based media (MEF/MES), where IOB5 was the only strain with fully colonized plates of these media types at week four (Figure 2-9). Colonies grown on malt extract-based media (MEF/MES) had significantly reduced linear growth in comparison to all media (Figure 2-10). Colonies grown on carrot-based agar media (CAF/CAS) were found to have the greatest linear growth diameter (cm) over four weeks across four different strains of *Inonotus obliquus* (Figures 2-9 & 2-10). While this does demonstrate the superiority of carrot agar for rapid linear growth, it does not demonstrate growth in three dimensions (colony density and aerial mycelium growth). Due to this drawback, carrot-based media look relatively close in performance to chaga-based media (CHF/CHS) and birch-based media (BAF/BAS) (Figure 2-10). When examining qualitative colony characteristics, carrot agar obviously outperforms these media; the growth is vigorous, thick, cottony, and fast (Figure 2-12). While the others are relatively diffuse and submerged (Figures 2-14 & 2-15). Carrot agar has been found to by other researchers to be an excellent choice when working with members of the Hymenochaetaceae (Mallett & Myrholm, 1995). Outside of this experiment, carrot agar was the standard medium used for quickly producing large amounts of *I. obliquus* mycelium in these studies.

With regards to fruiting on these media, after six months of 12/12 blue light stimulation and temperature modulation between 15 ºC and 20 ºC , there did not appear to be any difference between media that were made with full nutrition (20g malt extract) and starved nutrition (10g malt extract). Blue light stimulation, a reduction in temperature, and starvation are known as factors important for inducing sporulation in agaricomycetes (Sakamoto, 2018). In the Basidiomycota, starvation of substrates is an important signal for sexual reproduction (Plunkett, 1953). Muraguchi *et al.* (2015) observed that *Copronpopsis cinerea* (Schaeff.) Redhead, Vilgalys & Moncalvo is induced to fruit under low glucose concentrations. The variation in nutrition concentration may have been too slight to induce fruiting body formation in a meaningful way in this case. The results were evident that malt extract-based media (MEF/MES) were by far the best media for forming fruit bodies in the long-term (Table 2-11). Interestingly, these media performed the worst for linear growth diameter but were ideal here. This may be because the malt extract-based media are starving and stressing cultures, or the addition of yeast extract (B-vitamins) is affecting fruiting body formation. All the other media, save for carrot agar, which had trace B-vitamins, did not contain any supplemented B-vitamins (Sharma *et al.* 2012). Hawker (1942) demonstrated the concentrations of B-vitamins have an impact on fruiting body formation in fungi. Birch-based media (BAF/BAS) were anticipated to induce prolific fruiting body formation due to containing substrate from its main host tree (Gilberston & Ryvarden, 1986); however, it did not (Table 2-10). Chaga-based agar (CHF/CHS) was developed because perhaps compounds in the sterile conk induce fruitification in wild environments. Like in birch agar, chaga agar did not meaningfully induce fruiting body formation (Table 2-10). Finally, carrot-based media (CAF/CAS) performed by far the best for linear growth, but essentially did not induce fruiting body formation relative to ME-based media (Figure 2-10) (Table 2-10). It is known that high concentrations of nutrients can suppress fruiting body formation (Sakamoto, 2018). Carrots are highly nutritious and contain a wealth of vitamins and complex sugars (Sharma *et al.* 2012). It is likely that this media's diverse and highly nutritional content suppresses fruiting body formation in *I. obliquus*, but is ideal for vigorous mycelium production. These results indicate that compounds in birch wood and chaga do not meaningfully affect fruiting body formation, and is likely caused by a starvation effect.

IMPACT OF STRAIN AND LIGHT CONDITION ON FRUITING

The 180 2% MEA (see MEF recipe) plates were inoculated with four strains of *I. obliquus* and examined how different light conditions affected fruiting at room temperature over eleven weeks (20 ºC ± 2 ºC). These analyses revealed that strain selection is incredibly important for reliable and consistent fruiting body formation. Strain testing and selection are crucial to test fruiting capacity and characteristics in mushroom cultivation (Myronycheva, *et al.* 2017; Rong *et al.* 2016). IOB2 formed almost all observed fruiting bodies over eleven weeks, while IOB1, IOB3, and IOB5 only fruited minimally (Figure 2-19). Through the breeding of progeny and genetic modification of strains, it is possible that fruiting capacity can be improved, as well as the prevalence of specific desired traits (i.e. large fruiting body formation/yield) (Kothe, 2001; Barh *et al.* 2019;). IOB2 is the most reliably fruiting strain and is analyzed most frequently in Chapter 3.

The 180 inoculated plates were placed under three different light conditions (blue light (BL), white light (WL), darkness (DK)) at room temperature (20 ºC ± 2 ºC) after 40 days of incubation in complete darkness. Temperature was not modulated in this experiment for simplicity. The BL and WL incubators were set at a 12/12 light cycle, while the DK incubator was not modulated for light. Colonies in BL formed the most basidiomata, followed by those in DK and then WL (Figure 2-20). Relative to BL, WL has a negative effect on fruiting body formation, while DK and BL are seen as equals (Table 2-21). BL was significantly different from WL and was not significantly different from DK; DK was not significantly different from WL (Table 2-21) ($p < 0.05$). Light is important for inducing fruiting body morphogenesis in fungi (Fuller *et al.* 2015; Sakamoto, 2018). It also regulates asexual spore production, pigment and carotenoid production, and secondary metabolite production (Bayram & Bayram, 2023). Fungi produce photoreceptors, which are photon absorbing protein molecules that use light-sensing chromophores (Fujisawa & Masuda, 2018). Once the chromophores absorb photons, the photoreceptor protein is converted to a signaling molecule, initiating nuclear signal transduction (Palczewski & Kiser, 2020). Fungi have evolved blue light receptors, red light sensors, and green light sensors (Bayram & Bayram, 2023). The most effective range of wavelength for fruiting body induction in basidiomycetes has been identified at between 280nm (ultraviolet) and 520nm (blue light) (Kitamoto *et al.* 1972; Durand & Furuya 1985). In ascomycete fungi, blue light photoreceptors WC1 and WC2 have been identified (Fuller *et al.* 2015). For Agaricomycetes, the role that light plays in fruiting is inconsistent across taxa, as many are able to form basidiomata in complete darkness (Sakamoto, 2018). *Inonotus* *obliquus* is no exception and appears able to complete its sexual cycle in complete darkness. The adaptation to sporulate in complete darkness is incredibly advantageous for a fungus that forms basidiomata under the bark (Bunyard, 2015).

COMMENTS ON THE EFFECTS OF GRAVITY

While the effect of plate orientation did not meaningful impact fruiting body formation, it did affect the direction of pore elongation (Figure 2-27). This was expected as agaricomyceteous fungi display gravitropism, which is a ubiquitous adaptation where the hymenia of basidiomata is developed angled towards the ground for basidiospore dispersal (Kern, 1999). Buller (1922) suggests that the life cycle and ecology of the basidiomata affect the degree of gravitropism. In the case of *I. obliquus*, this is seen as the oblique direction of pore formation relative to its substrate.

PREVIOUS EXAMINATIONS OF LABORATORY SPORULATION OF *INONOTUS OBLIQUUS*

Campbell and Davidson (1938) were the first to report the *in vitro* sporulation of *I. obliquus*. The formation of basidiomata *in vitro* enabled them to associate the sterile conk with the cryptic poroid fruit body (Figure 2-28).

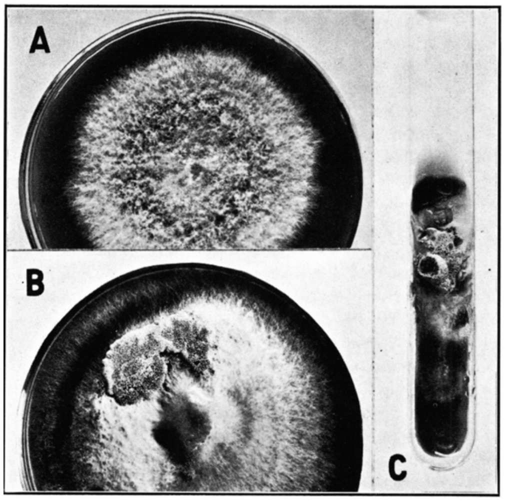

Figure 2-28. Fruitbodies Campbell & Davidson (1938)

Very recently, Sun *et al.* (2023) (in Mandarin) were able to sporulate *I. obliquus* under laboratory conditions and were the first to examine mating and fruiting characteristics. They were able to bag cultivate the fruit body on supplemented soybean hulls and form it *in vitro* (Figure 2-29). They incubated the bags at 26 ºC for 40 days and placed them in a 12/12 white light cycle incubator modulated between 10 °C and 22 °C. The germination rate, single-spored fruiting, mating system, nuclear behaviour, and mating locus will be discussed in Chapter 3.

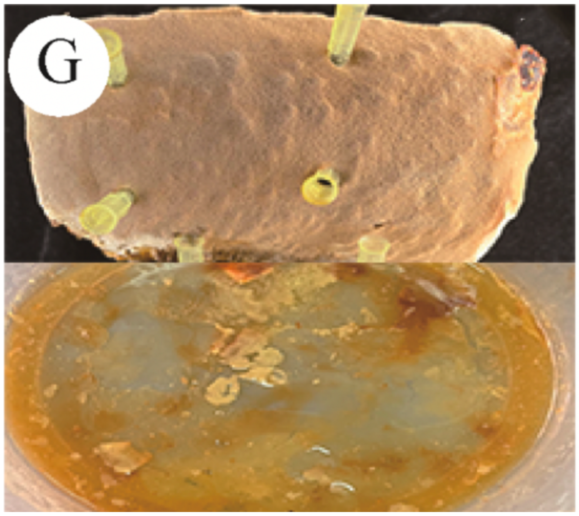

Figure 2-29. Fruitbodies Sun *et al*. (2023)

CONCLUSION

In this chapter, a protocol for isolating axenic cultures of *I. obliquus* from sterile conk fragments was demonstrated. Carrot agar was found to be the ideal medium for fast culturing of *I. obliquus* mycelium for inoculum and research purposes; it is simple to make and cost-effective. Strain IOB2 was identified as a prolific fruiter that could potentially be shared amongst researchers for future study as a model strain. 2% modified MEA is a readily available agar medium that initiates fruiting body formation at room temperature in complete darkness or with mild light stimulation. Under these findings, *I. obliquus* can be a very reliable fungus to manipulate in the laboratory and has the potential to have its fruit body studied for mating, chemistry, etc. Laboratory manipulation of the sexual cycle of *I. obliquus* enables the development of novel strains and breeding programs for wild and artificial cultivation. We lack a clear formal understanding of the sexual cycle, ecology, and physiology of *I. obliquus,* which are essential for the conservation and management of this taxon. This work aims to enable researchers to study the otherwise cryptic basidiomata of this fungus by presenting simple protocols.

.

LITERATURE CITED

Barh, A., Sharma, V. P., Annepu, S. K., Kamal, S., Sharma, S., & Bhatt, P. 2019. Genetic improvement in *Pleurotus* (oyster mushroom): a review. *3 Biotech*, *9*(9), 322.

Bayram, Ö. S., & Bayram, Ö. 2023. An anatomy of fungal eye: fungal photoreceptors and signalling mechanisms. *Journal of Fungi*, *9*(5), 591.

Buller, A. H. R. 1922. Researches on fungi. (Vol. 2). *Longmans, Green and Company*. London. 510 pp.

Bunyard, B. A. 2015. First record of insect mycophagy of the commercially-important "chaga" fungus *Inonotus obliquus* (Ach. ex Pers.) Pilát (Hymenochaetales: Hymenochaetaceae) in North America. *Proceedings of the Entomological Society of Washington*, *117*(4), 452–457.

Campbell, W. A., & Davidson, R. W. 1938. A *Poria* as the fruiting stage of the fungus causing the sterile conks on birch. *Mycologia*, *30*(5), 553–560.

Canan, K., Quark, M., Russell, S., Ostuni, S., Rockefeller, A., Williams, J., Culliton, S., Geurin, Z., & Birkebak, J. 2024. Introducing the Ohio mushroom DNA lab: early lessons and contributions from a new community-driven Nanopore sequencing laboratory. *McIlvainea. Vol. 33.* 29 pp.

Černý, A. 1976. Lesnická fytopatologie. *Státni zemědělské nakladatelstvi*, Praha. (in Czech)

Durand, R., & Furuya, M. 1985. Action spectra for stimulatory and inhibitory effects of UV and blue light on fruit-body formation in *Coprinus congregatus*. *Plant and cell physiology*, *26*(6), 1175-1183.

Ern, P. T. Y., Quan, T. Y., Yee, F. S., & Yin, A. C. Y. 2023. Therapeutic properties of *Inonotus obliquus* (Chaga mushroom): A review. *Mycology*, *15*(2), 1–18.

Fujisawa, T., & Masuda, S. 2018. Light-induced chromophore and protein responses and mechanical signal transduction of BLUF proteins. *Biophysical reviews*, *10*(2), 327-337.

Fuller, K. K., Loros, J. J., & Dunlap, J. C. 2015. Fungal photobiology: visible light as a signal for stress, space and time. *Current genetics*, *61*(3), 275-288.

Gilbertson, R. L., & Ryvarden, L. 1986. North American polypores. Vol. I. *Abortiporus-Lindtneria. Fungiflora.* Norway. 433 pp.

Hawker, L. E. 1942. The effect of vitamin B_1 on the concentration of glucose optimal for the fruiting of certain fungi. *Annals of Botany*, *6*(24), 631-636.

Kern, V. D. 1999. Gravitropism of basidiomycetous fungi—on Earth and in microgravity. *Advances in Space Research*, *24*(6), 697-706.

Kitamoto, Y., Suzuki, A., & Furukawa, S. 1972. An action spectrum for light-induced primordium formation in a basidiomycete, *Favolus arcularius* (Fr) Ames. *Plant Physiology*, *49*(3), 338-340.

Kothe, E. 2001. Mating-type genes for basidiomycete strain improvement in mushroom farming. *Applied microbiology and biotechnology*, *56*(5), 602-612.

Lee, Min-Woong, Hyeon-Hur, Kwang-Choon Chang, Tae-Soo Lee, Kang-Hyeon Ka, and L. Jankovsky. 2008. Introduction to distribution and ecology of sterile conks of *Inonotus obliquus*. *Mycobiology* 36(4):199–202.

Lewis, F., Butler, A., & Gilbert, L. 2011. A unified approach to model selection using the likelihood ratio test. *Methods in Ecology and Evolution*, *2*(2), 155–162.

Lõhmus, A., & Lõhmus, P. 2024. A heart-rot fungus, *Inonotus obliquus* (chaga), mediates microhabitat creation in birch snags and contributes to forest fungal diversity. *Global Ecology and Conservation*, *56*, e03319.

Mallett, K. I., & Myrholm, C. L. 1995. The mating system of *Phellinus tremulae*. *Mycologia*, *87*(5), 597–603.

Miina, J., Peltola, R., Veteli, P., Linnakoski, R., Escribano, M. C., Haveri-Heikkilä, J., Mattila, P., Marnila, P., Pihlava, J.-M., Hellström, J., Sarjala, T., Silvan, N., Kurttila, M., & Vanhanen, H. 2021. Inoculation success of *Inonotus obliquus* in living birch (Betula spp.). *Forest Ecology and Management*, *492*, 119244.

Muraguchi, H., Umezawa, K., Niikura, M., Yoshida, M., Kozaki, T., Ishii, K., & Pukkila, P. J. 2015. Strand-specific RNA-seq analyses of fruiting body development in *Coprinopsis cinerea*. *PloS one*, *10*(10), e0141586.

Myronycheva, O., Bandura, I., Bisko, N., Grygansky, A. P., & Karlsson, O. 2017. Assessment of the growth and fruiting of 19 oyster mushroom strains for indoor cultivation on lignocellulosic wastes. *BioResources*, *12*(3), 4606-4626.

Palczewski, K., & Kiser, P. D. 2020. Shedding new light on the generation of the visual chromophore. *Proceedings of the National Academy of Sciences*, *117*(33), 19629-19638.

Nimon, K. F. 2012. Statistical Assumptions of Substantive Analyses Across the General Linear Model: A Mini-Review. *Frontiers in Psychology*, *3*. 5pp.

Plunkett, B. E. 1953. Nutritional and other aspects of fruit-body production in pure cultures of Collybia velutipes (Curt.) Fr. *Annals of Botany*, *17*(2), 193-218.

Rivoire, B. 2020. Polypores de France et d'Europe. *Orilénas, Mycopolydev*. 874 p.

Rong, C. B., Song, S., Niu, Y. R., Xu, F., Liu, Y., Zhao, S., & Wang, S. X. 2016. Selection of a highly productive strain of *Pholiota adiposa*. *Mycosphere*, *7*(2), 226-235.

Russell, S. D. 2023. ONT DNA Barcoding Fungal Amplicons w/MinION & Flongle. https://slack.protocols.io:8443/view/ont-dna-barcoding-fungal-amplicons-w-minion-amp-fl-cq2avyae.html

Sakamoto, Y. 2018. Influences of environmental factors on fruiting body induction, development and maturation in mushroom-forming fungi. *Fungal Biology Reviews*, *32*(4), 236–248.

Sharma, K. D., Karki, S., Thakur, N. S., & Attri, S. 2012. Chemical composition, functional properties and processing of carrot—a review. *Journal of food science and technology*, *49*(1), 22-32.

Shigo, A. L. 1965. The Pattern of decays and discolorations in northern hardwoods. *Phytopathology,* 55: 648-652

Sun, Y., Zhang, Y., Cao, X., Zhou, J., & Jiang, J. 2023. Characteristics related to sexual reproduction and mating type locus of *Inonotus obliquus*. *Mycosystema*, 42(2), 520–529.

Thomas, P. W., Elkhateeb, W. A., & Daba, G. M. 2020. Chaga (*Inonotus obliquus*): a medical marvel but a conservation dilemma. *Sydowia*, *72*, 123–130.

APPENDIX I

THE EFFECT OF MEDIA ON COLONY DIAMETER AVERAGED OVER STRAIN BY WEEK AND OVERALL

Significant Pairwise Contrasts

Table 2-22. Significant pairwise contrasts – media over strain - overall

Contrast	Estimate (cm)	SE	df	t.ratio	p.value
BAF - BAS	0.33	0.06	284.49	5.37	4.48E-06
BAF - CAF	-0.75	0.06	284.49	-12.25	6.11E-13
BAF - CAS	-1.02	0.06	287.70	-16.49	5.69E-13
BAF - CHS	-0.46	0.06	284.49	-7.48	2.68E-11
BAF - MEF	2.80	0.06	284.49	45.51	6.10E-13
BAF - MES	2.77	0.06	290.93	44.70	7.43E-13
BAS - CAF	-1.08	0.06	284.49	-17.62	6.10E-13
BAS - CAS	-1.35	0.06	287.70	-21.85	5.69E-13
BAS - CHF	-0.43	0.06	287.70	-6.99	5.42E-10
BAS - CHS	-0.79	0.06	284.49	-12.85	6.10E-13
BAS - MEF	2.47	0.06	284.49	40.14	6.10E-13
BAS - MES	2.44	0.06	290.93	39.36	7.43E-13
CAF - CAS	-0.26	0.06	287.70	-4.28	6.61E-04
CAF - CHF	0.65	0.06	287.70	10.58	6.35E-13
CAF - CHS	0.29	0.06	284.49	4.77	7.96E-05
CAF - MEF	3.55	0.06	284.49	57.76	6.10E-13
CAF - MES	3.52	0.06	290.93	56.87	7.43E-13
CAS - CHF	0.92	0.06	290.93	14.82	7.43E-13
CAS - CHS	0.56	0.06	287.70	9.04	6.43E-13
CAS - MEF	3.82	0.06	287.70	61.86	5.69E-13
CAS - MES	3.79	0.06	294.16	60.96	7.53E-13
CHF - CHS	-0.36	0.06	287.70	-5.82	4.29E-07
CHF - MEF	2.90	0.06	287.70	47.00	5.69E-13
CHF - MES	2.87	0.06	294.16	46.19	7.53E-13
CHS - MEF	3.26	0.06	284.49	52.99	6.10E-13
CHS - MES	3.23	0.06	290.93	52.13	7.43E-13

Table 2-23. Significant pairwise contrasts – media over strain – week 1

Contrast	Week	Estimate (cm)	SE	df	t.ratio	p.value
BAF - CAS	1	-0.53	0.09	930.65	-5.83	2.16E-07
BAF - CHS	1	-0.36	0.09	924.02	-3.95	0.0021
BAF - MEF	1	1.12	0.09	924.02	12.31	<0.0001
BAF - MES	1	1.13	0.09	937.09	12.31	<0.0001
BAS - CAF	1	-0.28	0.09	924.02	-3.09	0.0430
BAS - CAS	1	-0.64	0.09	930.65	-6.99	1.47E-10
BAS - CHS	1	-0.46	0.09	924.02	-5.12	1.03E-05
BAS - MEF	1	1.01	0.09	924.02	11.15	<0.0001
BAS - MES	1	1.02	0.09	937.09	11.15	<0.0001
CAF - CAS	1	-0.36	0.09	930.65	-3.92	0.0024
CAF - MEF	1	1.29	0.09	924.02	14.23	<0.0001
CAF - MES	1	1.31	0.09	937.09	14.20	<0.0001
CAS - CHF	1	0.49	0.09	937.09	5.33	3.46E-06
CAS - MEF	1	1.65	0.09	930.65	18.07	8.05E-13
CAS - MES	1	1.66	0.09	943.34	18.00	<0.0001
CHF - CHS	1	-0.32	0.09	930.65	-3.46	0.0133
CHF - MEF	1	1.16	0.09	930.65	12.71	8.05E-13
CHF - MES	1	1.17	0.09	943.34	12.70	<0.0001
CHS - MEF	1	1.48	0.09	924.02	16.26	<0.0001
CHS - MES	1	1.49	0.09	937.09	16.21	<0.0001

Table 2-24. Significant pairwise contrasts – media over strain – week 2

Contrast	Week	Estimate (cm)	SE	df	t.ratio	p.value
BAF - BAS	2	0.41	0.09	924.02	4.51	0.0002
BAF - CAF	2	-1.83	0.09	924.02	-20.12	<0.0001
BAF - CAS	2	-2.37	0.09	930.65	-25.94	8.05E-13
BAF - CHF	2	-0.52	0.09	930.65	-5.67	5.42E-07
BAF - CHS	2	-1.07	0.09	924.02	-11.74	<0.0001
BAF - MEF	2	3.12	0.09	924.02	34.33	<0.0001
BAF - MES	2	3.11	0.09	937.09	33.80	<0.0001
BAS - CAF	2	-2.24	0.09	924.02	-24.63	<0.0001
BAS - CAS	2	-2.78	0.09	930.65	-30.43	8.05E-13
BAS - CHF	2	-0.93	0.09	930.65	-10.15	8.80E-13
BAS - CHS	2	-1.48	0.09	924.02	-16.25	<0.0001
BAS - MEF	2	2.71	0.09	924.02	29.82	<0.0001
BAS - MES	2	2.70	0.09	937.09	29.34	<0.0001
CAF - CAS	2	-0.54	0.09	930.65	-5.95	1.08E-07
CAF - CHF	2	1.31	0.09	930.65	14.33	8.05E-13
CAF - CHS	2	0.76	0.09	924.02	8.38	<0.0001

CAF - MEF	2	4.95	0.09	924.02	54.45	<0.0001
CAF - MES	2	4.93	0.09	937.09	53.68	<0.0001
CAS - CHF	2	1.85	0.09	937.09	20.16	<0.0001
CAS - CHS	2	1.30	0.09	930.65	14.28	8.05E-13
CAS - MEF	2	5.49	0.09	930.65	60.07	8.05E-13
CAS - MES	2	5.48	0.09	943.34	59.25	<0.0001
CHF - CHS	2	-0.55	0.09	930.65	-6.00	7.79E-08
CHF - MEF	2	3.64	0.09	930.65	39.79	8.05E-13
CHF - MES	2	3.62	0.09	943.34	39.20	<0.0001
CHS - MEF	2	4.19	0.09	924.02	46.07	<0.0001
CHS - MES	2	4.17	0.09	937.09	45.40	<0.0001

Table 2-25. Significant pairwise contrasts – media over strain – week 3

Contrast	Week	Estimate (cm)	SE	df	t.ratio	p.value
BAF - BAS	3	0.72	0.09	924.02	7.93	1.45E-13
BAF - CAF	3	-1.01	0.09	924.02	-11.16	<0.0001
BAF - CAS	3	-1.17	0.09	930.65	-12.83	8.05E-13
BAF - CHS	3	-0.42	0.09	924.02	-4.58	0.0001
BAF - MEF	3	4.21	0.09	924.02	46.30	<0.0001
BAF - MES	3	3.97	0.09	937.09	43.22	<0.0001
BAS - CAF	3	-1.73	0.09	924.02	-19.08	<0.0001
BAS - CAS	3	-1.89	0.09	930.65	-20.71	8.05E-13
BAS - CHF	3	-0.67	0.09	930.65	-7.38	1.09E-11
BAS - CHS	3	-1.14	0.09	924.02	-12.51	<0.0001
BAS - MEF	3	3.49	0.09	924.02	38.37	<0.0001
BAS - MES	3	3.25	0.09	937.09	35.38	<0.0001
CAF - CHF	3	1.06	0.09	930.65	11.60	8.09E-13
CAF - CHS	3	0.60	0.09	924.02	6.58	2.24E-09
CAF - MEF	3	5.22	0.09	924.02	57.46	<0.0001
CAF - MES	3	4.99	0.09	937.09	54.25	<0.0001
CAS - CHF	3	1.22	0.09	937.09	13.25	<0.0001
CAS - CHS	3	0.76	0.09	930.65	8.28	9.06E-13
CAS - MEF	3	5.38	0.09	930.65	58.86	8.05E-13
CAS - MES	3	5.14	0.09	943.34	55.65	<0.0001
CHF - CHS	3	-0.46	0.09	930.65	-5.06	1.41E-05
CHF - MEF	3	4.16	0.09	930.65	45.53	8.05E-13
CHF - MES	3	3.93	0.09	943.34	42.47	<0.0001
CHS - MEF	3	4.62	0.09	924.02	50.88	<0.0001
CHS - MES	3	4.39	0.09	937.09	47.75	<0.0001

Table 2-26. Significant pairwise contrasts – media over strain – week 4

Contrast	Week	Estimate (cm)	SE	df	t.ratio	p.value
BAF - MEF	4	2.76	0.09	924.02	30.38	<0.0001
BAF - MES	4	2.86	0.09	937.09	31.13	<0.0001
BAS - MEF	4	2.67	0.09	924.02	29.43	<0.0001
BAS - MES	4	2.77	0.09	937.09	30.19	<0.0001
CAF - MEF	4	2.76	0.09	924.02	30.38	<0.0001
CAF - MES	4	2.86	0.09	937.09	31.13	<0.0001
CAS - MEF	4	2.76	0.09	930.65	30.17	8.05E-13
CAS - MES	4	2.86	0.09	943.34	30.91	<0.0001
CHF - MEF	4	2.65	0.09	930.65	28.98	8.05E-13
CHF - MES	4	2.75	0.09	943.34	29.74	<0.0001
CHS - MEF	4	2.76	0.09	924.02	30.38	<0.0001
CHS - MES	4	2.86	0.09	937.09	31.13	<0.0001

Figures and Tables for each week – media

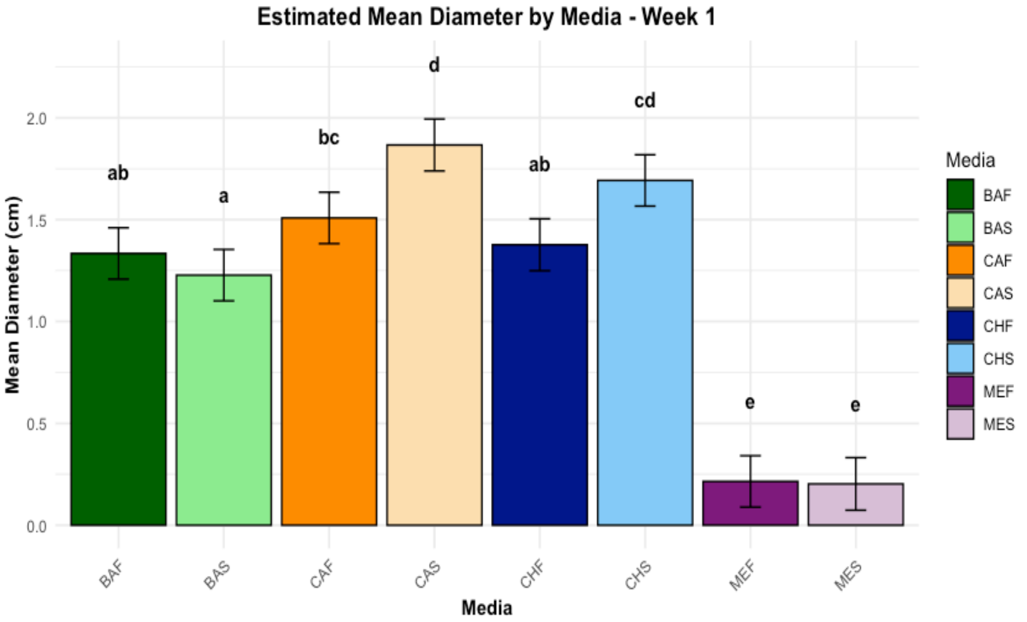

Figure 2-30. Media over strain – week 1

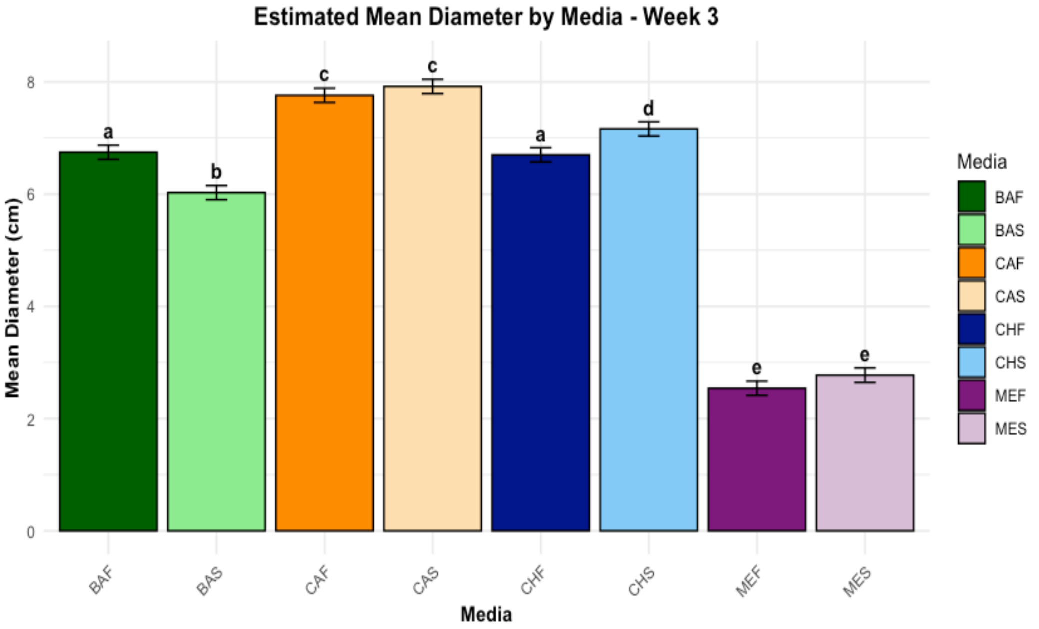

Figure 2-31. Media over strain – week 3

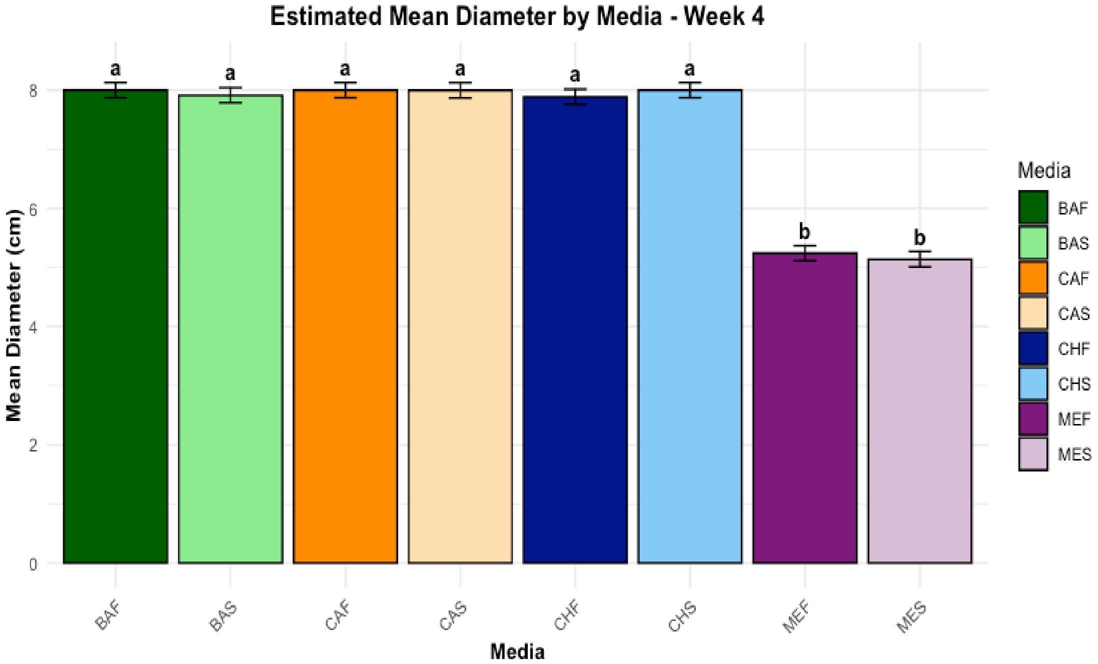

Figure 2-32. Media over strain – week 4

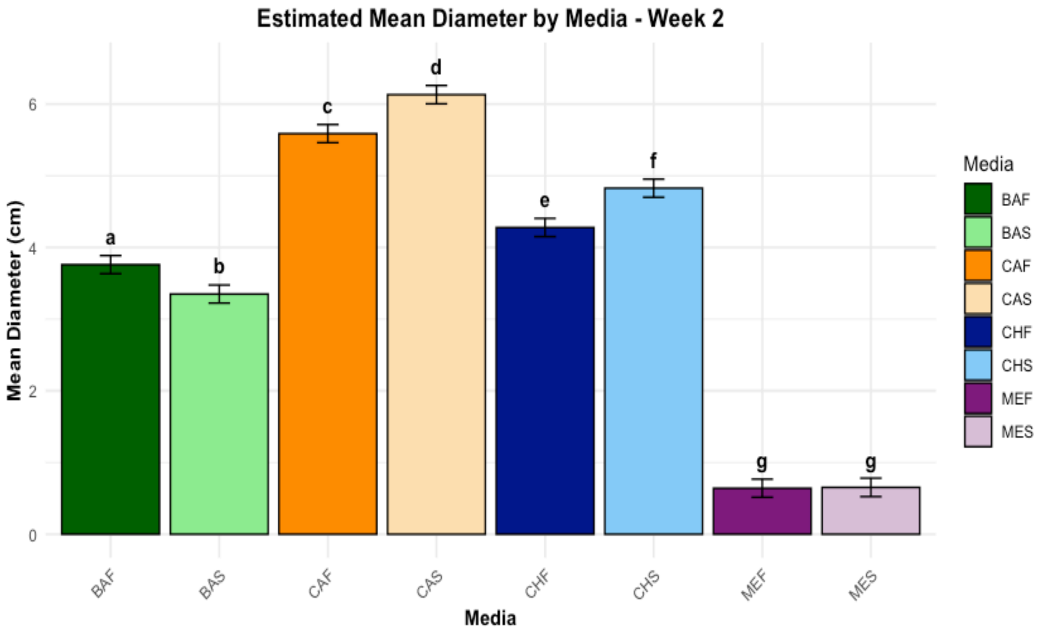

Figure 2-33. Media over strain – week 2

Table 2-27. Media over strain – week 1

Media	Week	Estimated Diameter (cm)	SE	df	95% CoI: L	95% CoI: U	CLD
BAF	1	1.33	0.06	924.02	1.21	1.46	ab
BAS	1	1.23	0.06	924.02	1.10	1.35	a
CAF	1	1.51	0.06	924.02	1.38	1.63	bc
CAS	1	1.87	0.06	937.09	1.74	1.99	d
CHF	1	1.38	0.06	937.09	1.25	1.50	ab
CHS	1	1.69	0.06	924.02	1.57	1.82	cd
MEF	1	0.21	0.06	924.02	0.09	0.34	e
MES	1	0.20	0.07	949.42	0.07	0.33	e

Table 2-28. Media over strain – week 2

Media	Week	Estimated Diameter (cm)	SE	df	95% CoI: L	95% CoI: U	CLD
BAF	2	3.76	0.06	924.02	3.63	3.89	a
BAS	2	3.35	0.06	924.02	3.22	3.48	b
CAF	2	5.59	0.06	924.02	5.46	5.71	c
CAS	2	6.13	0.06	937.09	6.00	6.26	d
CHF	2	4.28	0.06	937.09	4.15	4.41	e
CHS	2	4.83	0.06	924.02	4.70	4.95	f
MEF	2	0.64	0.06	924.02	0.52	0.77	g
MES	2	0.65	0.07	949.42	0.52	0.78	g

Table 2-29. Media over strain – week 3

Media	Week	Estimated Diameter (cm)	SE	df	95% CoI: L	95% CoI: U	CLD
BAF	3	6.75	0.06	924.02	6.62	6.87	a
BAS	3	6.03	0.06	924.02	5.90	6.15	b
CAF	3	7.76	0.06	924.02	7.63	7.89	c
CAS	3	7.92	0.06	937.09	7.79	8.05	c
CHF	3	6.70	0.06	937.09	6.57	6.83	a
CHS	3	7.16	0.06	924.02	7.04	7.29	d
MEF	3	2.54	0.06	924.02	2.41	2.67	e
MES	3	2.77	0.07	949.42	2.64	2.90	e

Table 2-30. Media over strain – week 4

Media	Week	Estimated Diameter (cm	SE	df	95% CoI: L	95% CoI: U	CLD
BAF	4	8.00	0.06	924.02	7.87	8.13	a
BAS	4	7.91	0.06	924.02	7.79	8.04	a
CAF	4	8.00	0.06	924.02	7.87	8.13	a
CAS	4	8.00	0.06	937.09	7.87	8.12	a
CHF	4	7.89	0.06	937.09	7.76	8.02	a
CHS	4	8.00	0.06	924.02	7.87	8.13	a
MEF	4	5.24	0.06	924.02	5.11	5.37	b
MES	4	5.14	0.07	949.42	5.01	5.27	b

THE EFFECTS OF STRAIN ON COLONY DIAMETER AVERAGED OVER MEDIA BY WEEK AND OVERALL

Significant Pairwise Contrasts

Table 2-31. Significant pairwise contrasts of strain over media - overall

Contrast	Estimate (cm)	SE	df	t.ratio	p.value
IOB1 - IOB2	0.23	0.04	286.10	5.22	<0.0001
IOB1 - IOB3	0.34	0.04	287.70	7.84	<0.0001
IOB1 - IOB5	-0.53	0.04	286.10	-12.25	<0.0001
IOB2 - IOB5	-0.76	0.04	287.70	-17.44	<0.0001
IOB3 - IOB5	-0.88	0.04	289.32	-20.04	<0.0001

Table 2-32. Significant pairwise contrasts of strain over media – week 1

Contrast	Week	Estimate (cm)	SE	df	t.ratio	p.value
IOB1 - IOB2	1	0.21	0.06	927.36	3.23	0.01
IOB1 - IOB3	1	0.19	0.06	930.65	2.88	0.02
IOB1 - IOB5	1	-0.19	0.06	927.36	-2.90	0.02
IOB2 - IOB5	1	-0.39	0.06	930.65	-6.10	<0.0001
IOB3 - IOB5	1	-0.37	0.06	933.89	-5.75	<0.0001

Table 2-33. Significant pairwise contrasts of strain over media – week 2

Contrast	Week	Estimate (cm)	SE	df	t.ratio	p.value
IOB1 - IOB5	2	-0.52	0.06	927.36	-8.10	<0.0001
IOB2 - IOB5	2	-0.50	0.06	930.65	-7.80	<0.0001
IOB3 - IOB5	2	-0.55	0.06	933.89	-8.45	<0.0001

Table 2-34. Significant pairwise contrasts of strain over media – week 3

Contrast	Week	Estimate (cm)	SE	df	t.ratio	p.value
IOB1 - IOB2	3	0.44	0.06	927.36	6.79	<0.0001
IOB1 - IOB3	3	0.69	0.06	930.65	10.75	<0.0001
IOB1 - IOB5	3	-0.79	0.06	927.36	-12.28	<0.0001
IOB2 - IOB3	3	0.26	0.06	933.89	3.97	0.0004
IOB2 - IOB5	3	-1.23	0.06	930.65	-19.01	<0.0001
IOB3 - IOB5	3	-1.49	0.06	933.89	-22.93	<0.0001

Table 2-35. Significant pairwise contrasts of strain over media – week 4

Contrast	Week	Estimate (cm)	SE	df	t.ratio	p.value
IOB1 - IOB2	4	0.28	0.06	927.36	4.39	<0.0001
IOB1 - IOB3	4	0.46	0.06	930.65	7.15	<0.0001
IOB1 - IOB5	4	-0.64	0.06	927.36	-9.87	<0.0001
IOB2 - IOB3	4	0.18	0.06	933.89	2.77	0.0311
IOB2 - IOB5	4	-0.92	0.06	930.65	-14.22	<0.0001
IOB3 - IOB5	4	-1.10	0.06	933.89	-16.94	<0.0001

Tables and Figures

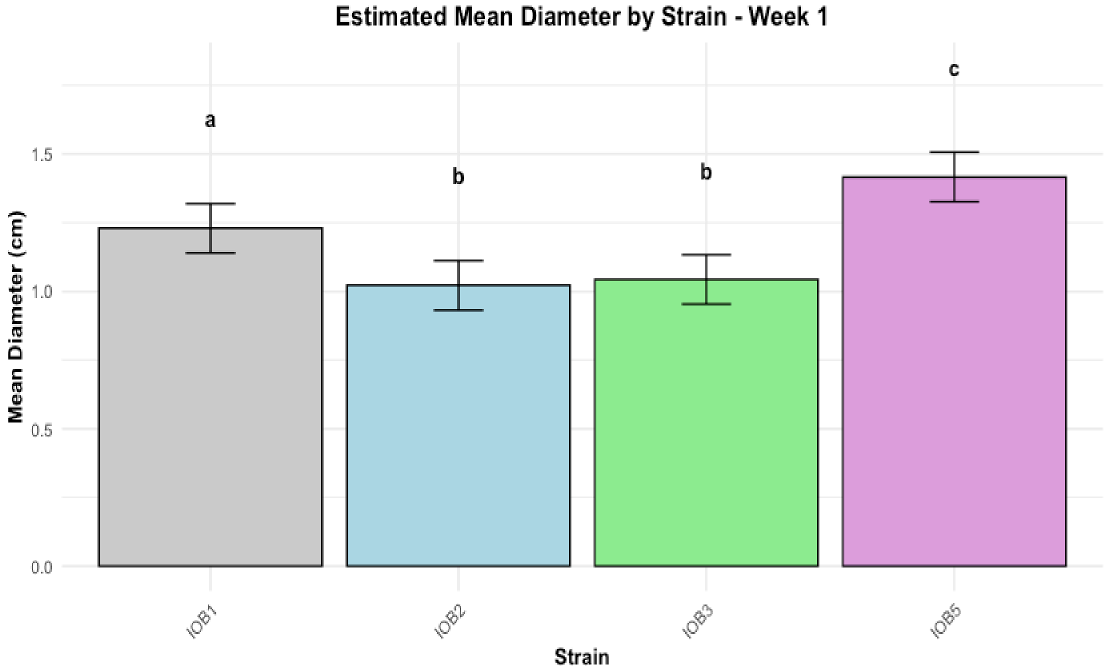

Figure 2-34. Strain over media – week 1

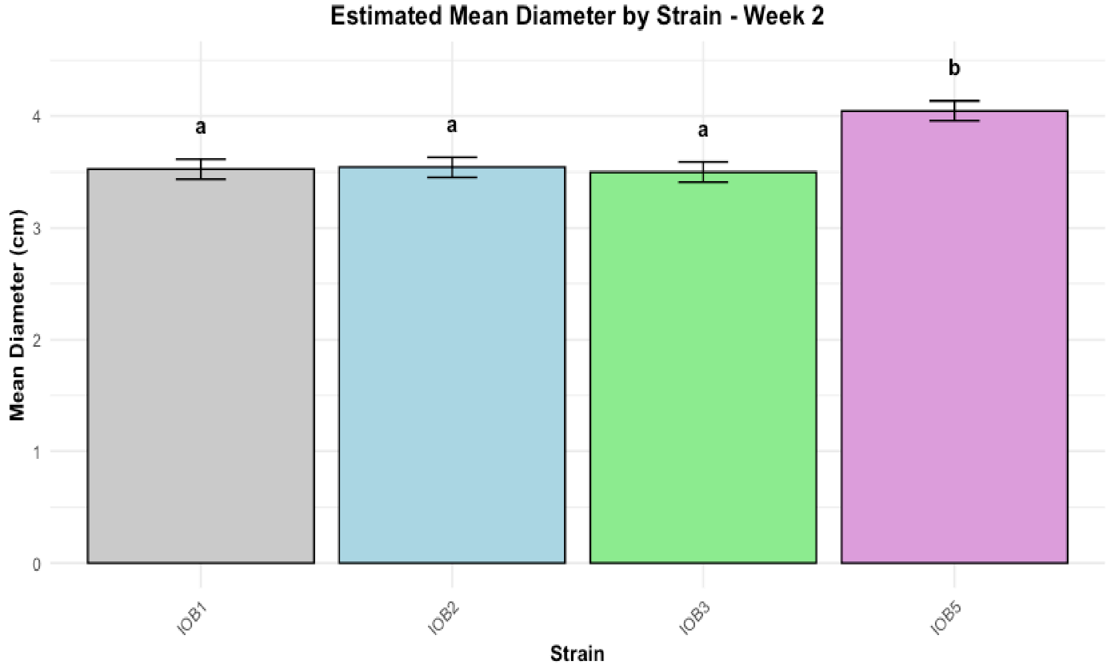

Figure 2-35. Strain over media – week 2

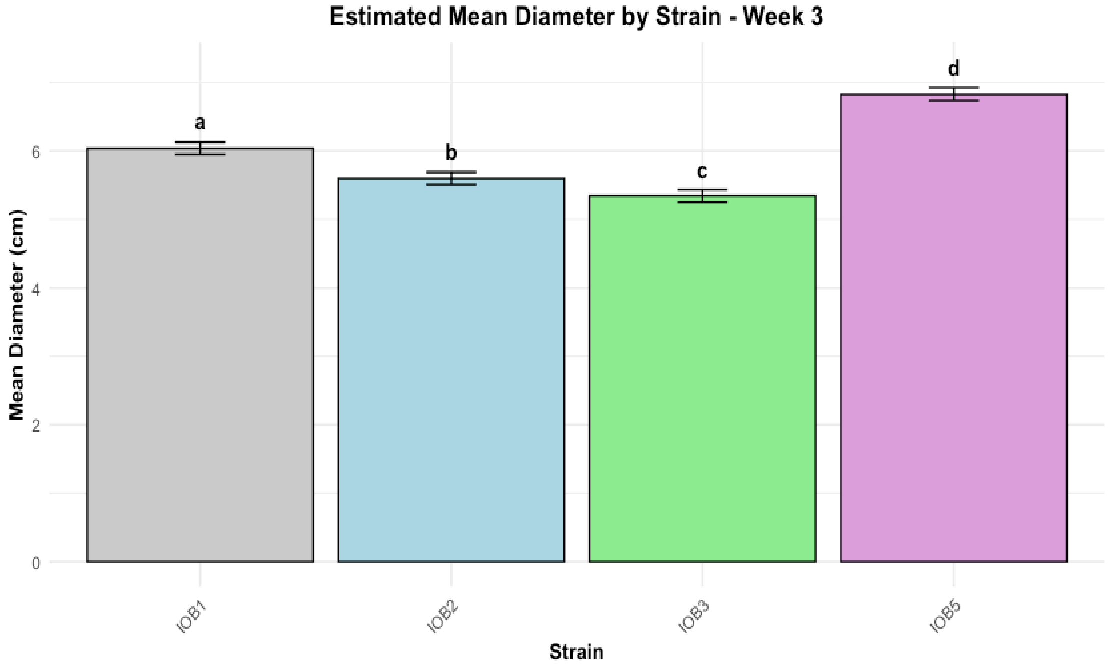

Figure 2-36. Strain over media – week 3

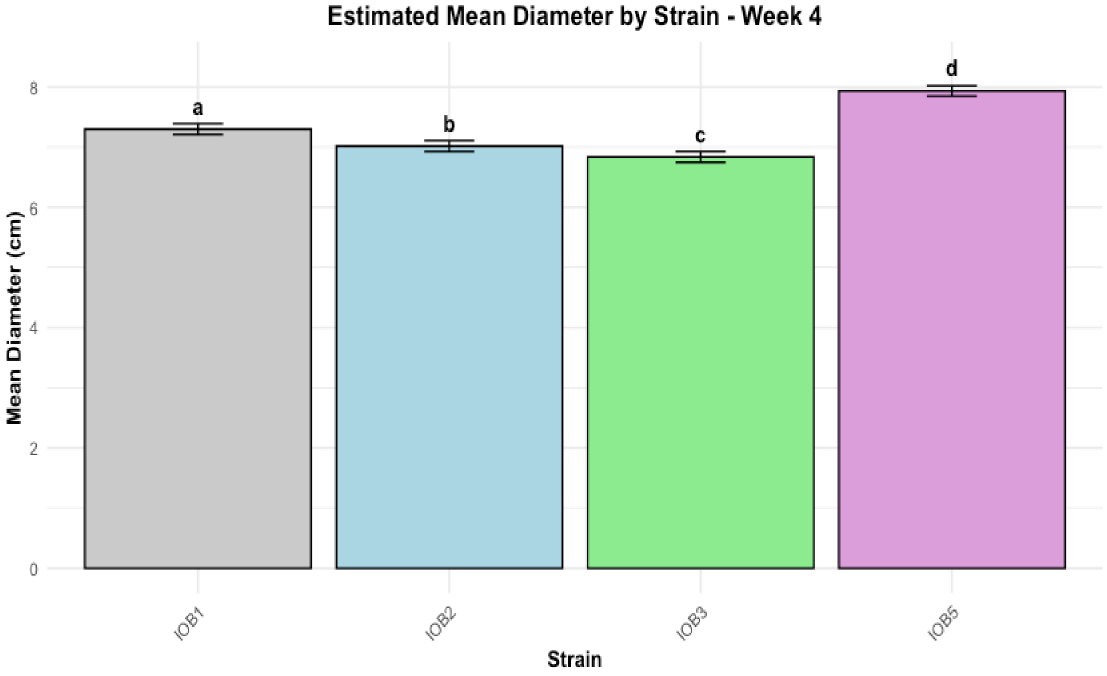

Figure 2-37. Strain over media – week 4

Table 2-36. Strain over media – week 1

Strain	Week	Estimated Diameter (cm)	SE	df	95% CoI: L	95% CoI: U	CLD
IOB1	1	1.23	0.05	924.02	1.14	1.32	a
IOB2	1	1.02	0.05	930.65	0.93	1.11	b
IOB3	1	1.04	0.05	937.09	0.95	1.13	b
IOB5	1	1.42	0.05	930.65	1.33	1.51	c

Table 2-37. Strain over media – week 2

Strain	Week	Estimated Diameter (cm)	SE	df	95% CoI: L	95% CoI: U	CLD
IOB1	2	3.53	0.05	924.02	3.44	3.61	a
IOB2	2	3.54	0.05	930.65	3.45	3.63	a
IOB3	2	3.50	0.05	937.09	3.41	3.59	a
IOB5	2	4.05	0.05	930.65	3.96	4.14	b

Table 2-38. Strain over media – week 3

Strain	Week	Estimated Diameter (cm)	SE	df	95% CoI: L	95% CoI: U	CLD
IOB1	3	6.04	0.05	924.02	5.95	6.13	a
IOB2	3	5.60	0.05	930.65	5.51	5.69	b
IOB3	3	5.34	0.05	937.09	5.25	5.43	c
IOB5	3	6.83	0.05	930.65	6.74	6.92	d

Table 2-39. Strain over media – week 4

Strain	Week	Estimated Diameter (cm)	SE	df	95% CoI: L	95% CoI: U	CLD
IOB1	4	7.30	0.05	924.02	7.21	7.39	a
IOB2	4	7.02	0.05	930.65	6.93	7.11	b
IOB3	4	6.84	0.05	937.09	6.75	6.93	c
IOB5	4	7.94	0.05	930.65	7.85	8.03	d

THE EFFECTS OF MEDIA ON COLONY DIAMETER BY STRAIN AVERAGED OVER WEEKS

Significant Pairwise Contrasts

Table 2-40. Significant pairwise contrasts – media by strain – IOB1

Contrast	Strain	Estimate (cm)	SE	df	t.ratio	p.value
BAF - BAS	IOB1	0.52	0.12	284.49	4.19	0.0009
BAF - CHF	IOB1	-0.38	0.12	284.49	-3.13	0.0404
BAF - MEF	IOB1	3.25	0.12	284.49	26.37	<0.0001
BAF - MES	IOB1	3.20	0.12	284.49	25.99	<0.0001
BAS - CAS	IOB1	-0.88	0.12	284.49	-7.17	<0.0001
BAS - CHF	IOB1	-0.90	0.12	284.49	-7.32	<0.0001
BAS - CHS	IOB1	-0.85	0.12	284.49	-6.95	<0.0001
BAS - MEF	IOB1	2.73	0.12	284.49	22.18	<0.0001
BAS - MES	IOB1	2.68	0.12	284.49	21.80	<0.0001
CAF - CAS	IOB1	-0.59	0.12	284.49	-4.78	0.0001
CAF - CHF	IOB1	-0.61	0.12	284.49	-4.93	<0.0001
CAF - CHS	IOB1	-0.56	0.12	284.49	-4.55	0.0002
CAF - MEF	IOB1	3.02	0.12	284.49	24.57	<0.0001
CAF - MES	IOB1	2.98	0.12	284.49	24.19	<0.0001
CAS - MEF	IOB1	3.61	0.12	284.49	29.35	<0.0001
CAS - MES	IOB1	3.57	0.12	284.49	28.97	<0.0001
CHF - MEF	IOB1	3.63	0.12	284.49	29.50	<0.0001
CHF - MES	IOB1	3.58	0.12	284.49	29.12	<0.0001
CHS - MEF	IOB1	3.58	0.12	284.49	29.12	<0.0001

CHS - MES	IOB1	3.54	0.12	284.49	28.74	<0.0001

Table 2-41. Significant pairwise contrasts – media by strain – IOB2

Contrast	Strain	Estimate (cm)	SE	df	t.ratio	p.value
BAF - CAF	IOB2	-1.31	0.12	284.49	-10.64	<0.0001
BAF - CAS	IOB2	-1.65	0.12	284.49	-13.41	<0.0001
BAF - CHS	IOB2	-0.62	0.12	284.49	-5.01	<0.0001
BAF - MEF	IOB2	2.42	0.12	284.49	19.70	<0.0001
BAF - MES	IOB2	3.23	0.12	297.40	25.90	<0.0001
BAS - CAF	IOB2	-1.47	0.12	284.49	-11.95	<0.0001
BAS - CAS	IOB2	-1.81	0.12	284.49	-14.72	<0.0001
BAS - CHS	IOB2	-0.78	0.12	284.49	-6.32	<0.0001
BAS - MEF	IOB2	2.26	0.12	284.49	18.39	<0.0001
BAS - MES	IOB2	3.06	0.12	297.40	24.60	<0.0001
CAF - CHF	IOB2	1.53	0.12	284.49	12.43	<0.0001
CAF - CHS	IOB2	0.69	0.12	284.49	5.64	<0.0001
CAF - MEF	IOB2	3.74	0.12	284.49	30.34	<0.0001
CAF - MES	IOB2	4.54	0.12	297.40	36.41	<0.0001
CAS - CHF	IOB2	1.87	0.12	284.49	15.20	<0.0001
CAS - CHS	IOB2	1.04	0.12	284.49	8.41	<0.0001
CAS - MEF	IOB2	4.08	0.12	284.49	33.11	<0.0001
CAS - MES	IOB2	4.88	0.12	297.40	39.15	<0.0001
CHF - CHS	IOB2	-0.84	0.12	284.49	-6.79	<0.0001
CHF - MEF	IOB2	2.21	0.12	284.49	17.91	<0.0001
CHF - MES	IOB2	3.01	0.12	297.40	24.13	<0.0001
CHS - MEF	IOB2	3.04	0.12	284.49	24.71	<0.0001
CHS - MES	IOB2	3.84	0.12	297.40	30.84	<0.0001
MEF - MES	IOB2	0.80	0.12	297.40	6.43	<0.0001

Table 2-42. Significant pairwise contrasts – media by strain – IOB3

Contrast	Strain	Estimate (cm)	SE	df	t.ratio	p.value
BAF - CAF	IOB3	-1.34	0.12	284.49	-10.88	<0.0001
BAF - CAS	IOB3	-1.39	0.12	284.49	-11.29	<0.0001
BAF - CHS	IOB3	-0.65	0.12	284.49	-5.29	<0.0001
BAF - MEF	IOB3	3.53	0.12	284.49	28.69	<0.0001
BAF - MES	IOB3	3.15	0.12	297.40	25.31	<0.0001
BAS - CAF	IOB3	-1.57	0.12	284.49	-12.76	<0.0001
BAS - CAS	IOB3	-1.62	0.12	284.49	-13.18	<0.0001
BAS - CHS	IOB3	-0.88	0.12	284.49	-7.18	<0.0001
BAS - MEF	IOB3	3.30	0.12	284.49	26.80	<0.0001
BAS - MES	IOB3	2.92	0.12	297.40	23.44	<0.0001
CAF - CHF	IOB3	1.30	0.12	297.40	10.47	<0.0001
CAF - CHS	IOB3	0.69	0.12	284.49	5.59	<0.0001
CAF - MEF	IOB3	4.87	0.12	284.49	39.56	<0.0001
CAF - MES	IOB3	4.49	0.12	297.40	36.05	<0.0001

CAS - CHF	IOB3	1.36	0.12	297.40	10.88	<0.0001
CAS - CHS	IOB3	0.74	0.12	284.49	6.00	<0.0001
CAS - MEF	IOB3	4.92	0.12	284.49	39.98	<0.0001
CAS - MES	IOB3	4.54	0.12	297.40	36.46	<0.0001
CHF - CHS	IOB3	-0.62	0.12	297.40	-4.95	<0.0001
CHF - MEF	IOB3	3.57	0.12	297.40	28.62	<0.0001
CHF - MES	IOB3	3.19	0.13	310.44	25.29	<0.0001
CHS - MEF	IOB3	4.18	0.12	284.49	33.98	<0.0001
CHS - MES	IOB3	3.80	0.12	297.40	30.53	<0.0001

Table 2-43. Significant pairwise contrasts – media by strain – IOB5

Contrast	Strain	Estimate (cm)	SE	df	t.ratio	p.value
BAF - BAS	IOB5	0.41	0.12	284.49	3.35	0.0203
BAF - CAF	IOB5	-0.59	0.12	284.49	-4.78	0.0001
BAF - CAS	IOB5	-0.67	0.12	297.40	-5.34	<0.0001
BAF - MEF	IOB5	2.00	0.12	284.49	16.26	<0.0001
BAF - MES	IOB5	1.49	0.12	284.49	12.12	<0.0001
BAS - CAF	IOB5	-1.00	0.12	284.49	-8.13	<0.0001
BAS - CAS	IOB5	-1.08	0.12	297.40	-8.65	<0.0001
BAS - CHF	IOB5	-0.62	0.12	284.49	-5.01	<0.0001
BAS - CHS	IOB5	-0.65	0.12	284.49	-5.26	<0.0001
BAS - MEF	IOB5	1.59	0.12	284.49	12.91	<0.0001
BAS - MES	IOB5	1.08	0.12	284.49	8.77	<0.0001
CAF - CHF	IOB5	0.39	0.12	284.49	3.13	0.0404
CAF - MEF	IOB5	2.59	0.12	284.49	21.04	<0.0001
CAF - MES	IOB5	2.08	0.12	284.49	16.91	<0.0001
CAS - CHF	IOB5	0.46	0.12	297.40	3.71	0.0061
CAS - CHS	IOB5	0.43	0.12	297.40	3.45	0.0144
CAS - MEF	IOB5	2.67	0.12	297.40	21.40	<0.0001
CAS - MES	IOB5	2.16	0.12	297.40	17.32	<0.0001
CHF - MEF	IOB5	2.21	0.12	284.49	17.91	<0.0001
CHF - MES	IOB5	1.70	0.12	284.49	13.78	<0.0001
CHS - MEF	IOB5	2.24	0.12	284.49	18.17	<0.0001
CHS - MES	IOB5	1.73	0.12	284.49	14.03	<0.0001
MEF - MES	IOB5	-0.51	0.12	284.49	-4.13	0.0012

Figures and Tables

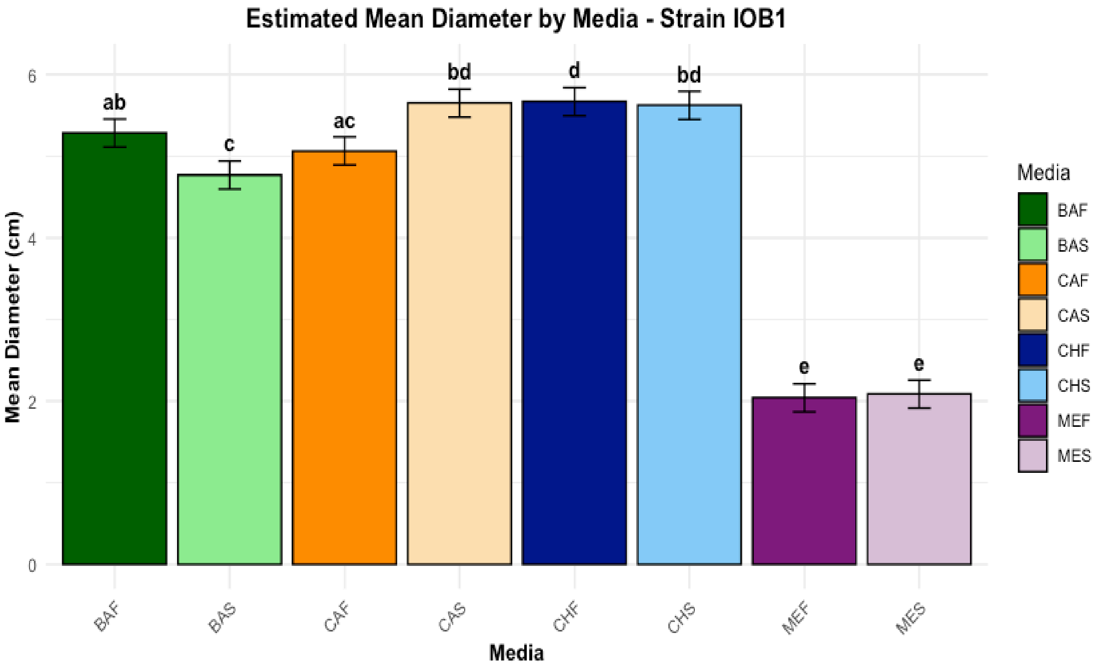

Figure 2-38. Media by strain – IOB1

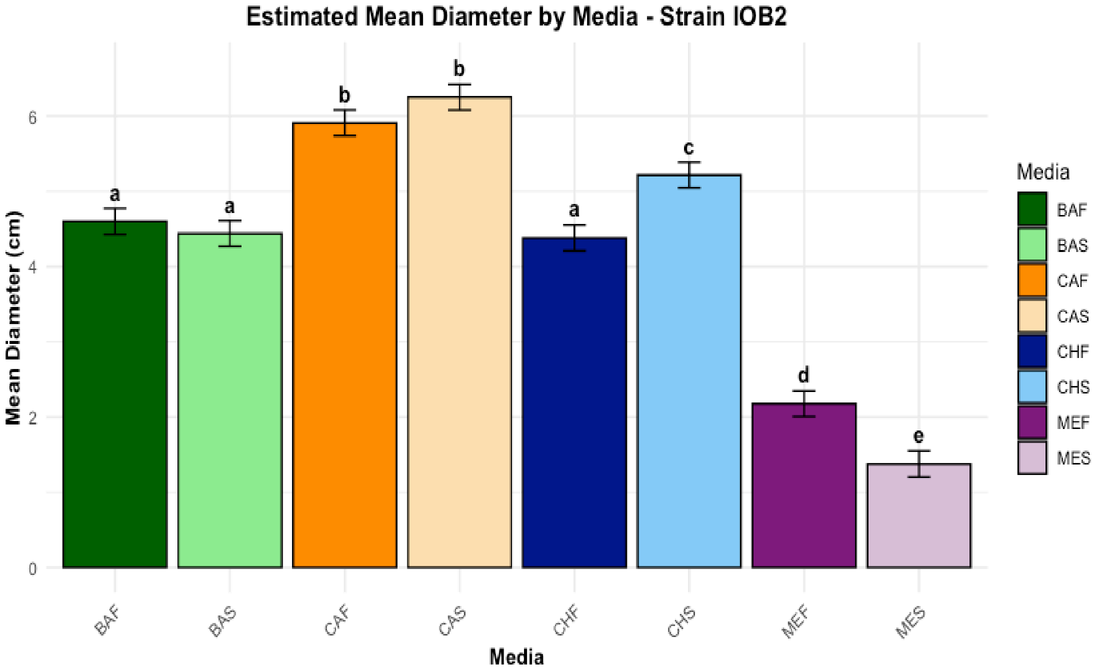

Figure 2-39. Media by strain – IOB2

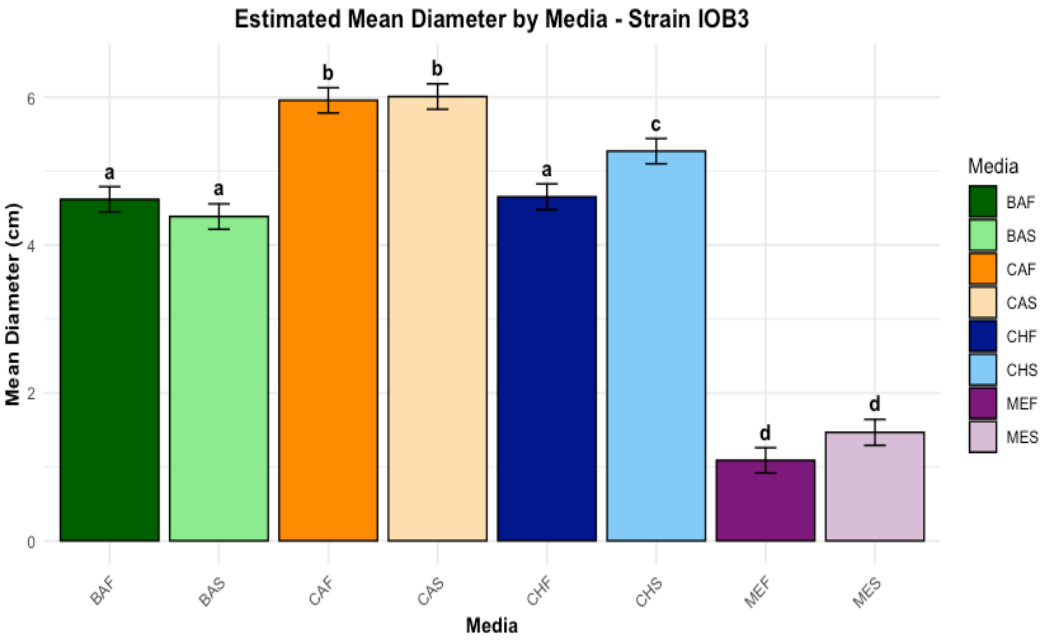

Figure 2-40. Media by strain – IOB3

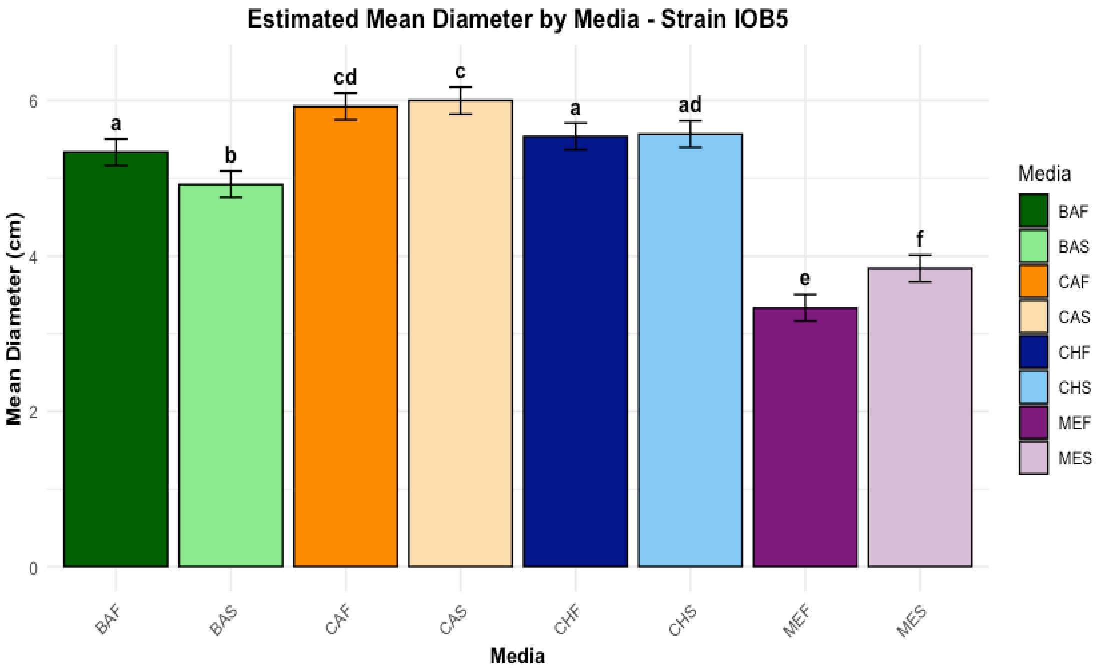

Figure 2-41. Media by strain – IOB5

Table 2-44. Media by strain – IOB1

Media	Strain	Estimated Diameter (cm)	SE	df	95% CoI: L	95% CoI: U	CLD
BAF	IOB1	5.29	0.09	284.49	5.11	5.46	ab
BAS	IOB1	4.77	0.09	284.49	4.60	4.94	c
CAF	IOB1	5.06	0.09	284.49	4.89	5.23	ac
CAS	IOB1	5.65	0.09	284.49	5.48	5.82	bd
CHF	IOB1	5.67	0.09	284.49	5.50	5.84	d
CHS	IOB1	5.62	0.09	284.49	5.45	5.80	bd
MEF	IOB1	2.04	0.09	284.49	1.87	2.21	e
MES	IOB1	2.09	0.09	284.49	1.91	2.26	e

Table 2-45. Media by strain – IOB2

Media	Strain	Estimated Diameter (cm)	SE	df	95% CoI: L	95% CoI: U	CLD
BAF	IOB2	4.60	0.09	284.49	4.43	4.77	a
BAS	IOB2	4.44	0.09	284.49	4.27	4.61	a
CAF	IOB2	5.91	0.09	284.49	5.74	6.08	b
CAS	IOB2	6.25	0.09	284.49	6.08	6.43	b
CHF	IOB2	4.38	0.09	284.49	4.21	4.55	a
CHS	IOB2	5.22	0.09	284.49	5.05	5.39	c
MEF	IOB2	2.18	0.09	284.49	2.01	2.35	d
MES	IOB2	1.38	0.09	310.44	1.20	1.55	e

Table 2-46. Media by strain – IOB3

Media	Strain	Estimated Diameter (cm)	SE	df	95% CoI: L	95% CoI: U	CLD
BAF	IOB3	4.62	0.09	284.49	4.45	4.79	a
BAS	IOB3	4.39	0.09	284.49	4.21	4.56	a
CAF	IOB3	5.96	0.09	284.49	5.79	6.13	b
CAS	IOB3	6.01	0.09	284.49	5.84	6.18	b
CHF	IOB3	4.65	0.09	310.44	4.48	4.83	a
CHS	IOB3	5.27	0.09	284.49	5.10	5.44	c
MEF	IOB3	1.09	0.09	284.49	0.92	1.26	d
MES	IOB3	1.47	0.09	310.44	1.29	1.64	d

Table 2-46. Media by strain – IOB5

Media	Strain	Estimated Diameter (cm)	SE	df	95% CoI: L	95% CoI: U	CLD
BAF	IOB5	5.33	0.09	284.49	5.16	5.51	a
BAS	IOB5	4.92	0.09	284.49	4.75	5.09	b
CAF	IOB5	5.92	0.09	284.49	5.75	6.09	cd
CAS	IOB5	6.00	0.09	310.44	5.82	6.17	c
CHF	IOB5	5.54	0.09	284.49	5.37	5.71	a
CHS	IOB5	5.57	0.09	284.49	5.40	5.74	ad
MEF	IOB5	3.33	0.09	284.49	3.16	3.50	e
MES	IOB5	3.84	0.09	284.49	3.67	4.01	f

CHAPTER 3:

INONOTUS OBLIQUUS (HYMENOCHAETACEAE) AMPHITHALLISM:

MATING SYSTEM AND CHARACTERIZATION OF HIGHLY VARIABLE BASIDIOSPORE NUCLEAR BEHAVIOURS

ABSTRACT

Inonotus obliquus(Ach. ex Pers.) Pilàt is a parasitic white heart rot fungus of circumboreal distribution belonging to the family Hymenochaetaceae. It is primarily hosted on birch, but can occur on other hardwoods. Typically, this fungus is recognized by a charcoal-like sterile conk with a yellowish-brown interior that forms on the host tree. As the name suggests, the sterile conk does not produce any basidiospores. Once in an infection cycle of approximately 10 - 80 years, a spore-producing resupinate and poroid basidiomata will form beneath the bark of a recently dead host. The mating system of this fungus has been speculated to be amphithallic (primarily pseudohomothallic + tetrapolar heterothallic).

Laboratory produced *I. obliquus* basidiomata were analyzed for variability in nuclear behaviour over maturation. Nuclear examination was carried out using Hoechst 33342 and fluorescence microscopy. It was discovered that the basidiospores of *I. obliquus* have highly variable nuclear characteristics, as they can contain between 1 and 6 nuclei in different ratios at different points in development. A Bayesian logistic mixed-effects model was run to examine these differences and displayed frequent credibility. The presence of both homokaryotic and heterokaryotic basidiospores confirms an amphithallic mating system. Comparisons made between the present work and comparable work by Chinese researchers on *I. obliquus* showed both similarity and major differences. It is possible these differences were caused by laboratory growing conditions, in protocol, or genetics. The post-meiotic nuclear events in *I. obliquus* are speculated: basidiospores are likely to possess multiple genotypes and varying nuclear ratios. This has important implications for ecology, dispersal, and population genetics. To date, this is the most well-characterized mating system in the Hymenochaetaceae.

INTRODUCTION

Studying mating in the Hymenochaetaceae has been notoriously difficult. Members of this family do not possess clamp connections, a classic feature for testing mating compatibility in Agaricomycetes (Kothe, 1996; Rajchenberg *et al.* 2015). Homokaryotic and Heterokaryotic cultures possess multinucleate hyphae and are typically not distinguishable based on micro or cultural characters (Mallett & Myrholm, 1995; Goldstein & Gilbertson, 1981; Rajchenberg, 2011;). Certain studies examining mating systems of this group using classical *in vitro* pairings have resulted in false positives (Mallett & Myrholm, 1995). Going forward, mating studies in this group should involve the use of various molecular techniques (Kauserud & Schumacher, 2001). *Inonotus obliquus* (Ach. ex Pers.) Pilàt is an especially difficult member to study as its basidiomata are notoriously rare and difficult to find (Bunyard, 2015). This species been shown to possess a variety of potential medicinal properties, is increasingly popular as a consumer product, and is an important wild harvested and cultivatable resource (Pilz, 2004; Thomas *et al.* 2020; Miina *et al.* 2021; Ern *et al.* 2023).

Recently, methods have been developed to form the basidiomata under laboratory conditions (see Chapter 2; Sun *et al.* 2023). This has enabled the study of its mating system and basidiospore nuclear characteristics. Sun *et al.* (2023) reported that *I. obliquus* primarily displays a pseudohomothallic (secondary homothallic) mating system along with being tetrapolar heterothallic; thus, can be characterized as amphithallic *sensu* Lange (1952). Sun *et al.* (2023) sequenced the *MAT* region of *I. obliquus* and found it was relatively similar to a typical agaricomyceteous *MAT* structure which contains two unlinked *MAT* A and *MAT* B that encode pairs of homeodomain regulatory proteins (HD1/HD2) and compliments of pheromone receptor and pheromone precursor genes respectively (Fraser *et al.* 2007). It was found to produce anucleate, uninucleate, binucleate, trinucleate, and tetranucleate basidiospores in varying proportions at different stages of basidiomata maturity. However, sample sizes and a formal statistical analysis were not presented. Therefore, the experiment was loosely based on sparse data through frequent spore printing of *in vitro I. obliquus* basidiomata, The following report examines how basidiospore nuclear type proportion shifts compare to the results of Sun *et al.* (2023) and speculates the potential implications of the proposed mating system and basidiospore nuclear behaviour.

MATERIALS AND METHODS

STRAINS AND CULTURING

Three wild strains of *Inonotus obliquus* (IOB2, IOB3, IOB5) were examined for maturity-driven basidiospore nuclear-type ratio variability. They were isolated from *I. obliquus* sterile conk fragments or infected wood (see Chapter 2). Identification of these strains were verified through ITS using Oxford Nanopore (see Chapter 2). It was found that IOB2 would fruit consistently and reliably *in vitro*, while the remaining strains (IOB3 and IOB5) would do so more inconsistently (see Chapter 2). Due to this, IOB2 had significantly far more basidiospores collected and analyzed for this study. The inoculum for each strain was grown on carrot agar (see Chapter 2) in complete darkness at room temperature (20°C ± 2) for 2-3 weeks. A 7mm cork borer was used to aseptically cut agar plugs of mycelium from the margin of each respective strain and transferred to the centre of 2% modified MEA plates (20g malt extract, 1g yeast extract, 15g agar, 1000ml water) and incubated in complete darkness for approximately 40 days. The *I. obliquus in vitro* fruiting protocol utilized in Chapter 2, and many fruit bodies from those experiments, were implemented here. To supplement these data, additional Petri dishes of IOB2 were made to fruit so their basidiospores could be analyzed

BASIDIOSPORE COLLECTION, HOECHST 33342 STAINING, AND EPIFLUORESCENCE MICROSCOPY

To analyze how the proportion of basidiospores of different nuclear types (uninucleate, binucleate, trinucleate, tetranucleate, pentanucleate, and hexanucleate) changed with hymenium maturity, three main steps were followed:

(1) Formation of fruiting bodies *in vitro*
(2) Frequent repeated basidiospore collection from live developing fruit bodies
(3) Staining of collected basidiospores with Hoechst 33342 and observation of basidiospores of different nuclear types with epifluorescence microscopy (Olympus IX51 Inverted Microscope)

1 – Fruiting Body Formation

Fruiting bodies were formed using the methods previously outlined (see Chapter 2). These sometimes formed under blue light, white light, or in complete darkness. Each was treated with the same collection, staining, and observation protocols that are outlined below. In total, 15 fruit bodies had their basidiospores temporally analyzed. The fruiting capacity of each strain (IOB1, IOB2, IOB3, and IOB5) significantly influenced the frequency of their basidiospore examination. Twelve were formed by IOB2, two by IOB3, one by IOB5, and zero by IOB1 (Table 3-1). IOB2 primarily influences the data collected here, while the others only supply a small amount of information.

2 – Basidiospore Collection

Basidiospores were collected by spore printing from developing fruiting bodies directly from Petri dishes onto specialized microscope slides, repeatedly throughout their development over an average of 9 days. The minimum was 1 day, and the maximum was 19 days (Table 3-1). These values represent the temporal range during which sampling took place from the onset of basidiospore production, not the number of days sampled. Agar plates containing fruit bodies were positioned face down without a lid and placed in a room-temperature incubator in complete darkness for 1 to 24 hours (Figures 3-1 & 3-2). The printing duration was determined by the rate of spore discharge and the maturity of the fruiting body (Figure 3-3). After spore collection, Petri dishes were placed in a downward-facing position so that pores continued to form in a direction conducive to repeated printing (see Chapter 2 for effects of gravity on fruiting bodies). To prevent desiccation of basidiomata during spore collection, humidity was increased by adding 1-2 mL of sterile water to the agar surface of fertile Petri dishes every few days, and a water-soaked tray of perlite was placed in the incubator. In low humidity, fruit bodies would often cease to produce spores and die. The specialized microscope slides were coated with a thin layer of egg albumin applied with a toothpick to serve as an organic fixative. This method was time-efficient, but spores would not properly fix if they were printed in a thick layer. Spores required to be cast in a layer that was one spore thick, such that each one was discrete. The slides were examined dry following fruit body printing with phase contrast microscopy using a Nikon Eclipse e400 to ensure that spores were cast appropriately for analysis. The basidiospores would fix as soon as they landed on these slides; therefore, they were in the near-exact relative position from which they were cast from basidia.

Over their development, fruit bodies were placed into one of three maturity categories that occupy a range of days: **Young** (1 – 3 days old), **Middle** (4 – 8 days old) and **Old** (9 – 10+ days old). Ideally, printing would commence when primordial pores became visible and was repeated frequently in the days following; however, this was not always the case. Occasionally, printing began when the fruit body was in a later developmental stage; thus, spore collection did not occur while the hymenium was in a young state. Also, basidiospores would sometimes only be collected in the first few days of development because of the cessation of spore production or fruiting body desiccation. These inconsistencies meant that some fruiting bodies had spores collected for only one or two of the maturity categories, not all three (Table 3-1).

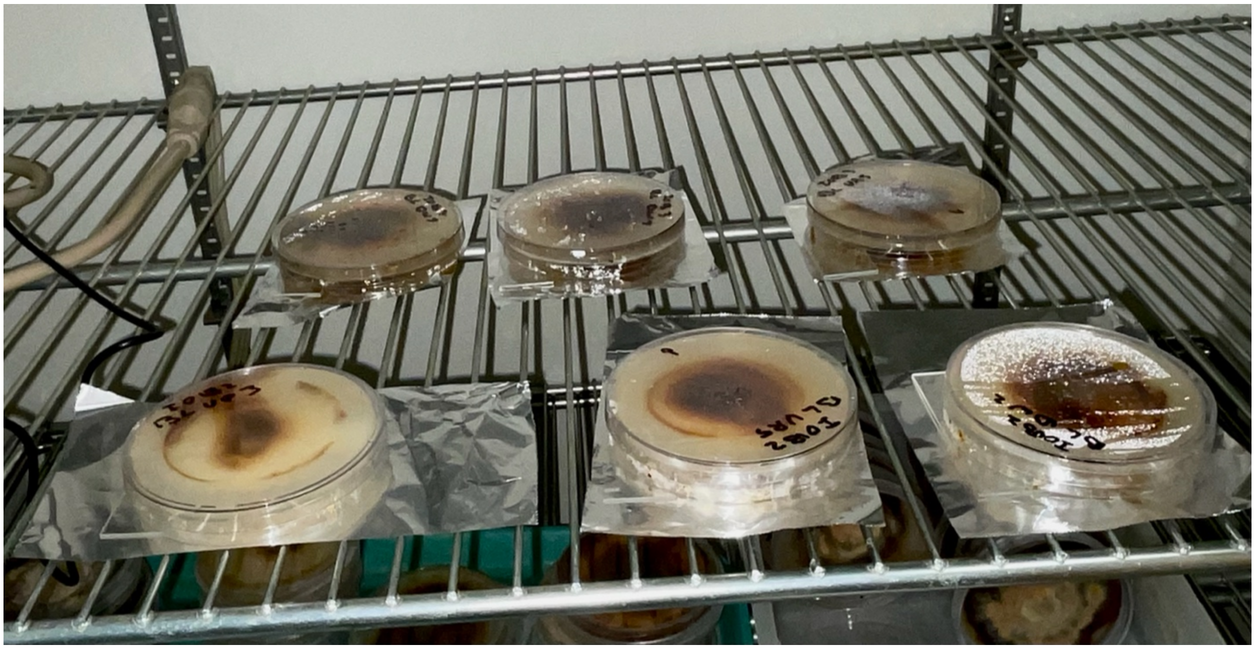

Figure 3-1. Inverted Petri dishes spore printing on microscope slides

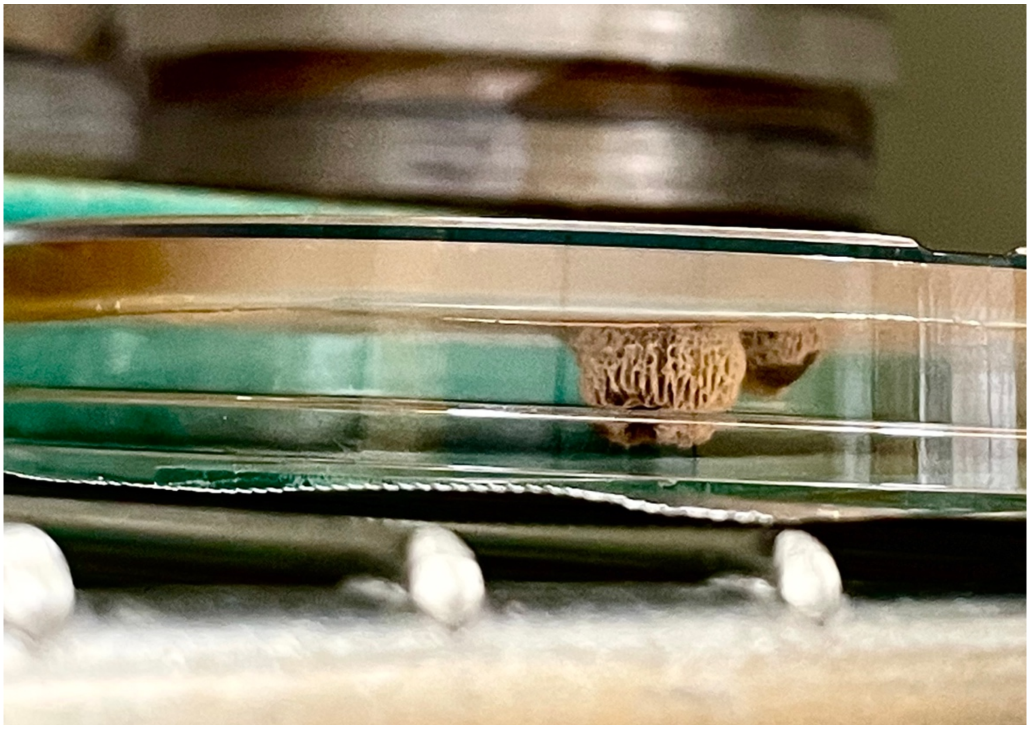

Figure 3-2. Side view of fruit body on inverted Petri dish

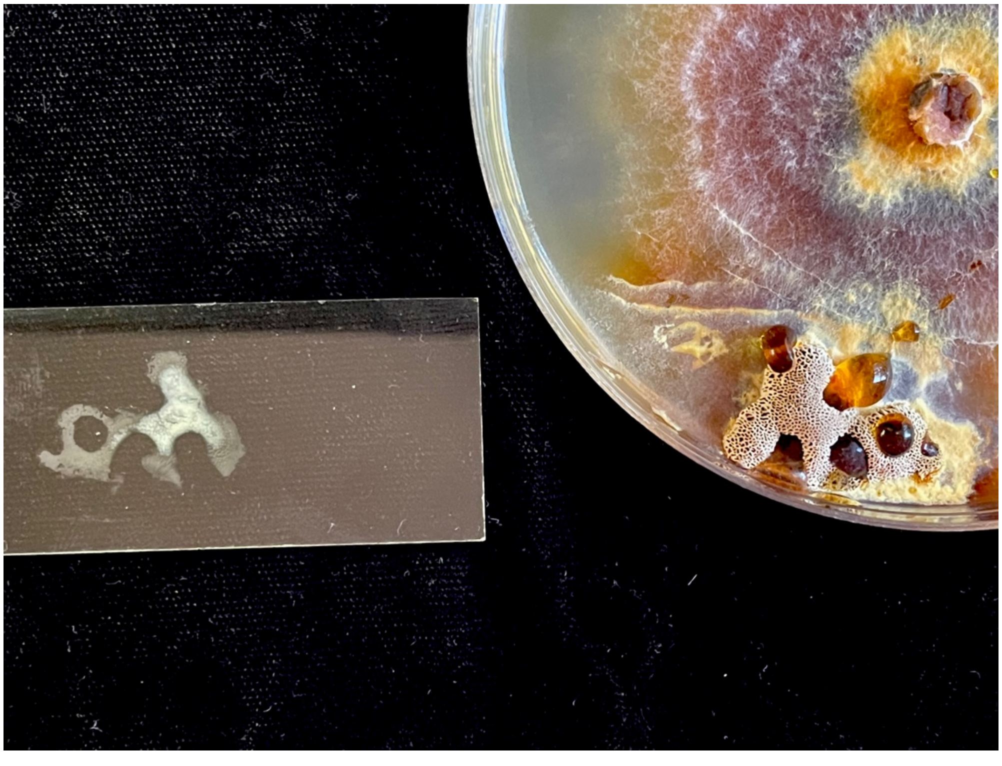

Figure 3-3. Resulting spore print of *in vitro* basidioma

3 – Basidiospore Nuclear Staining and Epifluorescence Microscopy

Collected spores were immediately stained with Hoechst 33342 (Invitrogen, Carlsbad, California, USA, Catalogue #: H3570) at a concentration of 5µg/ml (diluted from a stock of 10mg/ml in 1x or sometimes 10x PBS) for 30 minutes at room temperature in complete darkness and viewed with an Olympus IX51 Inverted Microscope equipped with a 100W mercury fluorescence system, a Cooled CCD digital camera, and a narrow UV filter cube with an excitation range of 360-370 nm (Figure 3-4).

Figure 3-4. Olympus IX51 Inverted Microscope

Overall, while Hoechst 33342 was simple to use in practice, it was incredibly temperamental in this application. This protocol required very consistent and controlled spore collection to work reliably. Optimal spore prints were as described above; relatively sparse and single-layered so that they could adhere to the albumin and be stained properly. When basidiomata were left to print too long in a humid environment, an accumulated and waterlogged spore mass would form. Upon drying, this resulted in a dense "spore crust". Even after rehydration and dilution, these spores strongly resisted the uptake of Hoechst 33342 in their nuclei. If the spore printing was not perfect, the stain would not uptake properly, leaving many with sometimes a brightly stained wall (Figure 3-5). As a result, certain collections could not have their basidiospores examined and are missing nuclear spore data across all three maturity categories. Exactly why this occurred is unknown and merits further investigation. When executed properly, the stain functioned beautifully and allowed for the observation of nuclear behaviour in basidiospores almost immediately after they had been ejected, providing insights into the post-shed nuclear status.

The basidiospores were recorded manually for how many discrete and discernible nuclei they contained and were placed into one of six categories: uninucleate, binucleate, trinucleate, tetranucleate, pentanucleate, and hexanucleate. Due to the staining challenges, spores that appeared anucleate were not recorded as such because of potential stain failure and a time constrained sampling window; however, they were likely present at times. Basidiospores which possessed nuclei that could not be distinguished or were heavily distorted were not counted in this study. It is important to consider that basidiospores were viewed in a single fixed axis, therefore, nuclei had the possibility of overlapping and being counted as having fewer nuclei than they truly contained. The difficulty of Hoechst 33342 and the variability of spore discharge caused spore count issues for certain fruit bodies on given days; therefore, the number of spores recorded was not consistent for each day and varied from 62 to 388, for an average of approximately 174 counts per fruit body per day. In total 11106 basidiospores where counted across 15 fruitbodies.

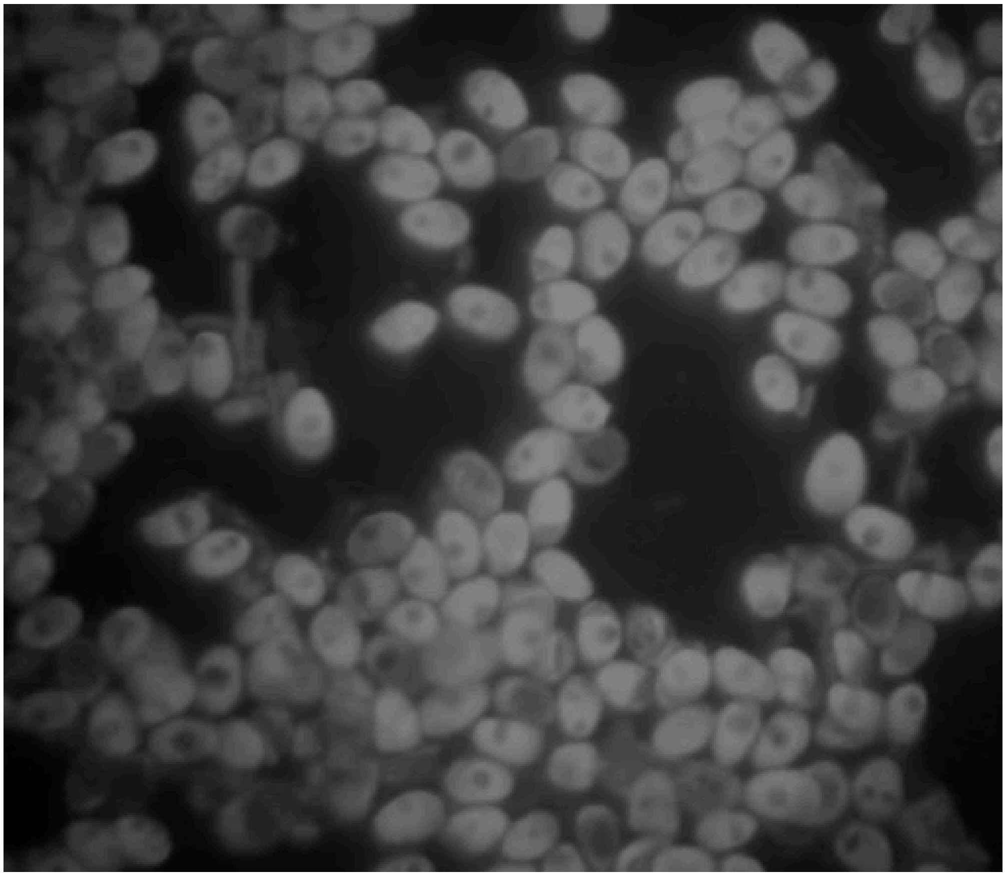

Figure 3-5. Unsuccessful staining reaction. * black dots are oil droplets not nuclei

Table 3-1. Comprehensive review of basidiospore data

Fruitbody Code	Total Spores (1-4)	Total Spores (5-6)	1N	2N	3N	4N	5N	6N	Maturity Category	Youngest Day	Oldest Day
10R_IOB2	213	0	86	113	12	2	0	0	Young	1	1
2R_IOB2	482	0	217	178	78	9	0	0	Young	1	2
3R_IOB2	1495	0	763	532	175	25	0	0	Young, Middle, Old	1	18
4R_IOB2	536	0	299	164	54	19	0	0	Old	15	19
5R_IOB2	652	2	257	296	84	15	2	0	Old	12	16
6R_IOB2	1104	0	545	452	92	15	0	0	Young, Middle, Old	1	12
7R_IOB2	1359	11	474	514	308	63	8	3	Young, Middle, Old	1	11
8R_IOB2	111	3	30	51	27	3	2	1	Young	1	1
BLDW5_IOB2	205	0	39	116	41	9	0	0	Young	1	2
BLUP5_IOB2	1587	0	954	424	170	39	0	0	Young, Middle, Old	1	12
DKUP4_IOB2	1165	0	676	294	166	29	0	0	Young, Middle, Old	1	14
DKUP5_IOB3	337	0	129	102	89	17	0	0	Young, Middle	1	6
DKVR5_IOB2	833	0	604	185	40	4	0	0	Young, Middle, Old	1	10
DKVR5_IOB3	235	0	129	83	22	1	0	0	Young	1	1
DKVR5_IOB5	776	0	462	159	121	34	0	0	Young, Middle	1	6
Total	11090	16	5664	3663	1479	284	12	4	Young, Middle, Old	1	19

Note: This describes the details of each fruit body. Codenames were applied, which indicate the individual fruitbody and which strain produced it (fruitbody_strain; e.g. 10R_IOB2). “Total Spores (1-4)” shows how many spores were counted across all maturity categories, which contained 1 to 4 nuclei, as these were the spores considered in statistical analysis. “Total Spores (5-6)” shows how many fruit bodies had penta or hexanucleate spores across all categories, which were few. Columns 1N = uninucleate, 2N = binucleate, 3N = trinucleate, 4N = tetranucleate, 5N = pentanucleate, 6N = hexanucleate, indicate how many spores of these types were counted in total across all maturity categories for each fruitbody. “Maturity Category” shows which maturity categories each fruit body was sampled in. “Youngest Day” and “Oldest Day” indicate how wide the spore sampling window was for each fruitbody. This does not mean they were sampled all those days, only the sampling window.

STATISTICAL ANALYSIS

Bayesian Framework and brms

To analyze the variability of basidiospore nuclear types over fruiting body development, a Bayesian mixed-effects categorical (multinomial) logit model was applied through the brms package in RStudio (Version 2024.12.0+467). The brm() function brms package was created by Paul-Christian Bürkner from the University of Münster. This package uses the probability-based programming language Stan to implement flexible Bayesian mixed-effect modelling into R that is more user-friendly (Bürkner, 2017). Bayesian statistics function in a framework that embraces uncertainty by using prior and current knowledge (likelihood) of data to develop a probabilistic posterior distribution (van de Schoot *et al.* 2021). Setting priors in a Bayesian model is a crucial step that regulates the model from making wild estimates, with the benefit of encoding prior knowledge of a phenomenon into model predictions (van de Schoot *et al.* 2021). In this case, priors were selected based on data in earlier research to regularize estimates and will be discussed further. The base model code will be provided (Appendix II).

The base model outputs in a logit model are on the log odds scale (Gelman & Hill, 2007). The range of estimates are presented in 95% credible intervals (CrI) (Hespanhol *et al.* 2019). A 95% credible interval (CrI) is not the same as a frequentist 95% confidence interval (CoI), which defines that if the experiment were repeated 100 times, and confidence intervals were calculated for each of them, 95 of those intervals would contain the true population mean (O'Brien *et al.* 2016; Hespanhol *et al.* 2019). 95% CrIs are based on the evidence provided by the data: there is a 95% probability that the true value lies in this interval (Hespanhol *et al.* 2019). In frequentist systems, statistical significance is defined by an arbitrary value (i.e. $p < 0.05$), but in a Bayesian framework, if a 95% CrI for a parameter estimate contains zero, evidence for an effect is lacking; thus, the model cannot make a meaningful prediction (McElreath, 2018; Hespanhol *et al.* 2019). The terms credible or not credible will be used to describe effects which do or do not contain zero in this analysis. This is not analogous classical statistical significance, but rather that evidence is lacking for an effect.

A mixed-effect model function in R uses Bayesian inference to generate posterior distributions through Markov chain Monte Carlo (MCMC) using Hamiltonian Monte Carlo (HMC), whereby thousands of dependent iterations are performed to explore a range of values which are likely to explain your model parameters (Bürkner, 2017; Betancourt, 2018). In this case, the model ran 4 chains with 2000 iterations for each, creating a total of 8000 model iterations; this is default in brms (Bürkner, 2017). Each chain is independent to test if the estimates come to a consensus (Betancourt, 2018). In the first 4000 iterations, the model begins at a completely random point in the parameter space and eventually arrives at a place that has likely explanations for your model parameter; this is termed a warm-up phase, where data is not being sampled from the model (Betancourt, 2018). In the following 4000 iterations, data is being drawn from the likely parameter space, where each iteration is a possible model (Betancourt, 2018). The likely parameter space is termed the typical set and is explored through conserved Markov transitions, which concentrates estimates towards the typical set (Betancourt, 2018).

Model Structure and Reasoning

In this model, the fixed effect was **Maturity** (Young, Middle, or Old), the response was categorical (family = categorical); **Nuclear type** (1N, 2N, 3N or 4N; uninucleate, binucleate, trinucleate, tetranucleate), and the random effect was individual fruit bodies (**1 | Replicate**). This dataset had three main notable structural issues: IOB2 (12 fruitbodies/replicates) was sampled proportionally far more than IOB3 (2 fruitbodies/replicates) and IOB5 (1 fruitbody/replicate), the number of total basidiospores sampled for a given fruitbody on a given day varied significantly from n = 62 to 388, and not all fruit bodies occurred across all maturity categories (Young, Middle, and Old) due to fruiting body death during the collection period and sampling complications

All the above factors are inherently considered through a mixed-effect or hierarchical model structure. Woven into these models is the use of a **partial pooling** framework that elegantly handles uneven data and prevents the over or underfitting of specific response variables that possess smaller or larger sample sizes (McElreath, 2018). In this framework, information is shared across replicates, such that the means of individual replicates are pushed and pulled between their mean and the grand mean of the overall dataset (McElreath, 2018).

Bayesian Workflow, Prior Selection, and Convergence

The model-building process followed a Bayesian workflow, which involves model comparison through prior/posterior predictive checking, as well as convergence. (Gelman *et al.* 2020). These checks are suitable for presentation in this section as they demonstrate that the model functions properly and does not make wild estimates. The following workflow follows a simplified version of the one presented by Gelman *et al.* (2020).

Firstly, the model exhibited an ideal convergence where all intercepts had a Rhat value of 1.00 (Appendix II). Prior selection is a crucial step in a Bayesian workflow that separates it from other frameworks (McElreath, 2018). Priors function by allowing you to encode previous knowledge on the phenomenon you are testing and are generated from a stance that your dataset has not been seen or analyzed (Gelman *et al.* 2017). In this case, weakly informative priors were chosen to ground estimates in reality, while also limiting the chance for wild estimates. Based on *I. obliquus* mating work of Sun *et al.* (2023), weakly informative priors were set to control basidiospore nuclear type proportion estimates. They found that uni- and binucleate spores predominated while multinucleate spores were much rarer; thus, weakly informative priors were set with this knowledge to regularize estimates (Appendix II). A prior predictive check ensures that the set priors (prior only model) produce reasonable estimates before the addition of your data through simulated data comparisons of the posterior (prior + data model) (Gelman *et al.* 2020). Data is simulated through the posterior_predict() function on the response scale (%) in this case (Bürkner, 2015). The prior predictive nuclear type distribution shows reasonable nuclear type proportions in a simulated prior only model; uni- and binucleate spores predominate, and multinucleate spores are much rarer (Figure 3-6). The credible intervals of this simulated data set are wide to allow data to inform the model. The posterior predictive nuclear type distribution (prior + data model) shows simulated proportions that are similar to the prior-only simulations, but are unique with tighter credible intervals (Figure 3-7). This demonstrates that priors ground the model in real-world knowledge, while not being overly restrictive, and allowing the data to meaningfully influence estimates.

Finally, a posterior predictive check was done by comparing simulated posterior data (prior + data model) to real-world data. This checks whether model-simulated data is comparable to your real-world dataset, which displays a well-fitted and behaved model Gelman *et al.* (2020). The simulated posterior predictive data show nuclear type proportions that closely match those in the dataset (Figure 3-8) (Table 3-3). Additionally, a density analysis shows that simulated nuclear type proportions were sampled tightly in the posterior, with a high sampling density around the real-world estimates and tight upper and lower estimates (Figure 3-9).

Chain convergence and prior/posterior predictive checks show that the model is well-behaved and fits well. Therefore, it will be used in this analysis.

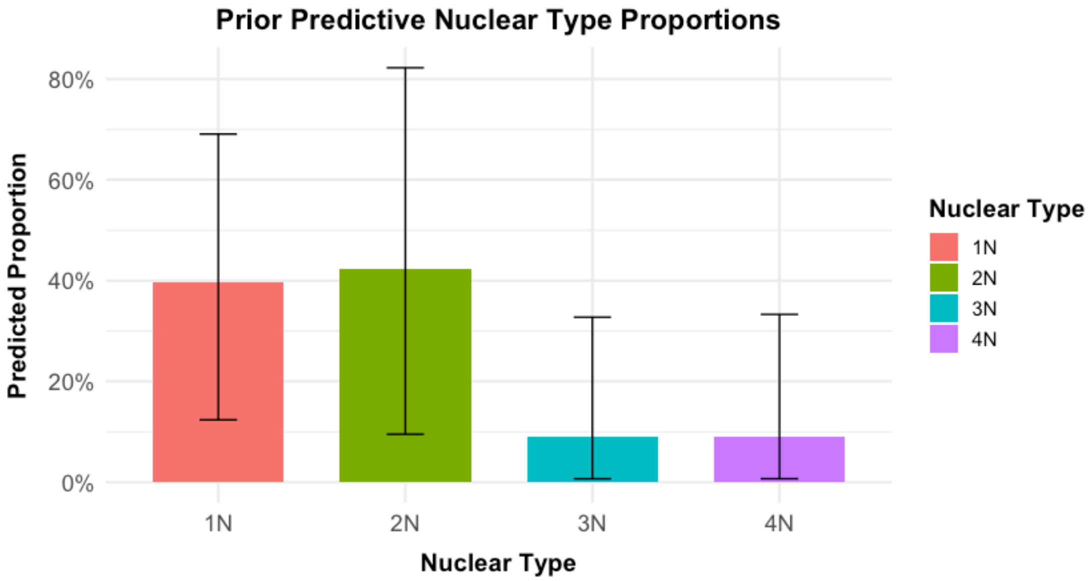

Figure 3-6. Prior predictive nuclear type proportions. Error bars: 95% credible interval

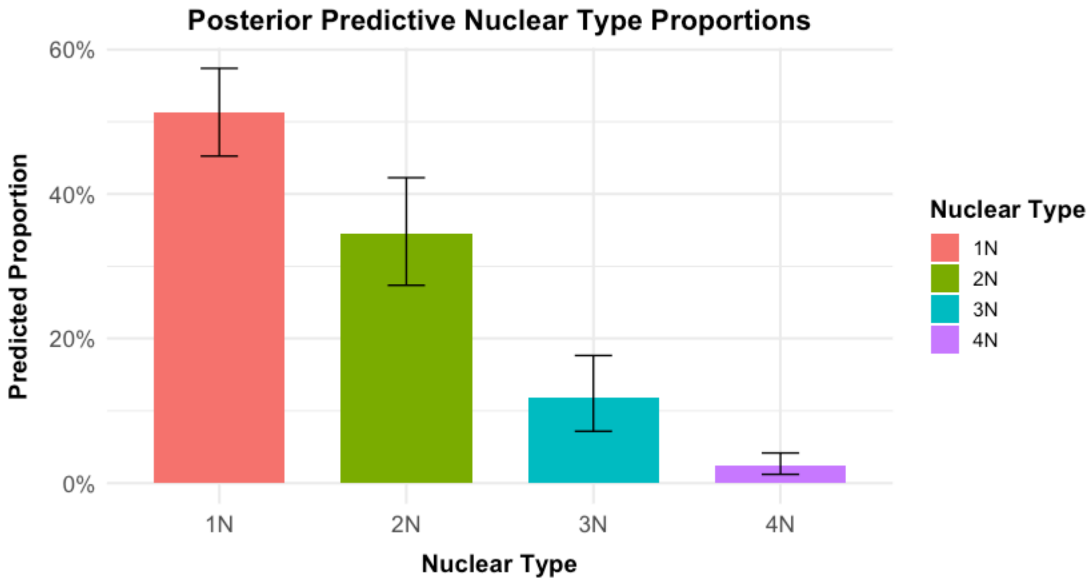

Figure 3-7. Posterior predictive nuclear type proportions. Error bars: 95% credible interval

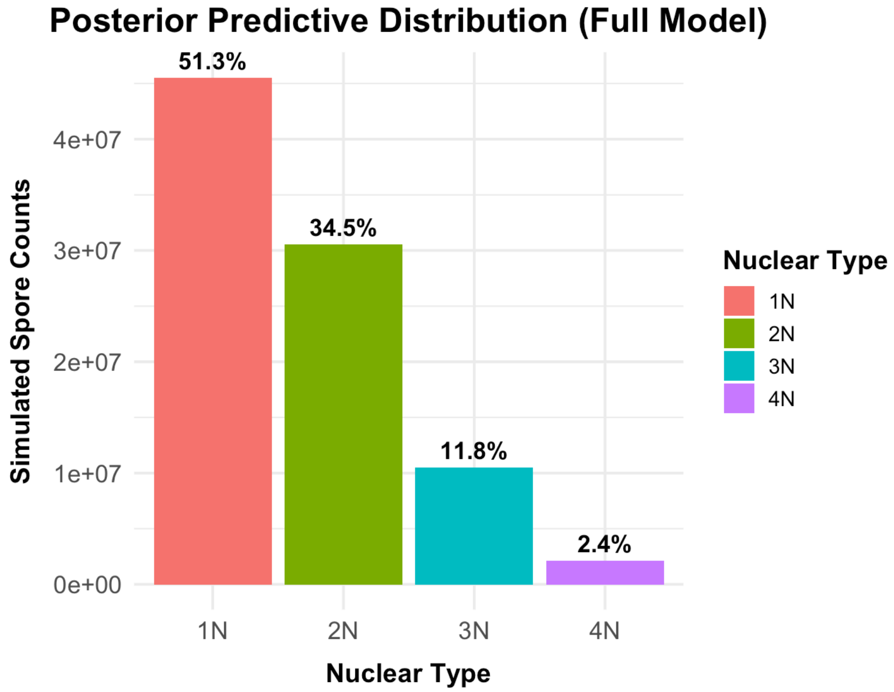

Figure 3-8. Posterior predictive distribution

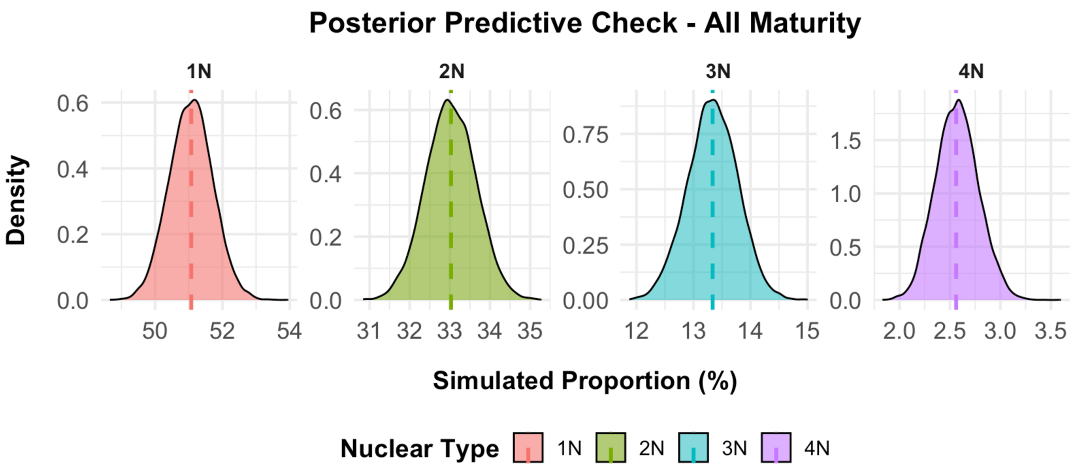

Figure 3-9. Posterior predictive density analysis

RESULTS

RAW DATA

In total, 11106 basidiospores were examined for nuclear type (Table 3-1). Of them, 5664 were uninucleate (1N), 3663 were binucleate (2N), 1479 were trinucleate (3N), 284 were tetranucleate (4N), 12 were pentanucleate (5N), and 4 were hexanucleate (6N). All basidiospore nuclear types were photographed (Figure 3-11), along with their variation from print to print (Figures 3-12 to 3-15). Additionally, hyphae happened to be stained by Hoechst 33342 occasionally and nuclei could be viewed (Figure 3-16). A formal analysis was not completed, but cells had high variability in nuclear contents (0 to ~30 nuclei per cell of those viewed). Each strain was viewed to possess 1N, 2N, 3N, and 4N basidiospores, but 5N and 6N basidiospores were restricted to IOB2 (Table 3-1). 9758 belonged to IOB2 (12 fruitbodies), 572 to IOB3 (2 fruitbodies), and 776 to IOB5 (1 fruitbody) (Table 3-2). Only spores that contained 1-4 nuclei were analyzed (11090), as the number of spores with 5-6 nuclei was well below 1%, therefore, their contribution to this report is anecdotal. Before any statistical analysis, in **Young** (fruitbodies 1 to 3 days old), a total of 3679 basidiospores were counted, 1391 were 1N (37.81%), 1387 were 2N (37.70%), 762 were 3N (20.71%), and 139 were

4N (3.78%) (Figure 3-10) (Table 3-3). In **Middle (**fruitbodies 4 – 8 days old), a total of 3604 basidiospores were counted, 2166 were 1N (60.10%), 1031 in 2N (28.61%), 338 in 3N (9.38%), and 69 in 4N (1.91%)(Figure 3-10) (Table 3-3). In **Old (**9 – 10 + days old**),** a total of 3807 basidiospores were counted, 2107 were 1N (55.35%), 1245 for 2N (32.70%), 379 were 3N (9.96%), and 76 were 4N (2.00%) (Figure 3-10) (Table 3-3).

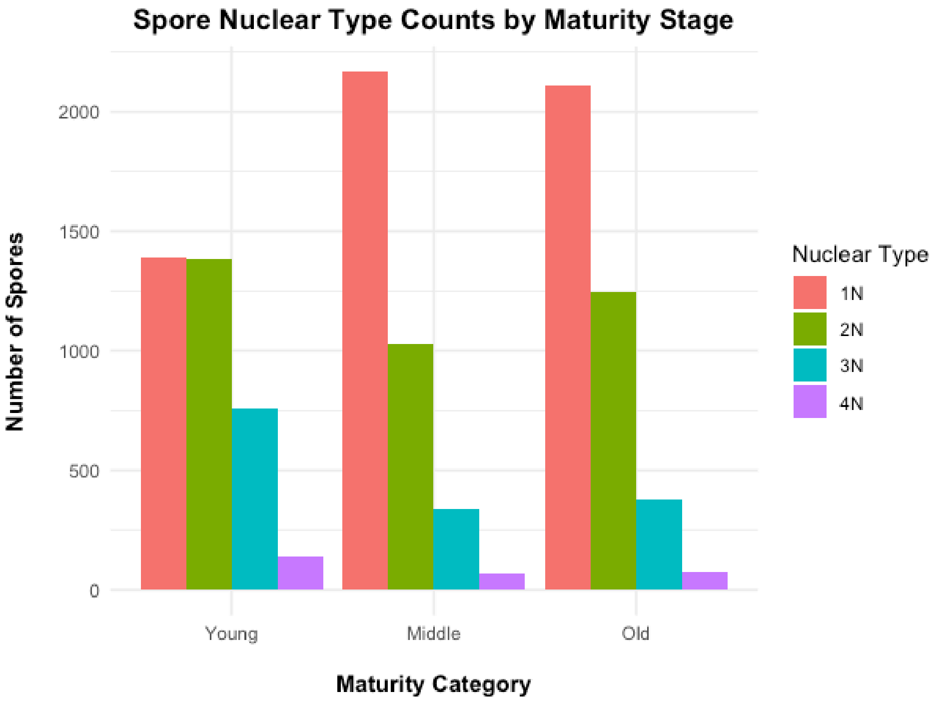

Figure 3-10. Raw counts of basidiospore nuclear types by maturity category

Table 3-2. Number of fruitbodies/total spores analyzed per strain

Strain	Number of Fruitbodies	Total Spores
IOB2	12	9758
IOB3	2	572
IOB5	1	776
All Strains	15	11106

Table 3-3. Counts and proportions of basidiospore nuclear types – maturity category

Maturity Category	1N	2N	3N	4N	Total
Young: spore count	1391	1387	762	139	3679
Young: proportion	37.81%	37.70%	20.71%	3.78%	100%
Middle: spore count	2166	1031	338	69	3604
Middle: proportion	60.10%	28.61%	9.38%	1.91%	100%
Old: spore count	2107	1245	379	76	3807
Old: proportion	55.35%	32.70%	9.96%	2.00%	100%
All: spore count	5664	3663	1479	284	11090
All: proportion	51.07%	33.03%	13.34%	2.56%	100%

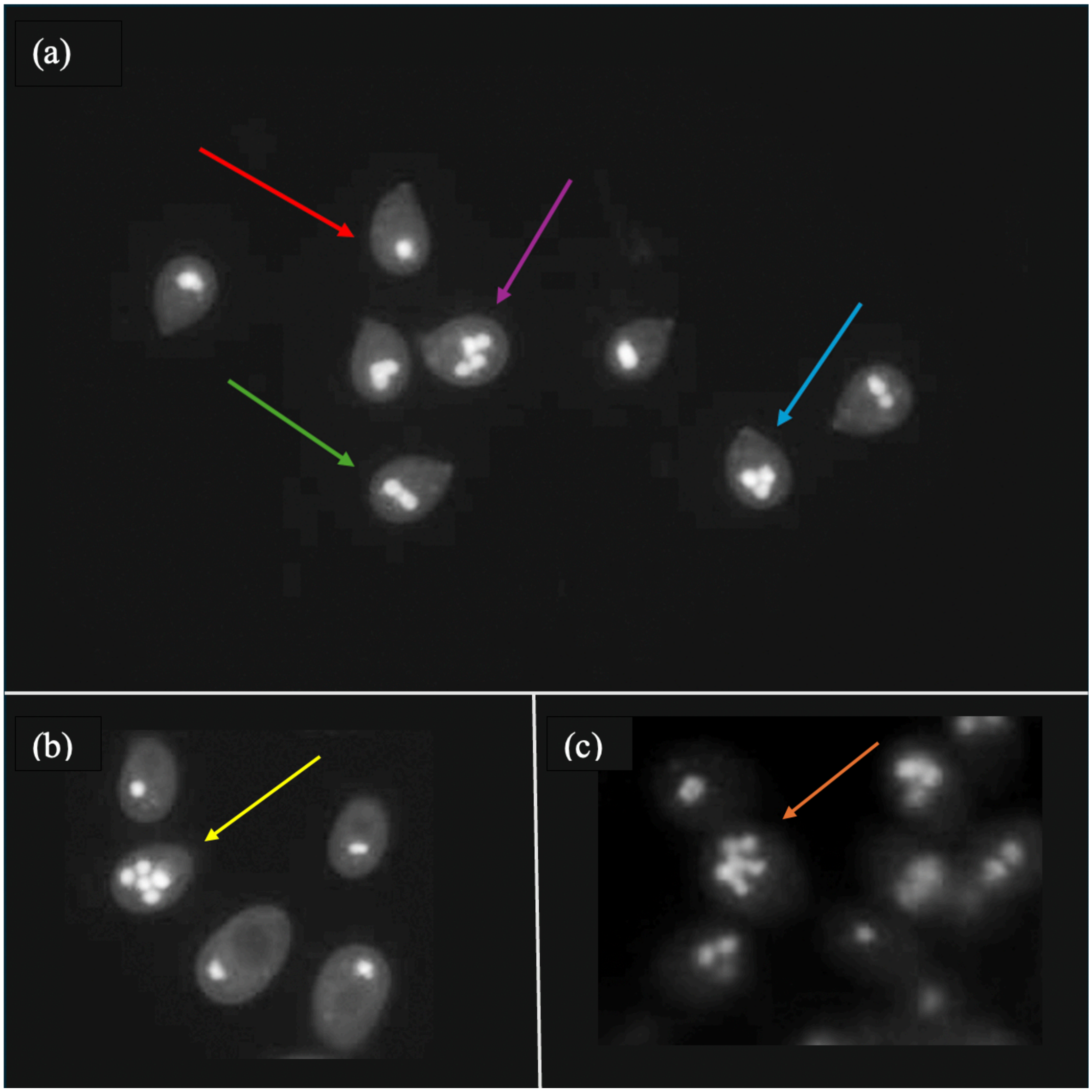

Figure 3-11. Uni, bi, tri, tetra, penta, and hexanucleate basidiospores (IOB2). (a) shows uninucleate (red arrow), binucleate (green arrow), trinucleate (blue arrow), and tetranucleate (purple arrow) basidiospores in close proximity to each other. (b) shows pentanucleate basidiospore (yellow arrow). (c) shows hexanucleate basidiospore (orange arrow)

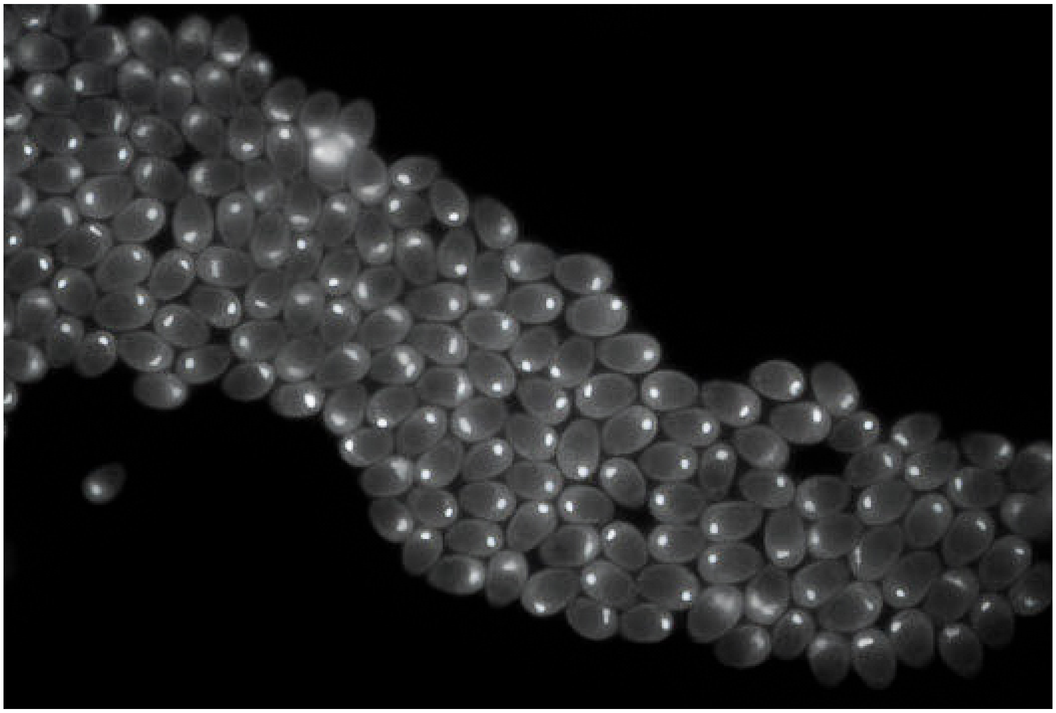

Figure 3-12. Basidiospore nuclear type variability (a). Note basidiospores are predominantly uninucleate

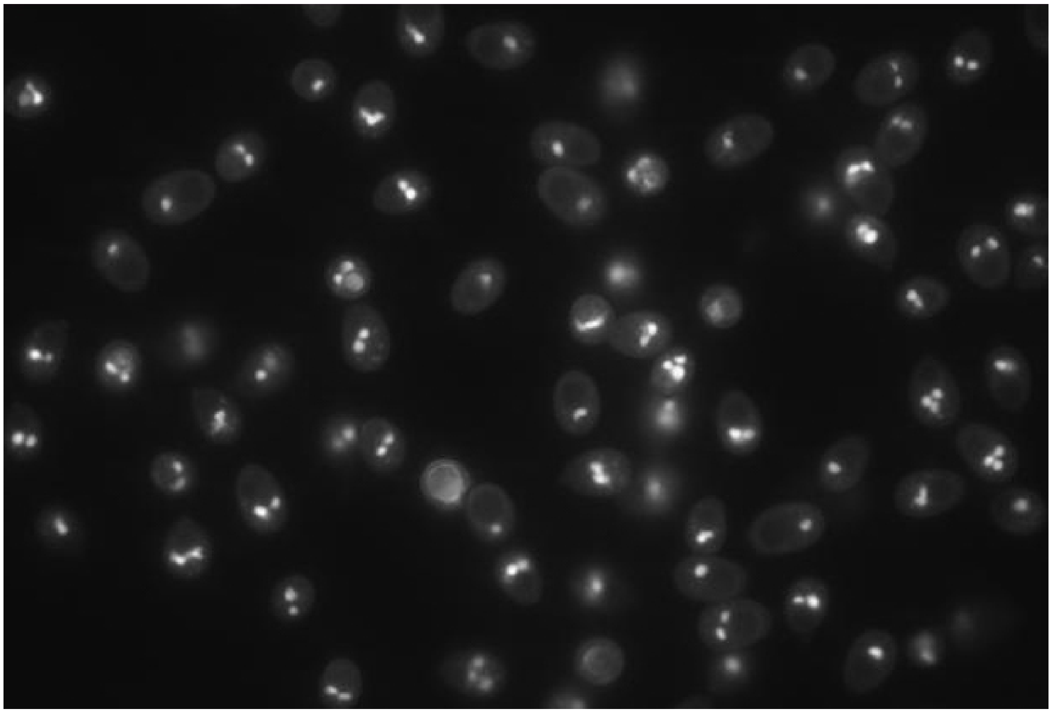

Figure 3-13. Basidiospore nuclear type variability (b). Note: basidiospores are variable – uni, bi, and trinucleate

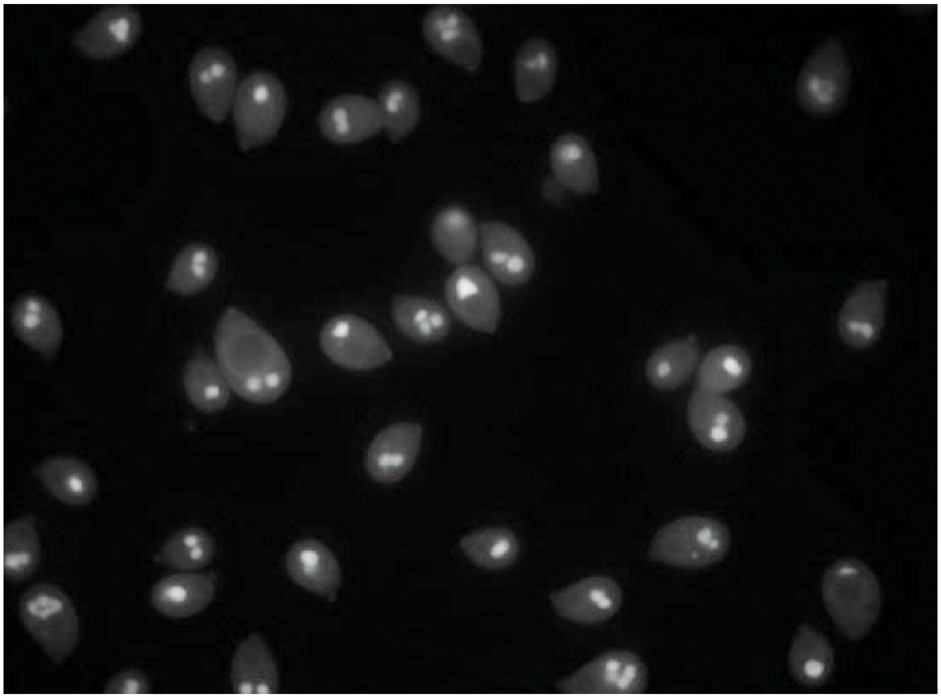

Figure 3-14. Basidiospore nuclear type variability (c). Note: basidiospores are variable in size and nuclear type

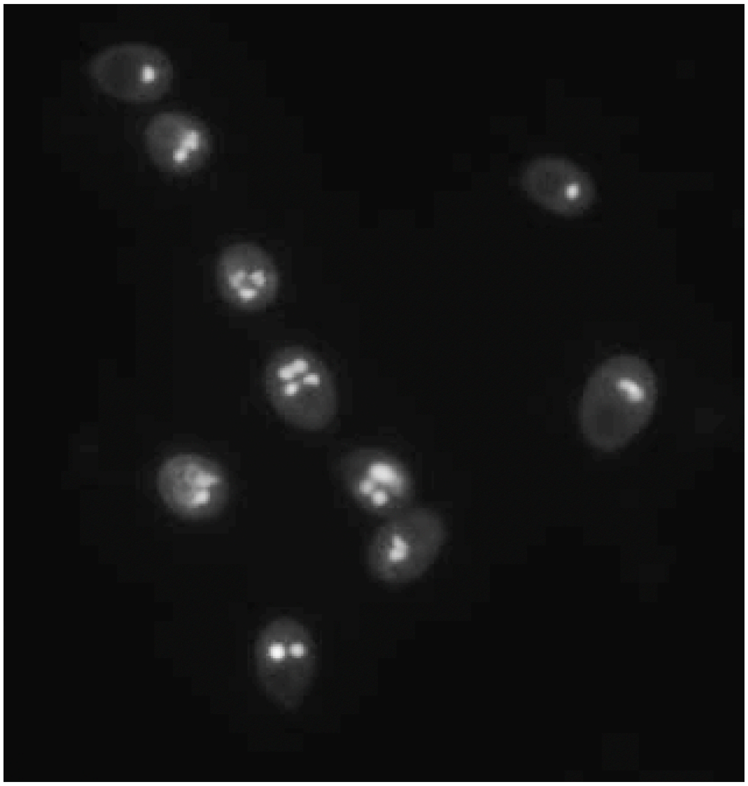

Figure 3-15. Basidiospore nuclear type variability (d). Note: basidiospores are variable in nuclear type – all four present

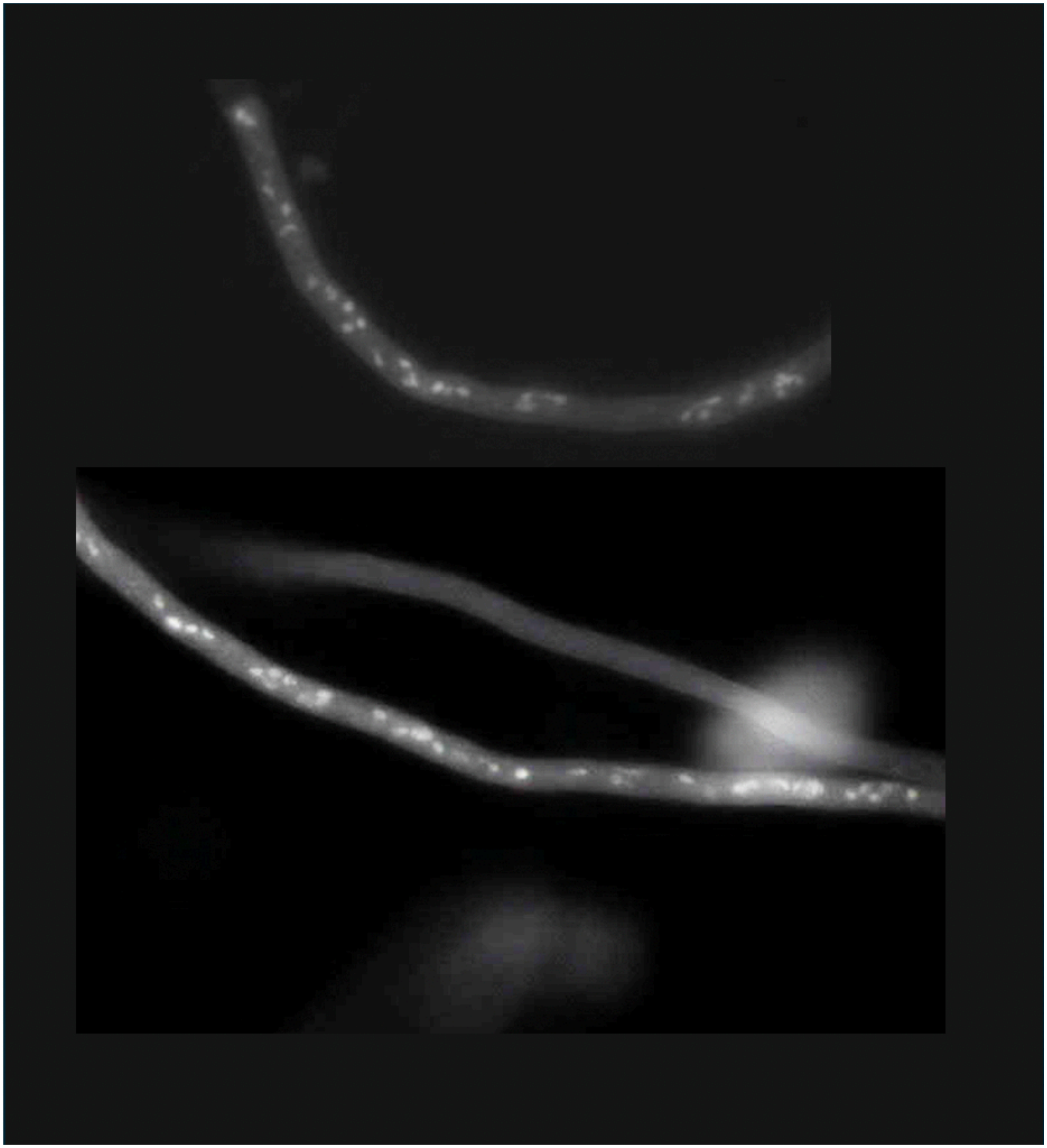

Figure 3-16. Multinucleate hyphae

MODEL RESULTS

A categorical (multinomial) mixed-effects Bayesian logistic model was run to analyze how the proportion of basidiospore nuclear type varied over the maturation of fruit bodies, utilizing the brms package in R. In brms, the model base outputs are on the log-odds scale, in which coefficients represent the shift from a reference category. In this case, the base model references are **1N** for **Nuclear Type** and **Young** for **Maturity.** The base outputs include first, hyperparameters that provide standard deviations (SD) for random effects (fruit bodies = (1 | Replicate) over the categorical response of **Nuclear Type.** Relative intercepts are generated which provide insights into how the 15 fruiting bodies deviated in basidiospore nuclear type proportions overall. There was reasonable log-odds SD between fruiting bodies (Table 3-4). Relative to 1N spores (baseline 0), 2N spores had the lowest SD (0.61; CrI: 0.41 - 0.94), 3N spores had the second highest SD (0.97; CrI: 0.41 - 0.94) and 4N had the highest SD (1.17; CrI: 0.72 – 1.86). As they were all positively correlated to 1N, 1N had the lowest relative SD across individual fruiting body basidiospore nuclear type proportion**.** This indicates that proportional counts of uninucleate basidiospores were the most consistent across fruiting bodies, while bi- and multinucleate spores were more variable.

Table 3-4. Log-odds estimated standard deviation between nuclear types

Contrast	Estimate (SD)	Est. Error	95% CrI: Lower	95% CrI: Upper	Rhat
2N v 1N	0.61	0.13	0.41	0.94	1.00
3N v 1N	0.97	0.21	0.65	1.47	1.00
4N v 1N	1.17	0.29	0.72	1.86	1.00

Secondly, intercepts for the fixed effect of **Maturity** relative to basidiospore **Nuclear Type** are created (see Appendix II). The base output is not included herein as complete pairwise log-odds contrasts were extrapolated through the arithmetic of intercept coefficients. The relative pairwise log-odds contrasts of basidiospore nuclear type within maturity categories (i.e. 2N v 1N in **Young**) and directional pairwise contrasts of single nuclear types between maturity categories (i.e. 2N in **Young** v 3N **Old**) are included in the main body of this section as they are intuitive to interpret (Table 3-6). If credible intervals of relationships (i.e. proportion of 2N vs 1N in **Young**) contained zero, this meant the model could not reasonably estimate if the relationship was a positive or negative one; thus, the proportions were not viewed as being credibly different. The relative pairwise log-odds contrasts of basidiospore nuclear type proportion over temporal shifts (2N vs 1N from **Young** to **Middle**), are confusing to interpret; thus, are not included in the main body of this section (see Appendix II). In order to intuitively present model results, the posterior_epred() function was utilized to extract population-level parameter effects (re_formula = NA) on the response scale (%) from the posterior (Heiss, 2021). Proportions of basidiospore nuclear types are presented as predicted probabilities (%) in each maturity category (Figure 3-17) (Table 3-5). The credible differences of basidiospore nuclear type proportions within and between maturity categories were analyzed through the retained pairwise log-odds contrasts (Table 3-6). Proportional shifts (%) of basidiospore nuclear types over a temporal scale (i.e **Young** to **Old**, **Middle** to **Old**) were extracted with the avg_comparisons () function from the marginaleffects R package (Arel-Bundock *et al.* 2024). Additionally, these explain if proportional shifts are credible (exclude 0). The results from the retained pairwise log-odds contrasts, and the credible and non-credible proportional shifts of basidiospore nuclear type over time, enabled the development of a compact letter display (CLD) that visually represents how nuclear type proportions relate within maturity categories and change between them (Figure 3-17) (Table 3-5). This does not represent statistical significance ($p < 0.05$), but that there was or was not enough evidence in the posterior for the model to predict a directional correlation between basidiospore nuclear type predicted proportions (%). Overall, the model found there to be sufficient evidence to indicate that basidiospore nuclear type did vary throughout fruiting body development (Figure 3-17) (Table 3-5).

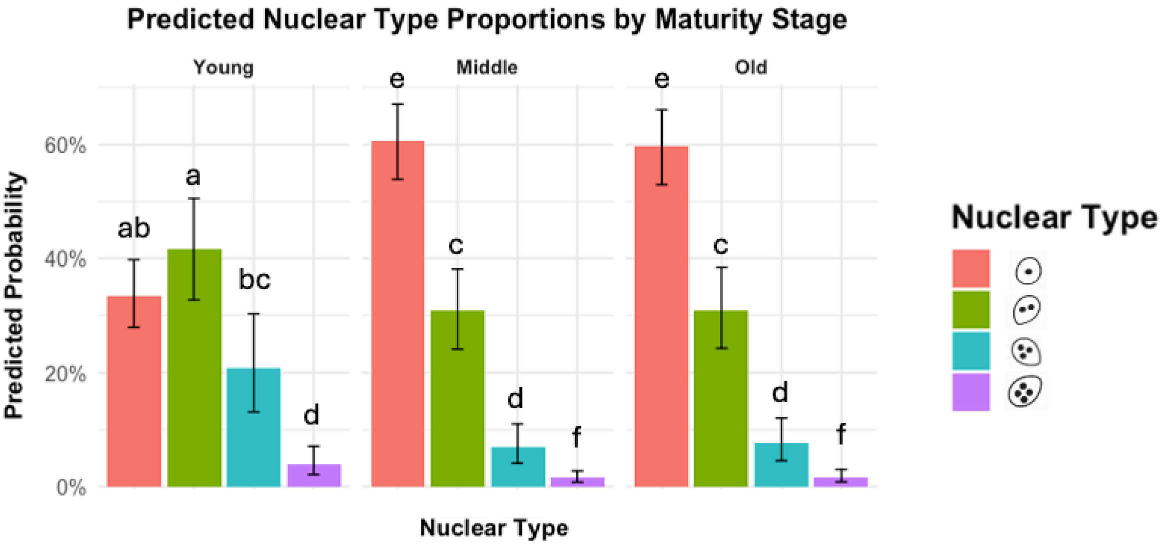

Figure 3-17. Predicted basidiospore nuclear type proportions. Error bars: 95% credible interval

Table 3-5. Predicted basidiospore nuclear type proportions

Maturity	Nuclear	Estimate (%)	95% CrI: Lower (%)	95% CrI: Upper (%)	SD (± %)	CLD
Young	1N	33.50	27.90	39.80	13.20	ab
Young	2N	41.60	32.80	50.60	9.62	a
Young	3N	20.90	13.10	30.30	11.00	bc
Young	4N	4.00	2.07	7.11	2.22	d
Middle	1N	60.70	53.90	67.10	13.70	e
Middle	2N	30.80	24.20	38.20	8.76	c
Middle	3N	6.99	4.09	10.90	6.20	d
Middle	4N	1.51	0.75	2.74	1.25	f
Old	1N	59.70	53.00	66.20	13.50	e
Old	2N	31.00	24.30	38.50	9.39	c
Old	3N	7.70	4.53	12.00	4.53	d
Old	4N	1.64	0.80	3.00	1.14	f

Predicted Basidiospore Nuclear Type Proportions

In the **Young** category (1-3 days old), 1N (ab) spores had a predicted probability of 33.4% (CrI: (%) 27.9 - 39.8), 2N spores (a) 41.6% (CrI: (%) 32.8 - 50.6), 3N spores (bc) 20.9% (CrI : (%) 13.1 - 30.3), and 4N (d) 4.0% (CrI: (%) 2.07 - 7.11). 2N spores slightly predominated here followed by 1N, 3N, and 4N respectively. (Table 3-5) Pairwise log-odds contrasts within **Young** showed that 1N spores (ab) were not credibly different from 2N (a) and 3N (bc) spores (Table 3-6). 2N (a) spores were credibly different from 3N spores (bc) (Table 3-6). All spore nuclear types were credibly different from 4N (d) spores (Table 3-6). In the **Middle** category (4-8 days old), 1N spores (e) had a predicted probability of 60.7% (CrI: (%) 53.9 - 67.1), 2N (c) 30.8% (CrI: (%) 24.2 - 38.2), 3N (d) 6.99% (CrI: (%) 4.09 - 10.9), and 4N (f) 1.51% (CrI: (%) 0.75 - 2.74) (Table 3-5). 1N spores predominated here followed by 2N, 3N, and 4N respectively. Pairwise log-odds contrasts within **Middle** showed that all nuclear types were credibly different from each other; 1N (e), 2N (c), 3N (d), and 4N (f) (Table 3-6). In the **Old** category, 1N (e) spores had a predicted probability of 59.7% (CrI: (%) 53.0 - 66.2), 2N (c) 31.0% (CrI: (%) 24.3 - 38.5), 3N (d) 7.70%

(CrI: (%) 4.53 - 12.0), and 4N (f) spores 1.64% (CrI: (%) 0.803 - 3.0) (Table 3-5). 1N spores predominated here followed by 2N, 3N, and 4N spores respectively. Pairwise log-odds contrasts within **Old** showed that all nuclear types were credibly different from each other; 1N (e), 2N (c), 3N (d), and 4N (f) (Table 3-6). Between maturity categories, the only basidiospores nuclear type proportions that were not credibly different from each other were 3N (bc) spores in **Young** compared to 2N (c) spores in **Middle** and **Old**; 4N (d) spores in **Young** compared to 3N (d) spores in **Middle** and **Old**; the proportion of all spores in **Middle** between **Old** (Table 3-6).

Table 3-6. Pairwise log-odds contrasts

Contrast	Estimate	95% CrI: Lower	95% CrI: Upper	Error	Contains 0 (Y/N)
2N v 1N Young	0.216	-0.112	0.544	0.168	Y
2N v 1N Middle	-0.685	-1.01	-0.351	0.168	N
2N v 1N Old	-0.661	-0.988	-0.328	0.169	N
1N v 3N Young	0.491	-0.003	1.01	0.255	Y
1N v 3N Middle	2.19	1.69	2.72	0.261	N
1N v 3N Old	2.08	1.58	2.6	0.259	N
3N v 2N Young	-0.707	-1.31	-0.103	0.304	N
3N v 2N Middle	-1.51	-2.11	-0.887	0.309	N
3N v 2N Old	-1.41	-2.02	-0.808	0.308	N
4N v 1N Young	-2.17	-2.78	-1.54	0.311	N
4N v 1N Middle	-3.74	-4.39	-3.08	0.327	N
4N v 1N Old	-3.64	-4.3	-2.97	0.333	N
2N v 4N Young	2.38	1.68	3.07	0.346	N
2N v 4N Middle	3.06	2.35	3.78	0.36	N
2N v 4N Old	2.98	2.25	3.72	0.366	N
4N v 3N Young	-1.68	-2.46	-0.882	0.398	N
4N v 3N Middle	-1.55	-2.37	-0.735	0.414	N
4N v 3N Old	-1.57	-2.4	-0.738	0.419	N
1N Middle v 1N Old	0.024	-0.103	0.148	0.0644	Y
2N Middle v 2N Old	-0.024	-0.148	0.103	0.0644	Y
3N Middle v 3N Old	-0.115	-0.311	0.0778	0.1	Y
4N Middle v 4N Old	-0.0994	-0.512	0.305	0.208	Y
3N Young v 1N Middle	-1.39	-1.92	-0.89	0.259	N
3N Young v 3N Middle	1.7	1.53	1.87	0.0864	N
3N Young v 2N Middle	0.194	-0.41	0.806	0.307	Y
3N Young vs 4N Middle	3.25	2.45	4.07	0.415	N
2N Young vs 1N Middle	-0.685	-1.01	-0.351	0.168	N
2N Young vs 2N Middle	0.901	0.774	1.03	0.0645	N
2N Young vs 3N Middle	2.41	1.78	3.02	0.312	N
2N Young vs 4N Middle	3.96	3.24	4.69	0.365	N
1N Young v 1N Middle	-0.901	-1.03	-0.774	0.0645	N
1N Young v 2N Middle	0.685	0.351	1.01	0.168	N
1N Young v 3N Middle	2.19	1.69	2.72	0.261	N
1N Young v 4N Middle	3.74	3.08	4.39	0.327	N
4N Young v 1N Middle	-3.07	-3.68	-2.43	0.316	N
4N Young v 2N Middle	-1.48	-2.18	-0.786	0.348	N
4N Young v 3N Middle	0.0226	-0.768	0.829	0.403	Y
4N Young v 4N Middle	1.58	1.26	1.9	0.163	N

Proportional Shifts of Basidiospore Nuclear Type Over Time

For 1N spores, there was an increase of 27.9% (CrI: (%) 25.2 – 30.6) when moving from **Young** to **Middle**, an increase of 26.9% (CrI: (%) 23.9 – 29.7) when moving from **Young** to **Old**, and a non-credible decrease of 1.03% (CrI: (%) – 1.49 – 3.52) when moving from **Middle** to **Old** (Table 3-7). For 2N spores, there was a decrease of 10.80% (CrI: (%) 8.30– 13.38) when moving from **Young** to **Middle**, a decrease of 10.6% (CrI: (%) 7.99 – 13.24) when moving from **Young** to **Old**, and a non-credible increase of 0.21% (CrI: (%) -2.42 – 2.10) when moving from **Middle** to **Old** (Table 3-7). For 3N, there was a 14.16% (CrI: (%) 11.96 – 16.54) decrease when moving from **Young** to **Middle**, a 13.48% (CrI: (%) 11.32 – 15.88) decrease from **Young** to **Old**, and a non-credible increase of 0.066% (CrI: (%) -1.89 – 0.48) from **Middle** to **Old** (Table 3-7). For 4N spores, the was a 2.86% (CrI: (%) 1.84 – 4.19) decrease when moving from **Young** to **Middle**, a comparable small decrease of 2.71% (CrI: (%) 1.64 – 4.09) when moving from **Young** to **Old**, and a non-credible increase of 0.13% (CrI: (%) – 0.85 – 0.49) when moving from **Middle** to **Old** (Table 3-7).

Table 3-7. Proportional shifts of basidiospore nuclear type over time

Contrast	Estimate (%)	95% CrI: Lower (%)	95% CrI: Upper (%)	Contains 0 (Y/N)
1N Young to Middle	27.90	25.20	30.60	N
1N Young to Old	26.90	23.90	29.70	N
1N Middle to Old	-1.03	-1.49	3.52	Y
2N Young to Middle	-10.80	-13.38	-8.30	N
2N Young to Old	-10.60	-13.24	-7.99	N
2N Middle to Old	0.21	-2.42	2.10	Y
3N Young to Middle	-14.16	-16.54	-11.96	N
3N Young to Old	-13.48	-15.88	-11.32	N
3N Middle to Old	0.06	-1.89	0.48	Y
4N Young to Middle	-2.86	-4.19	-1.84	N
4N Young to Old	-2.71	-4.09	-1.64	N
4N Middle to Old	0.13	-0.85	0.49	Y

DISCUSSION

Inonotus obliquus displayed incredible variation of nuclear behaviour in basidiospores throughout the maturation of hymenia, where uninucleate, binucleate, trinucleate, tetranucleate, pentanucleate, and hexanucleate states were observed. The observation of penta- and hexanucleate basidiospores is novel for this taxon. However, their prevalence was less than 1%; thus, their importance is debatable and was not included in analysis. The results in this section align with an amphithallic mating system proposed by Sun *et al*. (2023), as *I. obliquus* was observed to produce uninucleate (likely haploid) basidiospores, and bi/multinucleate basidiospores that contain at least two likely meiotic products required for mating ontogeny. The model predicted slightly different proportions from raw counts, especially for uni and binucleate spores in **Young** (Figures 3-10 & 3-17). Overall, tri and tetra nucleate spores were the least common across all stages, relative to uni and binucleate spores (Figure 3-17). Uninucleate spores were generally the most common across all stages, followed by binucleate spores (Figure 3-17). Binucleate (41.6% (CrI: (%) 32.8 - 50.6) trinucleate (20.9% (CrI: (%) 13.1 - 30.3)), and tetranucleate (4.0% (CrI: (%) 2.07 - 7.11)) were most common in the first 1 – 3 days (**Young)** (Figure 3-17). The proportion of uninucleate (33.4% (CrI: (%) 27.9 - 39.8)) basidiospores was reduced in the first 1 – 3 days relative to older stages and did not appear as credibly different from bi and trinucleate spores (Figure 3-17). The first 1 – 3 days (**Young**) possessed basidiospores that were highly variable compared to older stages (Figure 3-17). The proportion of trinucleate spores in 1 – 3 day old fruit bodies (20.9% (CrI: (%) 13.1 - 30.3) was not credibly different from the proportion of binucleate spores in 4 – 8 day old fruiting bodies (30.8% (CrI: (%) 24.2 - 38.2)) (Figure 3-17). Basidiospores that were released 4 – 8 days (**Middle**) and 9 – 10+ days (**Old**) after initial fruiting body formation had nearly identical nuclear type proportions (Figure 3-17); thus, nuclear type proportion shifts will be discussed in the context of 4 – 8 day old fruiting bodies (**Middle).**

The proportion of uninucleate basidiospores increased by 27.90% (CrI: (%) 25.2 – 30.6) in 4 – 8 day old (**Middle**) fruiting bodies (60.7% (CrI: (%) 53.9 - 67.1)) relative to 1 – 3 day old (**Young**) fruiting bodies and dominated (Table 7-3). The proportion of binucleate basidiospores decreased by 10.80% (CrI: (%) 8.30– 13.38) in 4 – 8 day old (**Middle**) fruiting bodies (30.8% (CrI: (%) 24.2 - 38.2)) relative to 1 – 3 day old (**Young**) fruiting bodies and dominated (Table 3-7). The proportion of trinucleate basidiospores decreased by 14.16% (CrI: (%) 11.96 – 16.54) in 4 – 8 day old (**Middle**) fruiting bodies (6.99% (CrI: (%) 4.09 - 10.9)) relative to 1 – 3 day old (**Young**) fruiting bodies and dominated (Table 3-7). The proportion of tetra nucleate basidiospores decreased by 2.86% (CrI: (%) 1.84 – 4.19) in 4 – 8 day old (**Middle**) fruiting bodies (1.51% (CrI: (%) 0.75 - 2.74)) relative to 1 – 3 day old (**Young**) fruiting bodies and dominated (Table 3-7).

COMPARISON OF BASIDIOSPORE NUCLEAR TYPE VARIABILITY RESULTS – SUN *ET AL.* 2023

The variability of basidiospore nuclear type proportions at different developmental stages of basidiomata observed is similar, but inherently different to the results observed by Sun *et al.* (2023). The results they provided were not incredibly detailed and explained only broad trends of nuclear type basidiospore proportion over eight days without providing the number of basidiospores counted, exact proportions of basidiospore nuclear types at all maturity stages or statistical methodology for analyzing these trends. Their description is as follows: in the first two days of spore production, basidiospores were mainly binucleate (53.5%), followed by uninucleate

(24.3%) and few tri, tetra, and anucleate basidiospores. In three to five days following initial spore production, basidiospores were primarily uninucleate (62.3%), followed by binucleate (25.7%), and there was no mention of tri, tetra, or anucleate basidiospores. In six to eight days following initial spore production, they were reported to be primarily anucleate; no mention of proportions was made. They reported basidiospores of *I. obliquus* had a low germination rate roughly between 0.23% and 4.55% depending on ejection time and media. Basidiospores were reported to be released for up to fifteen days from basidiomata and required ten days of incubation at 25 °C to form visible colonies. A birch sawdust agar medium induced a much higher rate of basidiospore germination (4.55%) compared to cornmeal yeast malt extract agar (CYM) (0.53%), and potato dextrose agar (PDA) (0.43%). Basidiospores released in the first two days had the highest germination rates of 0.62% on PDA, followed by 0.23% for basidiospores released three to five days, and no germination was observed in basidiospores released after six to eight days.

Basidiospore Nuclear Type Analysis Similarities

The primary similarities between observations made here and those presented in Sun *et al.* (2023) are firstly, that uninucleate, binucleate, trinucleate, and tetranucleate basidiospores were observed using Hoechst nuclear staining (Sun *et al.* (2023): Hoechst 33258; this report: Hoechst 33342) (Interchim, n.d.) and fluorescence microscopy. Secondly, that bi, tri, and tetranucleate basidiospores were most common in early developmental stages. In particular, the proportions of uninucleate to binucleate basidispores observed by Sun *et al.* (2023) at this stage were relatively similar to the predicted proportions generated in this report (Figure 3-17) (Table 3-5). This indicates a potential adaptation of *I. obliquus* to release a higher proportion of heterokaryotic (bi, tri, tetra) basidiospores early in basidiomata development. Thirdly, both reports show that the proportion of uninucleate basidiospores likely increases in later developmental stages (roughly 4 + days old), while bi, tri, and tetranucleate basidiospores become less common. This indicates a potential adaptation of *I. obliquus* to release a higher proportion of homokaryotic basidiospores in later developmental stages.

Basidiospore Nuclear Type Analysis Differences

The primary difference between this analysis and that of Sun *et al.* (2023) is that this analysis clearly outlines the amount of basidiospores counted (11090 spores in the analysis), clearly outlines methodology of the spore collection and staining process, provides complete predicted proportions with 95% credible intervals for each nuclear type in each maturity category, is transparent about the structure of the dataset, and uses robust statistics and modelling. The analysis of Sun *et al.* (2023), does not present the amount of basidiospores counted, does not clearly outline methodology of the spore collection and staining process other than providing stain concentrations and incubation times, only provides proportions for some types of spores without any measure of error, is not transparent about their dataset structure, and does not apparently use any statistics or modelling. The report Sun *et al.* (2023) provided covers a wider range of topics such as putative *MAT* genes, germination rates, and the fruiting of single spore isolates (SSI). This analysis was likely a small portion of their research. The second difference between this analysis and that of Sun *et al.* (2023) is that this present report did not examine for the prevalence of anucleate basidiospores. Sun *et al.* (2023) observed that basidiospores released from mature basidiomata were primarily anucleate. In this report, mature basidiomata of *I. obliquus* produce a full or partial complement of all basidiospore nuclear types. In mature basidiomata, essentially all basidiospores contained nuclei. A successful staining reaction was characterized by basidiospore cell walls that were transparent to allow the tally of nuclei (Figure 3-11). An unsuccessful staining reaction was characterized by a cell wall emitting bright fluorescence, where nuclei could not be viewed (Figure 3-5). Therefore, it is unlikely that unsuccessful staining reactions were anucleate basidiospores, and more so that a smaller proportion of anucleate basidiospores were present in successful staining, but not counted out of caution of false observations.

Inonotus obliquus is not the only agaricomycete to produce basidiospores with varying multinucleate characteristics. Calderoni *et al.* (2003) observed that *Stereum sanguinolentum* (Alb. & Schwein. : Fr.) Fr. produced basidiospores that on average were 5% uninucleate, 82% binucleate, 2% trinucleate, 1% tetranucleate, and 10% anucleate. Rebecca *et al.* (2021) observed that *Oudemansiella aparlosarca* (Berk. & Broome) Höhn. produced basidiospores that on average were 23.50% uninucleate, 54.70% binucleate, 16.38% multinucleate (3 to 4 nuclei), and 4.84% anucleate. In both of the cases, anucleate basidiospores were produced in relatively small proportion. As these fungi possess uni, bi, tri, and tetranucleate basidispores (as observed in *I. obliquus*), it is reasonable to assume that anucleate basidiospore production is a consequence of nuclear sorting mechanisms in agaricomycetes with high basidiospore nuclear variability. Due to the relatively low anucleate basidiospore production in multinucleate species by Rebecca *et al.* (2021) & Calderoni *et al.* (2003), and the putative prevalence of dominating anucleate basidiospores in mature basidiomata in *I. obliquus* (Sun *et al.* 2023), it is highly likely that the isolates of *I. obliquus* in this present study produced a small proportion of anucleate basidiospores in successful staining reactions, but were not counted. Under these assumptions, it is reasonable to state that the isolate examined by Sun *et al.* (2023) produced a relatively higher proportion of anucleate spores in maturity in comparison to isolates from this study, even though anucleate basidiospores were not explicitly tallied. Anecdotally, putative anucleate basidiospores where not nearly as common in mature basidiomata.

Sun *et al.* (2023) used a high concentration of Hoechst 33258 (50µg/ml) that was 10x stronger than the concentration of Hoechst 33342 (5µg/ml) used in this study. Relative to Hoechst 33258, Hoechst 33342 has a much better cell-permeating ability (Interchim, n.d.), which may explain the highly different concentrations between studies. Additionally, Sun *et al.* (2023) reported that basidiomata ceased basidiospore production after fifteen days but isolates not directly reported in this present study actively produced basidiospores for just over 30 days in ideal scenarios. This may indicate early fruiting body degradation or reduced spore production capacity in Chinese isolates of *I. obliquus,* that could be associated with degeneration of meiotic products in the basidium. Basidial nuclear degeneration is well described phenomena in post-meiotic events in agaricomycetes responsible for controlling the number of resultant nuclei in basidiospores (Duncan & Galbraith, 1972). This is seen in Patterns A, B, and C described by Duncan & Galbraith (1972). The observed variation of anucleate basidiospore proportion in mature basidiomata between these two studies is potentially caused by a combination of differences in laboratory conditions (media/substrate, temperature, light), nuclear stain capacity, genetic differences of North American and Chinese isolates of *I.obliquus*, fruiting body degradation, and reduced spore production in Chinese isolates. Examination of strains from different geographic regions, timed wild fruit body basidiospore analysis, and use of different stains is essential for elucidating a comprehensive understanding of *I. obliquus* basidiospore nuclear behaviour.

INONOTUS OBLIQUUS MATING - SPECULATIONS

Members of the hymenochaetoid clade (which includes Hymenochaetaceae) have not received any karyological treatment examining post-meiotic nuclear behaviour patterns; thus, the mechanisms for the achieved basidiospore nuclear status in *I. obliquus* remains unknown at this time. Multiple descriptions of *I. obliquus* confirm that basidia are tetraseterigmate (see Chapter 1). This information is important when speculating on the nuclear mechanisms that result in variable nuclear contents in *I. obliquus* basidiospores. In tetrasterigmate species, the occurrence of pseudohomothallism typically requires a post-meiotic mitosis in the basidium such that there are sufficient nuclei (8) to form 4 heterokaryotic spores (two nuclei per spore) with unlike mating compatible nuclei (Elliot & Challen, 1983). However, in *I. obliquus*, basidiospores can be anucleate, uninucleate, binucleate, trinucleate, and tetranucleate (very rarely penta and hexanucleate). Additionally, its tetrasterigmate condition rules out reduced sterigma number as a factor to contribute to bi or multinucleate spores as in *Laccaria fraterna* (Cooke & Mass.) Pegler (predominantly bisterigmate sometimes uni or tristerigmate) (Tommerup *et al.* 1991) and *Agaricus bisporus* (J.E. Lange) Imbach (predominatly bisterigmate) (Kamzolkina *et al.* 2006). In *Laccaria fraterna,* (Tommerup *et al.* 1991) describes a post-meiotic mitosis in basidispores following a standard meiosis in the basidium (Pattern D (Duncan & Galbraith, 1972)) Basidispores can potentially contain 1 – 8 nuclei; mediated by basidiospore post-meiotic mitosis and reduced sterigma number. The organism that most closely resembles the basidiospore nuclear status of *I. obliquus* and has preliminary karyological investigation of post meiotic events, is *Stereum sanguinolentum*; an amphithallic, tetrasterigmate agaricomycete that can produce anucleate, uninucleate, binucleate, trinucleate, and tetranucleate basidiospores (like *I. obliquus*) (Calderoni et al. 2003). Calderoni *et al.* (2003) describes two patterns in basidia: (1) a post-meiotic mitosis that results in eight haploid nuclei. (2) no post-meiotic mitosis resulting in four nuclei in the basidium. Unfortunately, Calderoni *et al.* (2003) did not detail nuclear segregation in basidiospores.

It is highly likely that *I. obliquus* is undergoing post-meiotic mitosis, but the question is, where? When viewing basidiospores for nuclear contents, often basidiomata were printed for an hour, with the basidiospores stained and viewed within 30 minutes. The last dispensed basidiospores would have landed on the slide approximately 30 minutes before viewing. Some basidiospores were already multinucleate, meaning it was unlikely that nuclei divided later. If post-meiotic mitosis occurred in basidiospores, it likely did so while still attached to sterigma before being shed. This would suggest than bi or multinucleate basidiospores are products of the mitosis of one or more nuclei, resulting in a homo allelic binucleate spore, an imbalanced nuclear ratio in trinucleate spores or a tetranucleate basidiospore with 2 sets of paired nuclei. The occurrence of post-meiotic mitosis in basidia is perhaps a more likely candidate in the case of *I. obliquus*. Additionally, as observed by Calderoni *et al.* (2003), it is possible that meiotic products of *I. obliquus* sometimes undergo post-meiotic mitosis in the basidum and sometimes do not, resulting in basidospores with reduced numbers. As detailed above, *Stereum sanguinolentum* and *Oudemansiella aparlosarca* were both found to produce anucleate, uninucleate, binucleate, trinucleate, and tetranucleate basidiospores, which suggests that the production of anucleate basidiospores may be a consequence of uneven distribution of the post-meiotic nuclei (Calderoni *et al.* 2003; Rebecca *et al.* 2021). For example, if one spore receives four nuclei, one receives three, and one receives one, then all eight nuclei are used and one spore will be anucleate. In tetrapolar heterothallic agaricomycetes, there are two fully possible mating compatible reactions that can occur in the eight possible interactions (25%). For example, if the four progeny are A1B1 = A, A1B2 = a, A2B1 = B, and A2B2 = b, then compatible reactions can occur between A + a and B + b as they are heteroallelic for mating type (Kothe, 1996). This means that in order for a SSI to form fertile basidiomata, it must be packaged with nuclei of one of those two compatible pairings. After a post-meiotic mitosis, each genotype is doubled meaning "there's enough compatibility to go around" for multiple spores, so to speak. It is likely that *I. obliquus* displays a non-random preferential sorting of mating compatible nuclei into the same spore, but that can only be proved through karyological and genomic investigation (Summerbell *et al.* 1989; Kamzolkina *et al.* 2006). James *et al.* (2009) examined the formation of trikaryons in *Heterobasidion parviporum* Niemelä & Korhonen through heterokaryon – homokaryon (he – ho) pairings by tracking unique nuclei using nucleus specific microsatellite markers. James *et al.* (2009) states that multinucleate (>2 per cell) heterokaryons are potential candidates for trikaryon formation. *Heterobasidion parviporum*, like *I. obliquus*, is multinucleate (>2 per cell). *Heterobasidion parviporum* was able to form trikaryons that contained nuclei of three distinct genotypes. The trikaryon was found to be semi-stable through multiple rounds of subculturing. This suggests that it is potentially possible for multinucleate basidiospores of *I. obliquus* to contain multiple nuclei all of unique genotype, or tri and tetranucleate spores to contain imbalanced nuclear ratios. It is also possible that trinucleate basidispores are trikaryotic (contains three unique genotypes) and could germinate to form a trikaryon. The same could be true for tetranucleate basidispores, where it possesses all four meiotic products and can germinate to form a "tetrakaryon". This is speculation and requires further investigation. James *et al.* (2009) suggests that fungi with multinucleate heterokaryotic cells have a greater potential for genetic diversity and recombination in relation to dikaryotic fungi. Additionally, James *et al.* (2008) viewed that imbalanced nuclear ratios (not 1:1) in multinucleate heterokaryons of *H. parviporum* affect gene transcription and growth rate. In multinucleate heterokaryons, the ratios of nuclei are frequently imbalanced, stable, caused by a combination genetic and epigenetic effects, and have a greater potential for genetic/phenotypic diversity.

In order to elucidate the nuclear ratios and genotypes present in *I. obliquus* heterokaryotic basidiospores and germinated mycelium, the use of nucleus specific satellite markers, and karyological investigations of basidia development/ post-meiotic patterns are required.

Sun *et al.* (2023) reported that 88.50% of the 96 single spore isolates (SSI) formed fertile fruiting bodies, and the highest rates of germination occurred in basidiospores that were shed from basidiomata in first two days (0.62%). Like the results in this present study, binucleate and multinucleate spores were at their highest proportion here. Bi and multinucleate spores may have higher rates of germination, which explains why such a high proportion of SSI's were able to fruit. In the observations of nuclear type proportions in this study and in Sun *et al.* (2023), uninucleate spores predominated when they were released four or more days following initial basidiospore formation (Figure 3-17). Those results should lead to more self-sterile SSI's, but they only exist in a very small relative proportion (11.5%). Gehrmann *et al.* (2018) described nucleus-specific gene expression in multinucleate heterokaryons of *Agaricus bisporus* and found that unique individual (P1 and P2) nuclei in heterokaryons can have greater expression of certain genes. One nucleus (P2) up-regulated almost three-fold more metabolism genes in comparison to P1. P1 dominated mRNA production relative to P2. While their findings were gathered from heterokaryotic mycelium, there isn't a reason why this couldn't be applied to heterokaryotic basidiospores. It is likely that containing more nuclei in a basidiospore could increase the chances of germination through the up-regulation of specific genes and diversity of gene expression.

Ecological Implications of an Amphithallic Mating System

Ecologically, *Inonotus obliquus* has a unique life-cycle in which generations can be incredibly long (80 +) years, and displays semelparous sporulation whereby basidiomata formation only forms once beneath bark of dead hosts (Černý, 1976; Shigo, 1965; Pringle & Taylor, 2002; Bunyard, 2015). It is very likely that the putative amphithallic mating system described by Sun *et al.* (2023) is an adaptation for a long-life cycle and a short lived semelparous sexual stage. Pseudohomothallism through the production of heterokaryotic basidiospores increases the success of colonizing new territory as it does not require a mating partner for sexual reproduction (Horton, 2006). Therefore, if a single heterokaryotic basidiospore happens to successfully infect a host, the colony will have no trouble forming a fruiting body in many decades. Production of bi or multinucleate spores may be advantageous as diversity of nuclei or nuclear ratios can have an effect on gene expression diversity, transcription, and growth rate (Gehrmann *et al.* 2018; James *et al.* 2008). Although, a drawback of this system is that genetic diversity is reduced through diploid selfing via automixis (Billiard *et al.* 2012). Contrarily, the production of homokaryotic basidiospores ensure that outcrossing can occur via the requirement of a mating compatible partner to form a heterokaryon (Kothe, 1996). Additionally, homokaryotic spores may be introduced to a stem already colonized by a compatible homokaryon, or mature heterokaryon, where it is possible that a trikaryon sensu James *et al.* (2009) could form. By this logic, the homokaryon can successfully incorporate its genome into a well-established colony that may have already prepared nutrient reserves for sporulation in the form of sterile conks, such that energy in early colonization is conserved. The predominance of heterokaryotic spores (bi, tri, and tetranucleate) in early development may present an opportunity to send out as much genetic information as possible, capable of establishing fertile colonies on their own, followed later by homokaryotic spores for outcrossing. The genetic mechanisms for nuclear sorting in *I. obliquus* would be an area of interest to study. Also, the genetic structure of *I. obliquus* populations may be unique and should be examined. The predominance of anucleate basidiospores by Sun *et al.* (2023) does not have any direct role in dispersal as they are sterile, but may be used to feed and attract insects.

CONCLUSION

This study provides a comprehensive and robust analysis of the variability of basidiospore nuclear type proportions for *I. obliquus* through maturation. Under laboratory conditions, this study and Sun *et al.* (2023) found that the basidiomata of *I. obliquus* produce basidiospores of highly variable nuclear type that appeared to change with fruiting body maturity (anucleate, uninucleate, binucleate, trinucleate, tetranucleate, and rarely penta/hexanucleate). Both studies saw a higher proportion of binucleate and multinucleate basidiospores in a young state, and a predominance of uninucleate basidiospores in a middle aged state, the predominace of anucleate spores in a old state was not observed here. This may be due to factors such as laboratory growing conditions, strain selection, staining protocol, or small spore sample sizes by Sun *et al.* (2023), as spore counts were not listed. It is possible that anucleate basidiospores are caused by an uneven distribution of post-meiotic nuclei in multinucleate spores. This leads to multinucleate spores that possess potentially multiple genotypes. The results here and of Sun *et al.* (2023) show a temporal shift of basidiospore nuclear type proportions is plausible, however, this may only exist under laboratory conditions and should be tested in the wild, or if not possible, with more strains.

LITERATURE CITED

Arel-Bundock, V., Greifer, N., & Heiss, A. 2024. How to interpret statistical models using marginaleffects for R and Python. *Journal of Statistical Software*, *111*, 1–32.

Betancourt, M. 2018. *A Conceptual Introduction to Hamiltonian Monte Carlo* (arXiv:1701.02434). arXiv.

Billiard, S., López-Villavicencio, M., Hood, M. E., & Giraud, T. 2012. Sex, outcrossing and mating types: unsolved questions in fungi and beyond. *Journal of Evolutionary Biology*, *25*(6), 1020–1038.

Bunyard, B. A. 2015. First record of insect mycophagy of the commercially-important "Chaga" fungus *Inonotus obliquus* (Ach. ex Pers.) Pilát (Hymenochaetales: Hymenochaetaceae) in North America. *Proceedings of the Entomological Society of Washington*, *117*(4), 452–457.

Bürkner, P.-C. 2015. *brms: Bayesian Regression Models using "Stan"* (p. 2.22.0) [Dataset].

Bürkner, P.-C. 2017. brms: An R package for Bayesian multilevel models using Stan. *Journal of Statistical Software*, *80*, 1–28.

Calderoni, M., Sieber, T. N., & Holdenrieder, O. 2003. *Stereum sanguinolentum*: is it an amphithallic basidiomycete? *Mycologia*, *95*(2), 232–238.

Černý, A. 1976. Lesnická fytopatologie. *Státni zemědělské nakladatelstvi*, Praha.

Duncan, E. G., & Galbraith, M. H. 1972. Post-meiotic events in the Homobasidiomycetidae. *Transactions of the British Mycological Society*, *58*(3), 387–392.

Elliott, T. J., & Challen, M. P. 1983. Genetic ratios in secondarily homothallic basidiomycetes. *Experimental Mycology*, *7*(2), 170–174.

Ern, P. T. Y., Quan, T. Y., Yee, F. S., & Yin, A. C. Y. 2023. Therapeutic properties of *Inonotus obliquus* (Chaga mushroom): A review. *Mycology*, *15*(2), 1–18.

Fraser, J. A., Hsueh, Y., Findley, K. M., Heitman, J. 2007. Evolution of the mating-type locus: the Basidiomycetes. In *Sex in Fungi: Molecular Determination and Evolutionary Implications* (J. Heitman, J. W. Kronstad, J. W. Taylor & L. A. Casselton, Eds.), Chapter 2, pp. 19–34. *ASM Press.*

Gehrmann, T., Pelkmans, J. F., Ohm, R. A., Vos, A. M., Sonnenberg, A. S. M., Baars, J. J. P., Wösten, H. A. B., Reinders, M. J. T., & Abeel, T. 2018. Nucleus-specific expression in the multinuclear mushroom-forming fungus *Agaricus bisporus* reveals different nuclear regulatory programs. *Proceedings of the National Academy of Sciences*, *115*(17), 4429–4434.

Gelman, A., & Hill, J. 2007. *Data analysis using regression and multilevel/hierarchical models*. Cambridge university press.

Gelman, A., Simpson, D., & Betancourt, M. 2017. The prior can generally only be understood in the context of the likelihood. *Entropy*, *19*(10), 555.

Gelman, A., Vehtari, A., Simpson, D., Margossian, C. C., Carpenter, B., Yao, Y., Kennedy, L., Gabry, J., Bürkner, P.-C., & Modrák, M. 2020. Bayesian Workflow. (arXiv:2011.01808). arXiv.

Goldstein, D., & Gilbertson, R. L. 1981. Cultural morphology and sexuality of *Inonotus arizonicus*. *Mycologia*, *73*(1), 167–180.

Heiss, A. 2021. A guide to correctly calculating posterior predictions and average marginal effects with multilievel Bayesian models. Andrew Heiss. 10.59350/wbn93-edb02

Hespanhol, L., Vallio, C. S., Costa, L. M., & Saragiotto, B. T. 2019. Understanding and interpreting confidence and credible intervals around effect estimates. *Brazilian Journal of Physical Therapy*, *23*(4), 290–301.

Horton, T. R. 2006. The number of nuclei in basidiospores of 63 species of ectomycorrhizal Homobasidiomycetes. *Mycologia*, *98*(2), 233-238.

Interchim**.** n.d.. Hoechst 33258, Hoechst 33342: Cell membrane-permeant, minor groove binding blue fluorescent DNA stains (Technical data sheet No. FT-61248A, Rev.T03E-H12E-F07VB). FluoProbes®

James, T. Y., Johansson, S. B., & Johannesson, H. 2009. Trikaryon formation and nuclear selection in pairings between heterokaryons and homokaryons of the root rot pathogen *Heterobasidion parviporum. Mycological research*, *113*(5), 583-590.

James, T. Y., Stenlid, J., Olson, Å., & Johannesson, H. 2008. Evolutionary significance of imbalanced nuclear ratios within heterokaryons of the basidiomycete fungus *Heterobasidion parviporum*. *Evolution*, *62*(9), 2279–2296.

Kamzolkina, O. V., Volkova, V. N., Kozlova, M. V., Pancheva, E. V., Dyakov, Y. T., & Callac, P. 2006. Karyological evidence for meiosis in the three different types of life cycles existing in Agaricus bisporus. *Mycologia*, *98*(5), 763–770.

Kauserud, H., & Schumacher, T. 2001. Outcrossing or inbreeding: DNA markers provide evidence for type of reproductive mode in Phellinus nigrolimitatus (Basidiomycota). *Mycological Research*, *105*(6), 676–683.

Kothe, E. 1996. Tetrapolar fungal mating types: Sexes by the thousands. *FEMS Microbiology Reviews*, *18*(1), 65–87.

Lange, M. 1952. Species concept in the genus *Coprinus*. A Study on the significance of intersterility. *Dansk Bot. Arkiv*. 14(6): 1-164.

Mallett, K. I., & Myrholm, C. L. 1995. The mating system of *Phellinus tremulae*. *Mycologia*, *87*(5), 597–603.

McElreath, R. 2018. Statistical rethinking: A Bayesian course with examples in R and Stan. Chapman and Hall/CRC.

Miina, J., Peltola, R., Veteli, P., Linnakoski, R., Escribano, M. C., Haveri-Heikkilä, J., Mattila, P., Marnila, P., Pihlava, J.-M., Hellström, J., Sarjala, T., Silvan, N., Kurttila, M., & Vanhanen, H. 2021. Inoculation success of *Inonotus obliquus* in living birch (Betula spp.). *Forest Ecology and Management*, *492*, 119244.

O'Brien, S. F., & Yi, Q. L. 2016. How do I interpret a confidence interval? *Transfusion*, *56*(7), 1680–1683.

Pilz, D. 2004. Chaga and other fungal resources: Assessment of sustainable commercial harvesting in Khabarovsk and Primorsky Krais, Russia. *Report Prepared for Winrock International, Morrilton, Arkansas and the FOREST Project, Khabarovsk, Russia*.

Pringle, A., & Taylor, J. 2002. The fitness of filamentous fungi. *Trends in Microbiology*, *10*(10), 474–481.

Rajchenberg, M. 2011. Nuclear behavior of the mycelium and the phylogeny of Polypores (Basidiomycota). *Mycologia*, *103*(4), 677–702.

Rajchenberg, M., Pildain, M. B., Bianchinotti, M. V., & Barroetaveña, C. 2015. The phylogenetic position of poroid Hymenochaetaceae (Hymenochaetales, Basidiomycota) from Patagonia, Argentina. *Mycologia*, *107*(4), 754–767.

Rebecca, R., Gao, Q., Cui, Y., Rong, C., Liu, Y., Zhao, W., Kumara, W., & Wang, S. 2021. Nuclear conditions of basidiospores and hyphal cells in the edible mushroom Oudemansiella aparlosarca. *MicrobiologyOpen*, *10*(5), e1233.

Shigo, A. L. 1965. The pattern of decays and discolorations in northern hardwoods. *Phytopathology*, 55: 648-652

Sun Y, Zhang YJ, Cao XY, Zhou JS, Jiang JH, 2023. Characteristics related to sexual reproduction and mating type locus of *Inonotus obliquus*. *Mycosystema*, 42(2): 520-529

Summerbell, R. C., Castle, A. J., Horgen, P. A., & Anderson, J. B. 1989. Inheritance of restriction fragment length polymorphisms in *Agaricus brunnescens*. *Genetics*, *123*(2), 293–300.

Thomas, P. W., Elkhateeb, W. A., & Daba, G. M. 2020. Chaga (*Inonotus obliquus*): A medical marvel but a conservation dilemma. *Sydowia*, *72*, 123–130.

Tommerup, I. C., Bougher, N. L., & Malajczuk, N. 1991. *Laccaria fraterna*, a common ectomycorrhizal fungus with mono- and bi-sporic basidia and multinucleate spores: Comparison with the quadristerigmate, binucleate spored *L. laccata* and the hypogeous relative *Hydnangium carneum*. *Mycological Research*, *95*(6), 689–698.

van de Schoot, R., Depaoli, S., King, R., Kramer, B., Märtens, K., Tadesse, M. G., Vannucci, M., Gelman, A., Veen, D., Willemsen, J., & Yau, C. 2021. Bayesian statistics and modelling. *Nature Reviews Methods Primers*, *1*(1), 1–26.

APPENDIX II

Base Model Code with priors

```
priors <- c(
+     # Intercepts (baseline: Maturity = "Young", vs. 1N)
+     prior(normal(0, 1), class = "Intercept", dpar = "mu2N"),
+     prior(normal(-2, 1), class = "Intercept", dpar = "mu3N"),
+     prior(normal(-2, 1), class = "Intercept", dpar = "mu4N"),
+
+     # Slopes for maturity (weakly informative, centered at 0)
+     prior(normal(0, 1), class = "b", dpar = "mu2N"),
+     prior(normal(0, 1), class = "b", dpar = "mu3N"),
+     prior(normal(0, 1), class = "b", dpar = "mu4N")
+ )
>
> full_model_yes <- brm(
+     formula = Nuclear_type ~ Maturity + (1 | Replicate),
+     family = categorical(),
+     data = Fully_Expanded_Spore_Data,
+     prior = priors,
+     chains = 4,
+     iter = 4000,
```

Table 3-8. Spore counts

Replicate	Maturity	1	2	3	4
3R_IO2	Middle_age	147	56	15	2
6R_IO2	Middle_age	299	325	66	10
7R_IO2	Middle_age	230	239	103	23
BLUP5_IO2	Middle_age	515	116	28	4
DKUP4_IO2	Middle_age	336	129	31	6
DKUP5_IO3	Middle_age	104	80	77	14
DKVR5_IO2	Middle_age	205	34	6	3
DKVR5_IO5	Middle_age	330	52	12	7
3R_IO2	Old	547	342	95	13
4R_IO2	Old	299	164	54	19
5R_IO2	Old	257	296	84	15
6R_IO2	Old	92	90	26	5
7R_IO2	Old	114	162	90	20
BLUP5_IO2	Old	289	134	27	4
DKUP4_IO2	Old	301	32	0	0
DKVR5_IO2	Old	208	25	3	0
10R_IO2	Young	86	113	12	2
2R_IO2	Young	217	178	78	9
3R_IO2	Young	69	134	65	10
6R_IO2	Young	154	37	0	0
7R_IO2	Young	130	113	115	20
8R_IO2	Young	30	51	27	3
BLDW5_IO2	Young	39	116	41	9
BLUP5_IO2	Young	150	174	115	31
DKUP4_IO2	Young	39	133	135	23
DKUP5_IO3	Young	25	22	12	3
DKVR5_IO2	Young	191	126	31	1
DKVR5_IO3	Young	129	83	22	1
DKVR5_IO5	Young	132	107	109	27

Table 3-9. Pairwise relative temporal log-odds contrasts of basidiospore nuclear types

Contrast	Estimate	95% CrI: Lower	95% CrI: Upper	Error	Contains 0 (Y/N)
2N v 1N Young to Middle	-0.901	-1.03	-0.774	0.0645	N
2N v 1N Young to Old	-0.877	-1.01	-0.742	0.069	N
2N v 1N Middle to Old	0.024	-0.103	0.148	0.0644	Y *
1N v 3N Young to Old	-1.58	-1.76	-1.4	0.0935	N
1N v 3N Young to Middle	1.7	1.53	1.87	0.0864	N
1N v 3N Middle to Old	-0.115	-0.311	0.0778	0.1	Y *
3N v 2N Young to Middle	-0.799	-0.973	-0.628	0.0876	N
3N v 2N Young to Old	-0.707	-0.893	-0.52	0.0955	N
3N v 2N Middle to Old	0.0914	-0.114	0.3	0.104	Y *
4N v 1N Young to Middle	-1.58	-1.9	-1.26	0.163	N
4N v 1N Young to Old	-1.48	-1.86	-1.1	0.19	N
4N v 1N Middle to Old	0.0994	-0.305	0.512	0.208	Y *
2N v 4N Young to Middle	0.675	0.356	0.993	0.162	N
2N v 4N Young to Old	0.6	0.224	0.977	0.193	N
2N v 4N Middle to old	-0.0755	-0.488	0.333	0.21	Y *
4N v 3N Young to Middle	0.124	-0.211	0.454	0.171	Y *
4N v 3N Young to Old	0.108	-0.288	0.499	0.203	Y *
4N v 3N Middle to Old	-0.0159	-0.46	0.425	0.224	Y *

Table 3-10. Base model output

Contrast	Estimate	Est.Error	95% CrI: Lower	95% CrI: Upper	Rhat
2N v 1N	0.22	0.17	-0.11	0.54	1.00
3N v 1N	-0.49	0.25	-1.01	0	1.00
4N v 1N	-2.17	0.31	-2.78	-1.54	1.00
2N v 1N Young to Middle	-0.9	0.06	-1.03	-0.77	1.00
2N v 1N Young to Old	-0.88	0.07	-1.01	-0.74	1.00
3N v 1N Young to Middle	-1.7	0.09	-1.87	-1.53	1.00
3N v 1N Young to Old	-1.58	0.09	-1.76	-1.4	1.00
4N v 1N Young to Middle	-1.58	0.16	-1.9	-1.26	1.00
4N vs 1N Young to Old	-1.48	0.19	-1.86	-1.1	1.00